THE SYNTHESIS OF

4-METHYL-3-THIOSEMICARBAZIDE (MTSC)

USING N,N-DIISOPROPYLETHYLAMINE AS BASE.

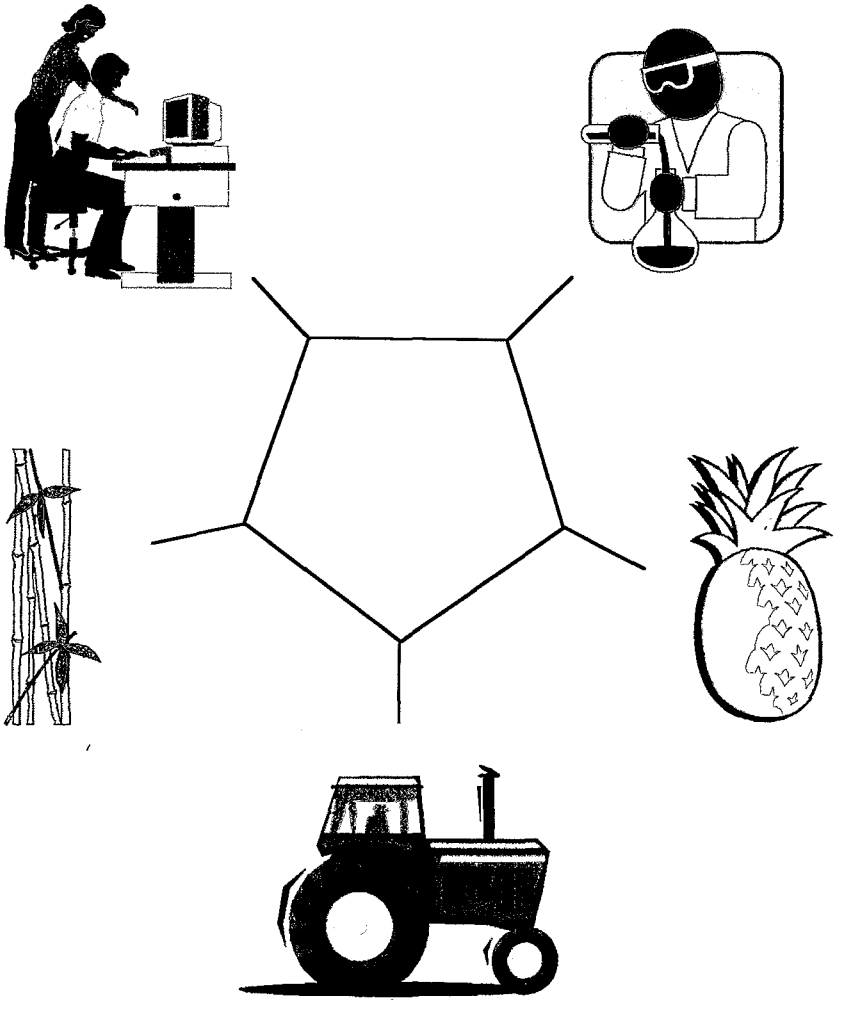

Colette de Klerk

10 December 1999

THE SYNTHESIS OF 4-METHYL-3-THIOSEMICARBAZIDE (MTSC) USING N,N-DIISOPROPYLETHYLAMINE AS BASE.

Colette de Klerk

Dissertation submitted in partial fulfillment of
the requirements for the degree of

MAGISTER SCIENTIAE

in Chemistry at the
Potchefstroomse Universiteit vir Christelike Hoër Onderwys

Supervisor : Prof. P. S. Steyn
Co-supervisor : Dr. A. Wiechers
Assistant supervisor: Prof. B. Zeelie

10 December 1999

Potchefstroom

CONTENTS

CHAPTER 2: The Synthesis of 4-methyl-3-thiosemicarbazide (MTSC)

Literature overview

CHAPTER 3: Experimental

ACKNOWLEDGEMENTS

- To my husband, Francois: Thank you for your love and support. I love you.
- To my parents in law: Thank you for helping me stay focussed.
- To Prof. Steyn: Thank you for making the time available during your busy schedule.
- To Prof. Zeelie and Dr. Wiechers: Thank you for your advice.
- To the National Research Foundation: Thank you for the financial support.
- To Dow AgroSciences: Thank you for affording me this opportunity.

SUMMARY

4-Methyl-3-thiosemicarbazide (MTSC) is an intermediate for the synthesis of 5-t-butyl-2-methylamino-1,3,4-thiadiazole (BTDA), the precursor of tebuthiuron, a broad-spectrum herbicide.

The current production process for MTSC being used at Sanachem's Devchem plant in Sasolburg entails the hydrazinolysis of ammonium N-methyldithiocarbamate. This method affords only a 60-65% yield of MTSC with purity of only 93-94%, while the manufacturing of BTDA of high purity (>98%) and yield requires MTSC of good quality (>97%). The current method also generates approximately 4kg of effluent for each kilogram of product. The effluent contains high concentrations of ammonium salts. An alternative base for the preparation of the methyldithiocarbamate intermediate was required.

N,N-Diisopropylethylamine (DIPEA) has been evaluated as a potential base for the preparation of the N-methyldithiocarbamate intermediate. The N,N-diisopropylethylammonium N-methyldithiocarbamate intermediate proved to be significantly more stable than its counterparts (Na^+, K^+, NH_4^+), resulting in a decrease in the formation of the by-products thiocarbohydrazide (TCH) and dimethylthiourea (DMTU). MTSC yields of 70-75% and purities of 97.5-98.5% were attained. Using DIPEA as base also reduced the amount of effluent produced. For each kilogram of MTSC only two kilograms of effluent were produced. This resulted in a reduction of waste disposal cost.

On completion of a factorial design, it was concluded that the yield of MTSC had to be sacrificed for purity. A yield of 73% and a purity of 98% for MTSC could be attained under the conditions for maximum purity. DIPEA proved to be an excellent alternative to NH_4OH as base for the preparation of N-methyldithiocarbamate as precursor of MTSC. Not only could better yields and purity for MTSC be achieved, but also a decrease in raw material cost.

Using DIPEA as base is more cost effective than using NH_4OH because it can be recovered and reused.

OPSOMMING

4-Metiel-3-tiosemikarbasied (MTSC) is 'n tussenproduk in die sintese van 5-t-butiel-2-metielamino-1,3,4-tiadiasool (BTDA), die voorloper van tebuthiuron, 'n breëspektrumonkruiddoder.

Die produksieproses vir MTSC wat tans by Sanachem se Devchem aanleg in Sasolburg bedryf word, behels die hidrasinolise van ammonium N-metiel-ditiokarbamaat. Hierdie metode lewer MTSC-opbrengste van slegs 60-65% en suiwerhede van slegs 93-94%. Die produksie van hoë kwaliteit BTDA (>98% suiwerheid) behels die gebruik van hoë kwaliteit MTSC (>97% suiwerheid). Hierdie produksieproses lewer groot volumes uitvloeisel. Tipies word 4kg uitvloeisel geproduseer vir elke kilogram MTSC. Die uitvloeisel bevat ook 'n hoë konsentrasie ammoniumsoute. 'n Alternatiewe basis vir die bereiding van die N-metielditiokarbamaat tussenproduk moes gevind word.

N,N-Diisopropieletielamien (DIPEA) is ge-evalueer as 'n moontlike basis vir die sintese van die N-metielditiokarbamaat tussenproduk. Die N,N-diisopropiel-etielammonium-N-metielditiokarbamaat tussenproduk is meer stabiel as die ooreenstemmende Na^+, K^+ en NH_4^+ soute. Hierdie verhoogde stabiliteit het 'n afname in die vorming van die byprodukte, tiokarbohidrasied en dimetieltioureum, tot gevolg gehad. MTSC-opbrengste van 70-75% en suiwerhede van 97.5-98.5% is verkry. Die gebruik van DIPEA as basis het ook 'n afname in die volume van die uitvloeisel tot gevolg gehad. Vir elke kilogram MTSC is slegs twee kilogram uitvloeisel geproduseer. Dit het 'n afname in die koste vir die verwydering van uitvloeisel tot gevolg gehad.

Na voltooiing van 'n faktoriaalontwerp, is gevind dat MTSC opbrengs opgeoffer moet word vir suiwerheid. 'n MTSC-opbrengs van 73% met 'n suiwerheid van 98% kan verkry word onder die optimum kondisies vir maksimum suiwerheid. DIPEA is 'n uitstekende plaasvervanger vir NH_4OH as basis vir die sintese van die N-metielditiokarbamaat tussenproduk vir MTSC.

Nie net is beter opbrengste en suiwerhede verkry nie, maar ook 'n afname in die koste van grondstowwe. Die gebruik van DIPEA as basis is meer ekonomies as die gebruik van NH_4OH, omdat DIPEA herwin kan word vir hergebruik.

LIST OF REACTION SCHEMES

LIST OF TABLES

LIST OF FIGURES

LIST OF ABBREVIATIONS

ANOVA	analysis of variance
BTDA	5-tert-butyl-2-methylamino-1,3,4-thiadiazole
COD	chemical oxygen demand
CS_2	carbon disulphide
DIPEA	N,N-diisopropylethylamine
DIPEADTC	N,N-diisopropyl ethylammonium N'-methyldithiocarbamate
DMSO-d_6	deuteriated dimethyl sulfoxide
DMTU	N,N'-dimethylthiourea
DMU	N,N'-dimethylurea
DTC^-	N-methyldithiocarbamate anion
HPLC	high performance liquid chromatography
MBT	2-mercaptobenzothiazole
MBTS	benzothiazole disulphide
MIC	methyl isocyanate
MITC	methyl isothiocyanate
MS	mean squares
MTSC	4-methyl-3-thiosemicarbazide
NMR	nuclear magnetic resonance
SS	sum of squares
TCH	thiocarbohydrazide
TDS	total dissolved solids
TEA	triethylamine
TMT	tris(mercapto)-1,3,5-triazine
UV	ultraviolet
ZMBT	zinc salt of MBT

CHAPTER 1

Tebuthiuron

1.1 Introduction

4-Methyl-3-thiosemicarbazide (MTSC) (**1**) is an intermediate in the synthesis of 5-*tert*-butyl-2-methylamino-1,3,4-thiadiazole (BTDA) (**2**), the precursor of 1-(5-*tert*-butyl-1,3,4-thiadiazol-2-yl)-1,3-dimethylurea or tebuthiuron (**3**). Tebuthiuron is a broad-spectrum herbicide for the control of herbaceous and woody plants, annual weeds, and perennial grass and broad-leaved weeds. It is used for the control of total vegetation in non-crop areas, undesirable woody plants in grassland and pastures, and grass and broad-leaved weeds in sugar cane. [1]

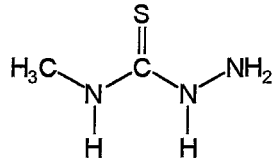

(**1**)

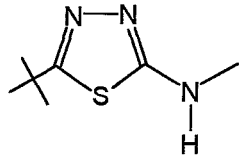

(**2**)

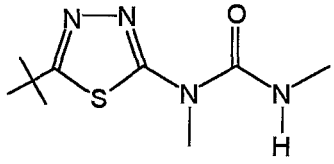

(**3**)

In Southern Africa, tebuthiuron is mainly used in the sugar cane farming industry, and to counteract bush encroachment in the Northern Cape Province and Namibia. It is, however, registered against twelve alien and native invasive weeds including silky hakea (*Hakea sericea*), one of the many woody, invasive, Australian weeds. Tebuthiuron was also proven effective against rock hakea (*Hakea gibbosa*) in the mountain fynbos of the Western Cape Province. [2]

1.2 The discovery and synthesis of Tebuthiuron

Tebuthiuron was discovered by J. F. Schwer and first introduced in Brazil by Eli Lilly & Co. in 1974. [1]

The synthesis of tebuthiuron during 1974-1985 involved the reaction of BTDA with methyl isocyanate (MIC). During 1974-1975 BTDA was produced by the reaction of MTSC and pivaloyl chloride and the subsequent cyclocondensation using sulfuric acid (Scheme 1.1). During 1976-1993 BTDA was produced by the reaction of MTSC with pivalic acid in the presence of polyphosphoric acid and sulphuric acid (Scheme 1.2).[3]

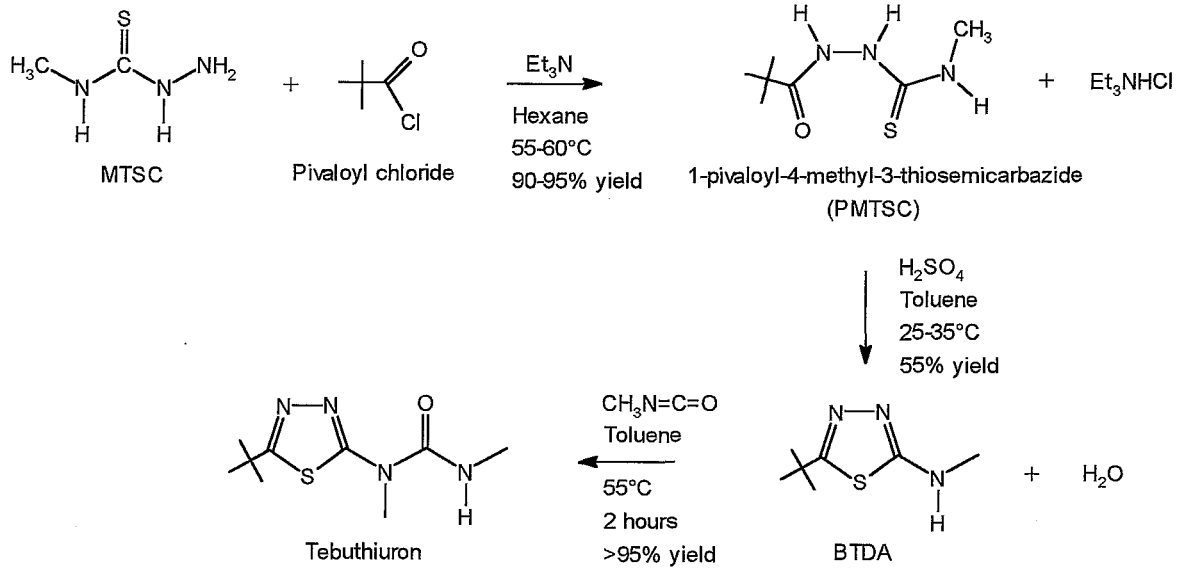

Scheme 1.1: Synthesis of tebuthiuron (1974-1975)

In 1985 a new process for the synthesis of tebuthiuron was introduced. This process involved using phosgene (Scheme 1.3) in stead of MIC, and it was produced in Cosmopolis, Brazil, during 1985 - 1988. This process was developed in response to the incident in Bhopal, India, where many people were killed due to the accidental release of MIC into the atmosphere.

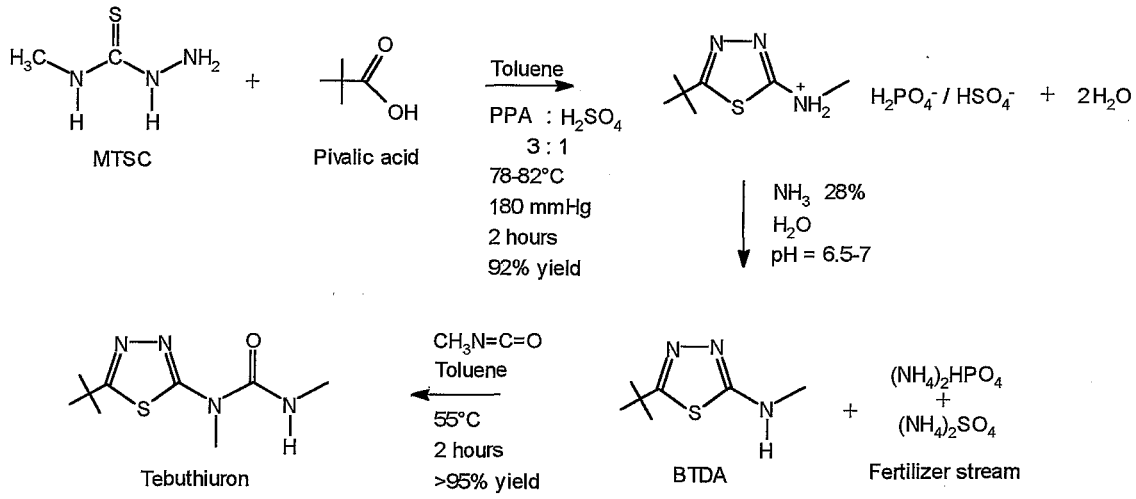

Scheme 1.2: Synthesis of tebuthiuron (1976-1985)

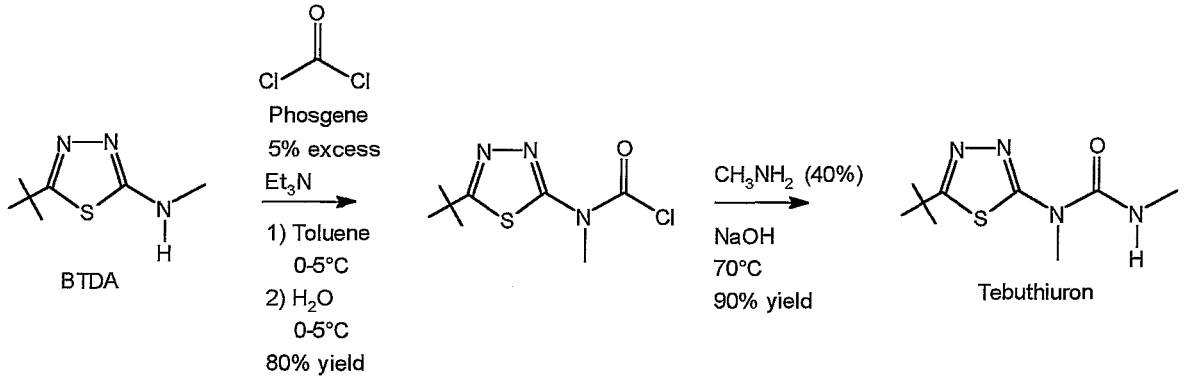

Scheme 1.3: Synthesis of tebuthiuron (1985-1988)

In response to Brazilian restrictions on the shipment of phosgene, a new process for the synthesis of tebuthiuron had to be developed in 1988. In this process N,N'-dimethylurea (DMU) replaced phosgene. It is described in Scheme 1.4.

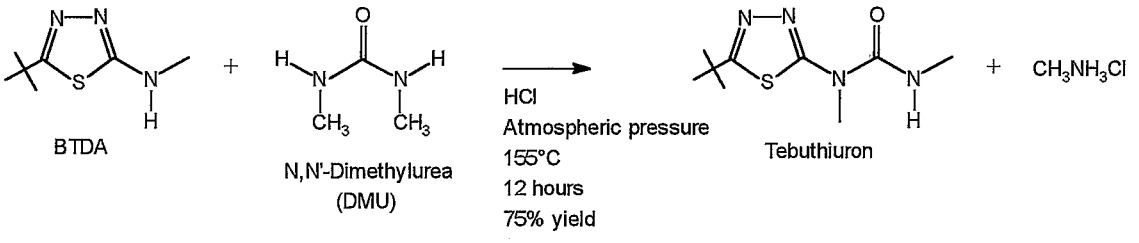

Scheme 1.4: Synthesis of tebuthiuron (1988-1999)

In 1993 a new process for the production of BTDA was introduced. BTDA was produced using toluene as solvent, resulting in the presence of a highly flammable solvent as part of the production process. To eliminate the use of toluene as solvent, a process was developed using one of the reagents (pivalic acid) as the reaction media. The newly developed process involved producing a slurry of MTSC in pivalic acid, and the subsequent reaction with a mixture of sulphuric acid and polyphosphoric acid to complete the cyclization to form BTDA (Scheme 1.5).

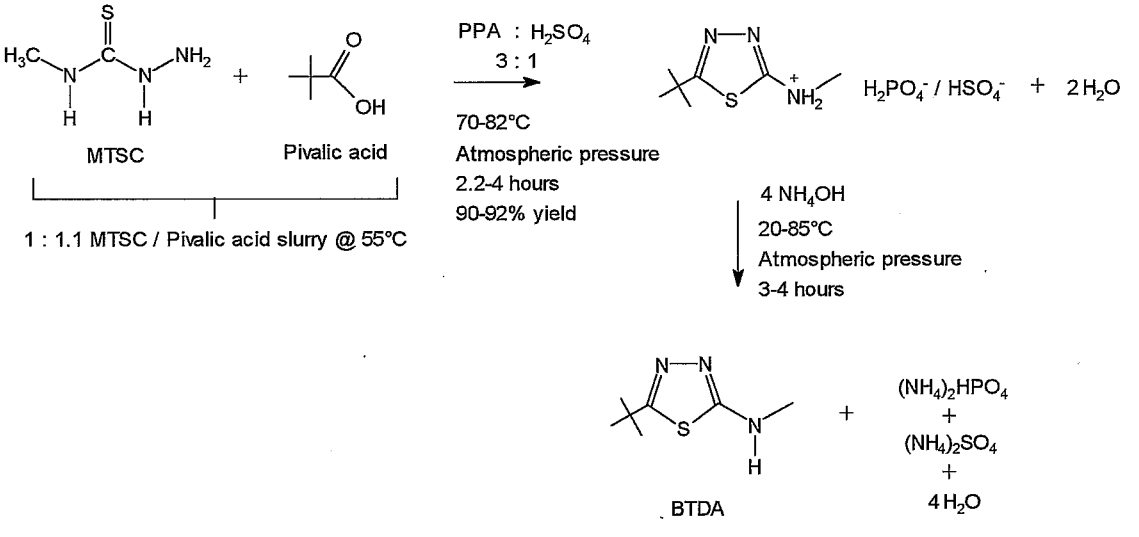

Scheme 1.5: Synthesis of BTDA (1993-1999)

The production facility in Cosmopolis, Brazil, was closed during 1999 and moved to South Africa. BTDA is produced in Sasolburg, while tebuthiuron is produced at Canelands, Durban. The production of BTDA involves the reaction of MTSC with pivaloyl chloride and the subsequent cyclocondensation using phosphorous oxytrichloride [4]. Tebuthiuron is then produced by the reaction of BTDA with MIC (Scheme 1.6).

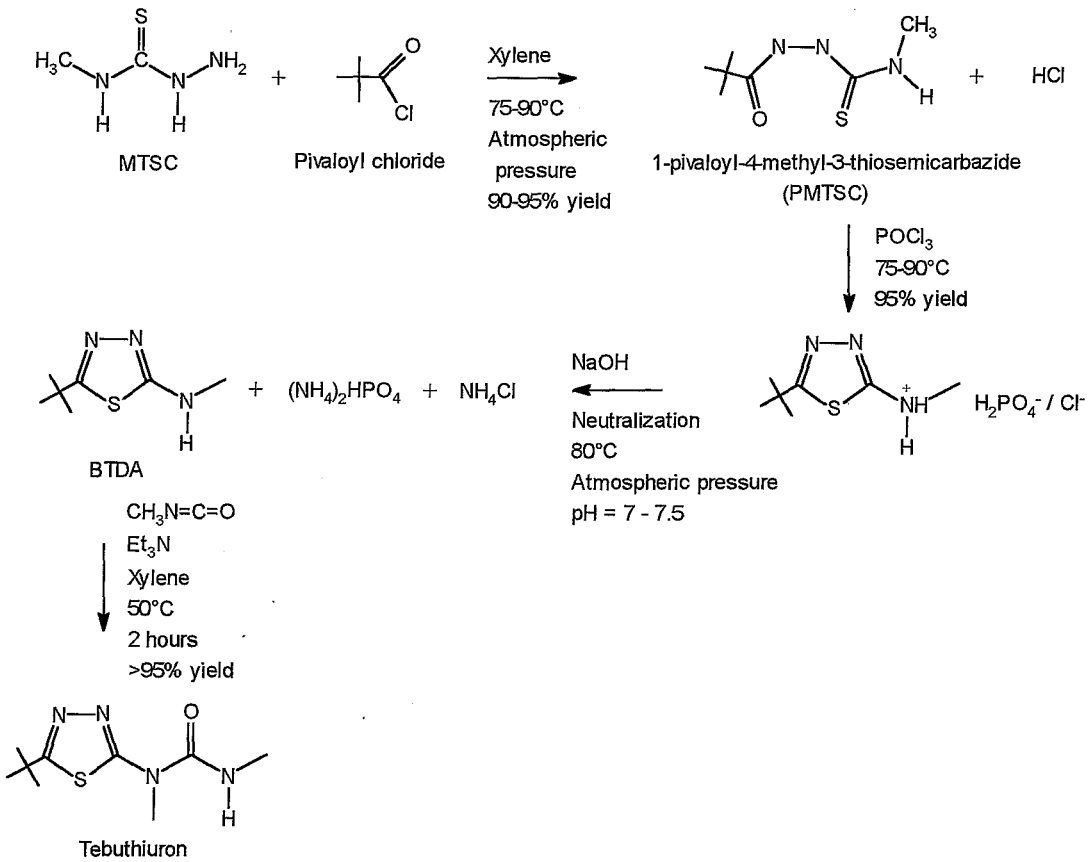

Scheme 1.6: Synthesis of Tebuthiuron (2000 -)

1.3 Mode of action and metabolic pathway

Tebuthiuron is a soil-applied herbicide, which is absorbed by the roots and translocated rapidly to the leaves *via* the xylem.[5],[6] It effects the Hill reaction by inhibiting electron transport in light reaction II during photosynthesis.[7],[8] This prevents the formation of adenosine-5'-triphosphate (ATP) and nicotinamide adenine dinucleotide-2'-phosphate (NADPH), which are required for carbon dioxide reduction.[9],[10],[11]

The main pathway of tebuthiuron metabolism in plants involves N-demethylation and hydroxylation of the *tert*-butyl side chain. Scheme 1.7 describes the metabolism of tebuthiuron in mammals. [12]

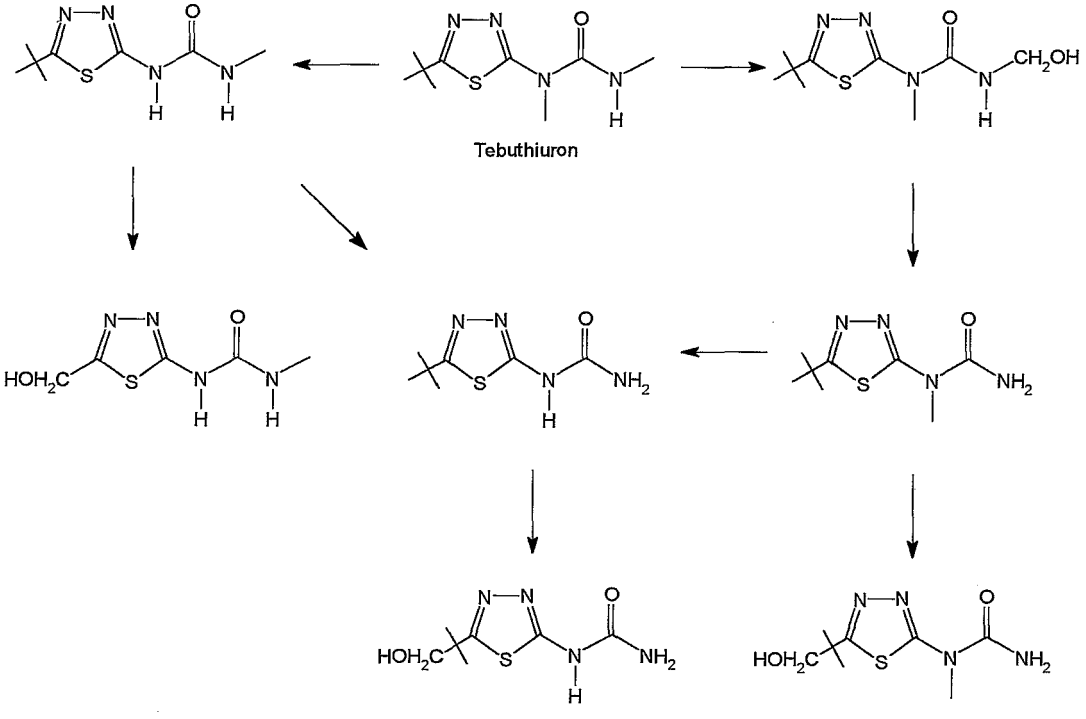

Scheme 1.7: Metabolism of tebuthiuron in mammals

CHAPTER 2.

The synthesis of 4-methyl-3-thiosemicarbazide (MTSC) Literature overview

2.1 Introduction

4-Methyl-3-thiosemicarbazide (MTSC) is produced by the reaction of methylamine, carbon disulphide (CS_2) and N,N-diisopropylethylamine (DIPEA), to produce an N-methyldithiocarbamate intermediate (equation 2.1), and its subsequent reaction with hydrazine hydrate (equation2.2).

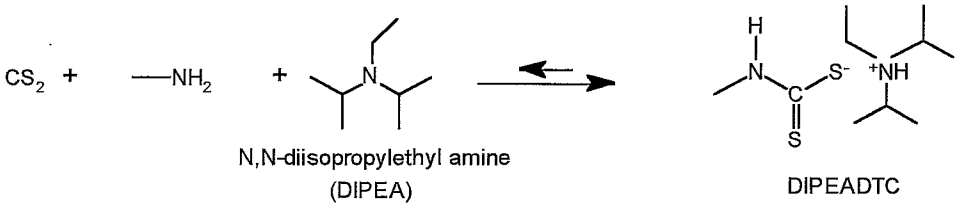

(2.1)

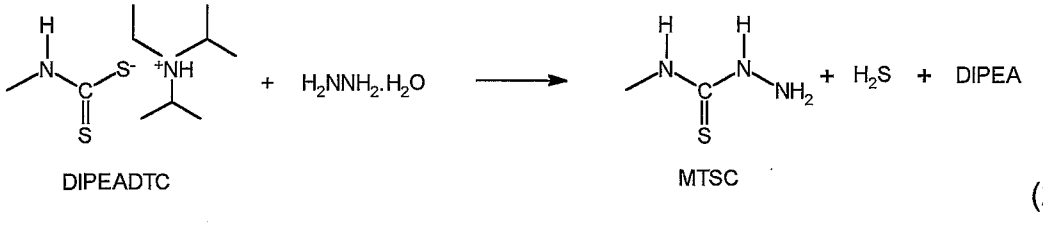

(2.2)

Carbon disulphide is an important reagent in the production of organosulphur compounds used as rubber chemicals or vulcanization accelerators, flotation agents and pesticides.[13]

2.2 Vulcanization accelerators

Vulcanization involves the cross-linking of polymer chains by mono-, di- or polysulphide bridges to improve the physical properties of the resulting rubber.[14] It makes the rubber more resilient and more stable at higher temperatures. The process of vulcanisation involves heating natural rubber or synthetic rubber in the presence of sulphur or a sulphur donor.[15]

CS_2 reacts with aniline in the presence of sulphur to form 2-mercaptobenzothiazole (MBT) (equation 2.3). This compound is the precursor of the benzothiazole accelerators.[16]

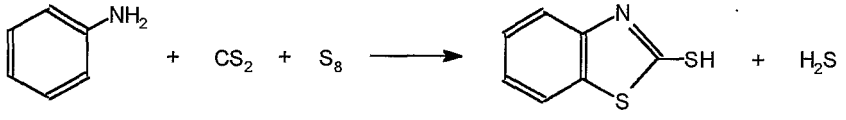

(2.3)

MBT can be oxidized to benzothiazole disulphide (MBTS) (**4**) and MBT can also react with zinc oxide to form the zinc salt of MBT (ZMBT) (**5**), which is used as an accelerator in the production of latex.

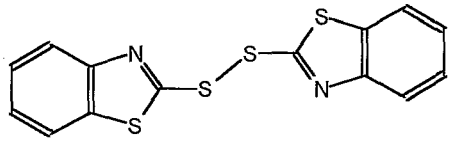

(**4**)

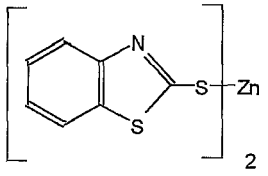

(**5**)

The reaction of CS_2 with aniline in the absence of sulphur forms thiocarbanilide, yet another important accelerator in the production of rubber (equation 2.4).[17]

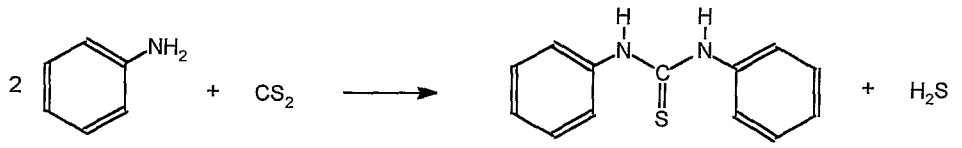

(2.4)

Dialkyl amines react with CS_2 in the presence of sodium hydroxide or excess amine to form dithiocarbamates (equations 2.5 and 2.6).

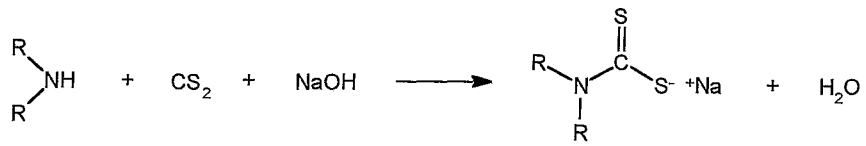

(2.5)

(2.6)

Dialkyldithiocarbamates are used as rubber accelerators when the sodium salt is converted to zinc or other metal salts, which are insoluble in water.[16] The use of different metals results in different properties of the resulting rubber. Copper salts are used when synthetic rubber is produced for O-rings and gaskets, and selenium or tellurium salts are used when rubber with good ageing properties is required.

The oxidation of dialkyldithiocarbamates results in the formation of tetraalkylthiuram disulphides, which are powerful vulcanization accelerators (equation 2.7).[18]

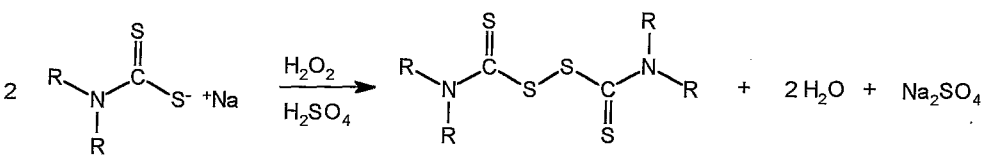

(2.7)

Another group of rubber accelerators called benzothiazolyl dithiocarbamates is prepared by the reaction of MBTS and tetraalkylthiuram disulphides (equation 2.8).[18]

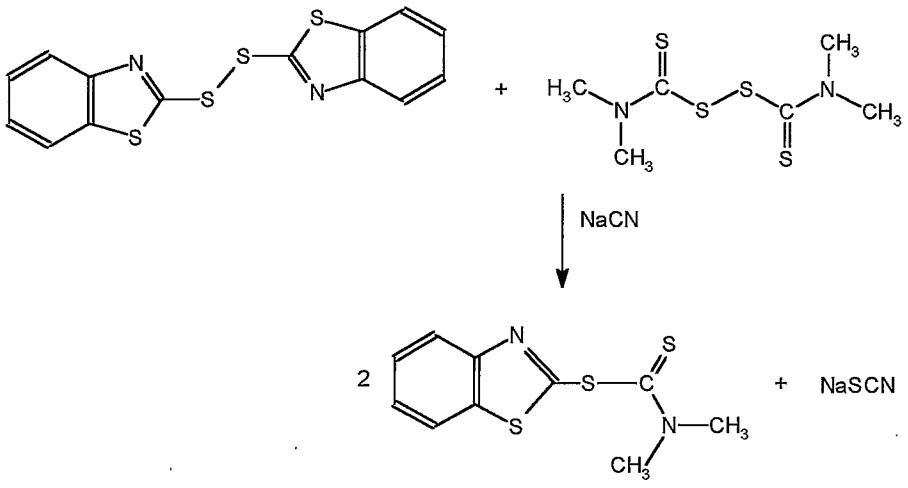

(2.8)

The oxidation of N,N-disubstituted dithiocarbamates or MBT in the presence of a primary or secondary amine results in the formation of thiocarbamoyl sulphenamides, another group of rubber accelerators (equations 2.9 and 2.10).[16], [18] Sulphenamides only become active accelerators when the sulphur – nitrogen bond dissociates.

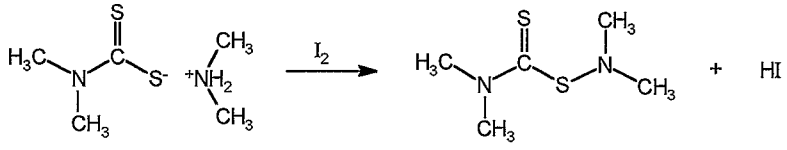

(2.9)

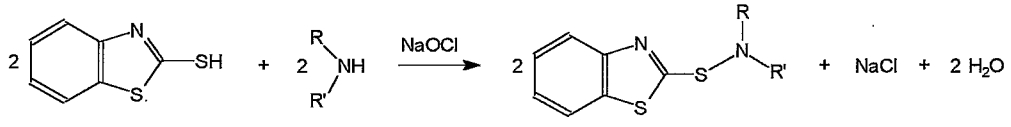

(2.10)

2.3 Flotation agents

The most common flotation collectors are xanthates. They can be prepared by the reaction of CS_2, sodium hydroxide and an alkyl alcohol (equation 2.11).[15], [19] Xanthates are used to collect sulphides and metallic minerals.[20]

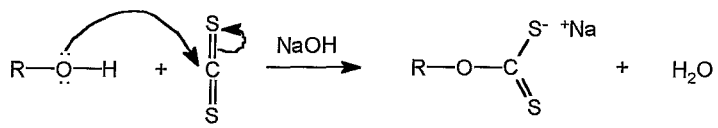

(2.11)

Xanthates can be oxidized to dixanthogens, a group of flotation collectors used to recover sulphides (equation 2.12).[21]

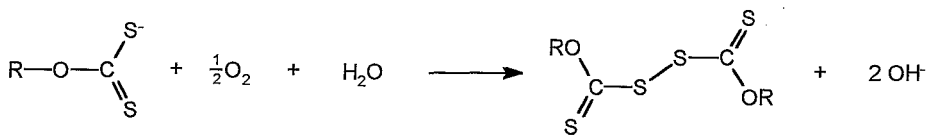

(2.12)

Xanthogen formates form another important group of flotation agents used to recover mineral sulphides.[18] They are prepared by heating dixanthogens in the presence of potassium cyanide (equation 2.13), or the reaction of the sodium xanthate salt with phosgene or cyanogen chloride (equation 2.14).[18]

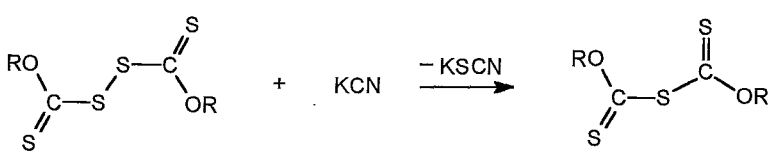

(2.13)

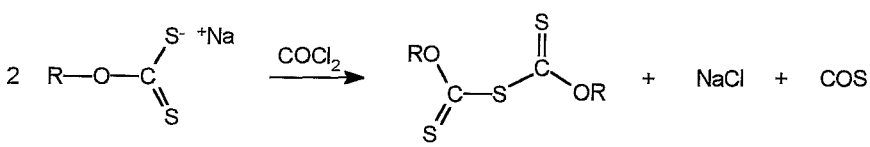

(2.14)

Other important flotation agents derived from CS_2 are thiocarbanilide (equation2.4), which is used as a collector for sulphides, and MBT (equation 2.3), which is used for the recovery of pyrite.[20]

2.4 Pesticides

Dithiocarbamates (equation 2.3) are among the most common pesticides derived from CS_2. Sodium N-methyldithiocarbamate (metam-sodium) (**6**) is used as a soil fumigant for the control of fungi, nematodes, weed seeds and insects in the soil.[1]

Ziram or zinc bis(N,N-dimethyldithiocarbamate) (**7**) is formed when sodium N,N-dimethyldithiocarbamate is treated with zinc sulphate. Ziram is used for fungicidal control in pome fruit, stone fruit, vines and flowers, but it is also a repellent for birds and rodents.[1]

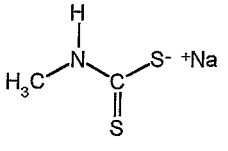

(**6**)

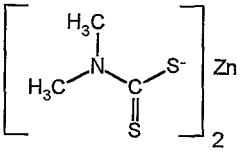

(**7**)

Methylammonium N-methyldithiocarbamate reacts with formaldehyde to form dazomet or 3,5-dimethyl-1,3,5-thiadiazinane-2-thione (equation 2.15).[18] Dazomet is used for the control of soil fungi, nematodes, germinating weed seeds and soil insects. It is also used as a slimicide in the pulp and paper industry, a preservative in adhesives and glues, and an accelerator in the production of polychloroprene.[1]

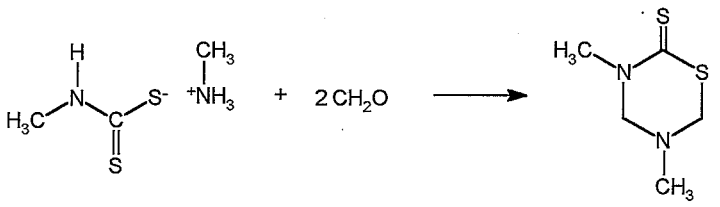

(2.15)

Nabam or disodium ethylenebis(dithiocarbamate) (**8**) is used as an algaecide in rice fields and as a fungicide to control some fungal diseases of cotton and onions.[1] Nabam is often combined with zinc sulphate or manganese sulphate to form polymeric zinc ethylenebis(dithiocarbamate) or zineb (**9**), and manganese ethylenebis(dithiocarbamate) or maneb (**10**).[1] Nabam is also often combined with a combination of manganese sulphate and zinc sulphate to form mancozeb (**11**), the zinc complex of polymeric manganese ethylenebis(dithiocarbamate).[1] Maneb, zineb and mancozeb are used as fungicides applied to the leaves of field crops, fruit and nut trees, and flowers.

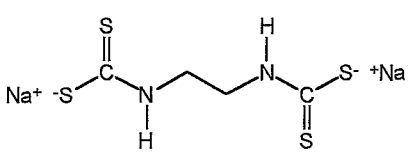

(**8**)

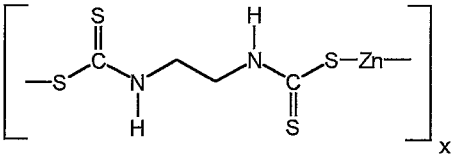

(**9**)

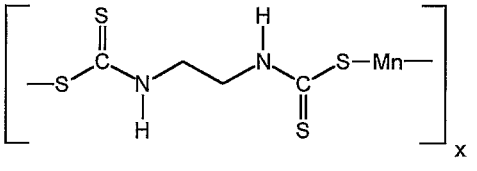

(**10**)

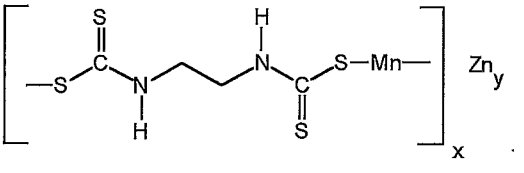

(**11**)

Sodium N-methyl dithiocarbamate can be oxidized by hydrogen peroxide to form methyl isothiocyanate (MITC) (equation 2.16).[22]

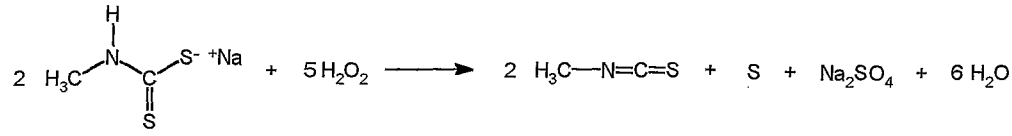

(2.16)

MITC is also formed when cyanuric chloride reacts with sodium N-methyldithiocarbamate (equation 2.17).[23] The byproduct, tris(mercapto)-1,3,5-triazine (TMT), is used as a heavy metal scavenger for removing trace elements from industrial waste water.[24]

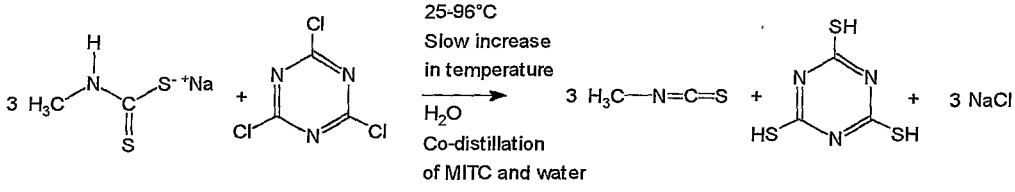

(2.17)

MITC is used directly as a fungicide and nematocide in soil, or as a raw material in the synthesis of 1,3,4-thiadiazoles, which are also very important herbicides.[22] The major commercial 1,3,4-thiadiazole herbicides include tebuthiuron (**12**), ethidimuron (**13**) and thiazafluron (**14**).

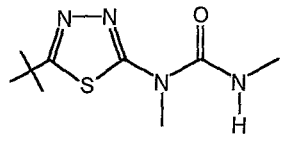

(**12**)

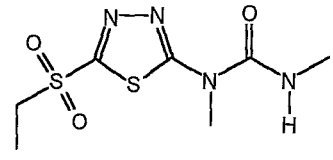

(**13**)

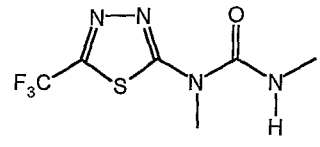

(**14**)

CS_2 reacts with chlorine in the presence of iodine to form sulfenyl chloride and sulphur monochloride (equation 2.18). Sulfenyl chloride then reacts with the sodium salt of tetrahydrophthalimide to form captan or N-

(trichloromethylthio)cyclohex-4-ene-1,2-dicarboximide (equation 2.19).[15] Captan is used as a foliar fungicide.[1]

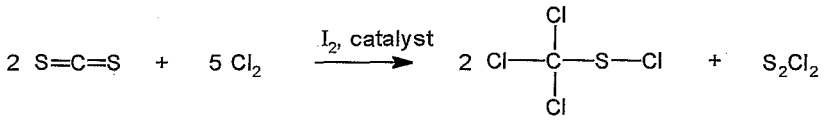

(2.18)

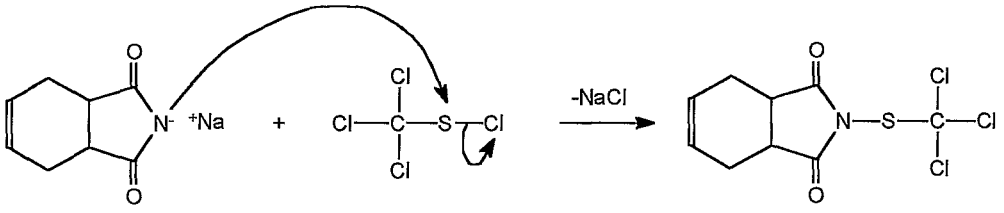

(2.19)

The reaction of CS_2 and hydrazine hydrate in the presence of H_2S forms thiocarbohydrazide (equation 2.20),[25] the precursor to metribuzin or 4-amino-6-*tert*-butyl-4,5-dihydro-3-methylthio-1,2,4-triazin-5-one (**15**), a herbicide for controlling broad leaf weeds and grass weeds in asparagus, potatoes, tomatoes, soya beans, sugar cane, pineapples and cereals.[1]

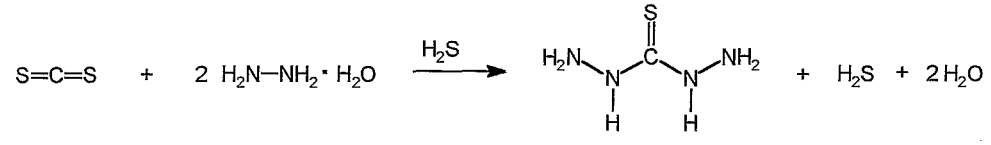

(2.20)

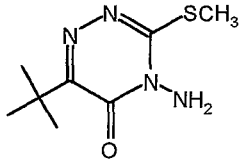

(**15**)

2.5 Other applications

Other applications of CS_2 and CS_2 derivatives include pharmaceuticals, fibres and solvents. CS_2 can be used as a reaction or extraction solvent, or as a reagent in the production of carbon tetrachloride, an important cleaning solvent and refrigerant.[17] CS_2 reacts with chlorine in the presence of iron catalysts to form carbon tetrachloride and sulphur monochloride (equation 2.21). The sulphur monochloride then acts as chlorinating agent to form carbon tetrachloride (equation 2.22).[13]

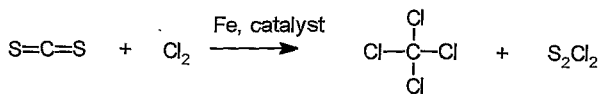

(2.21)

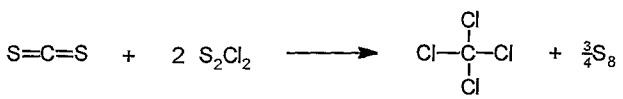

(2.22)

Carbon disulphide is used to convert cellulose to the xanthate (equation 2.23). The cellulose is then regenerated from the xanthate in sulphuric acid to form viscose rayon fibres and cellophane (equation 2.24). [17]

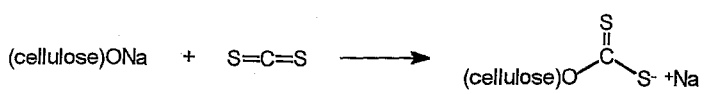

(2.23)

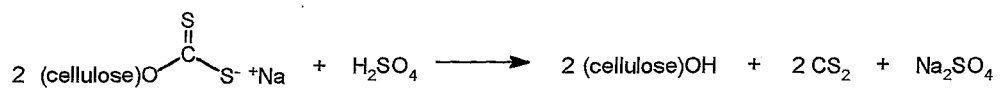

(2.24)

Compounds derived from CS_2 are also important pharmaceuticals. Disulfiram or tetraethylthiuram disulphide (**16**) is used as withdrawal agent in the treatment of alcoholism.[15] MITC is the starting material for the production of cimetidine (**17**) and ranitidine (**18**), which are important anti-ulcer drugs.[24]

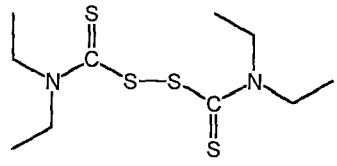

(**16**)

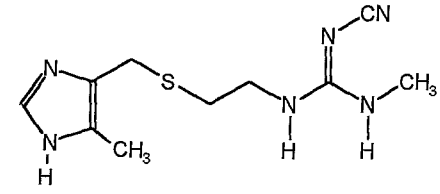

(**17**)

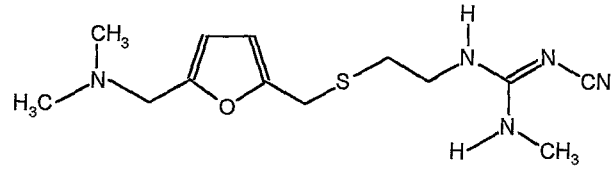

(**18**)

MITC reacts with sodium azide to form 5-mercapto-1-methyltetrazole (equation 2.25), a side-chain in the cefalosporin antibiotics, latamofex (**19**) and cefamandol (**20**).[22]

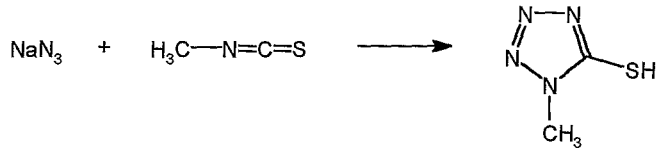

(2.25)

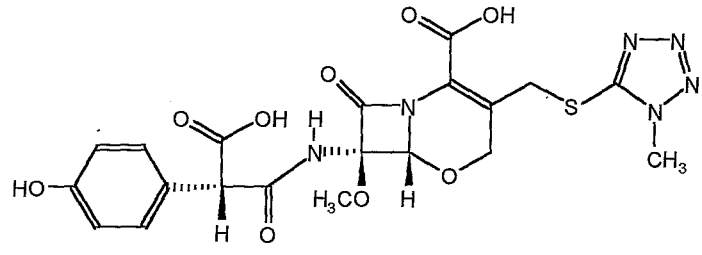

(**19**)

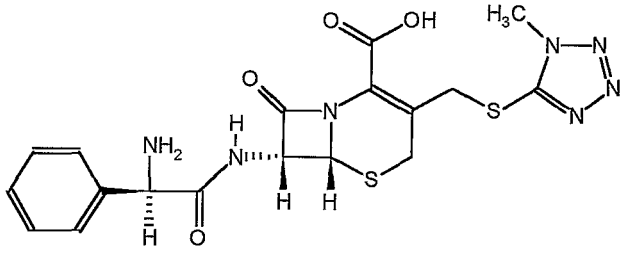

(**20**)

2.6 4-Methyl-3-thiosemicarbazide

Several synthetic methods for the preparation of MTSC are described in the patent literature. They can be summarized as follows:

- the reaction of methyl isothiocyanate with hydrazine hydrate,[26]
- the reaction of hydrazine hydrate and N-methyldithiocarbamate,[27], [28]
- the reaction of N,N'-dimethylthiuram disulphide with hydrazine hydrate,[29] and
- the thermal decomposition of aqueous solutions of ammonium/hydrazinium N-methyldithiocarbamate.[30]

In this study the reaction of N-alkyldithiocarbamate with hydrazine hydrate is investigated.

2.6.1 The synthesis of N-methyldithiocarbamate

N-Methyldithiocarbamate is produced by the reaction of methylamine, carbon disulphide, and a base. This base may be a primary amine, tertiary amine, or alkali metal hydroxide. [31], [32] First the N-methyldithiocarbamic acid is formed, which then reacts with the base to form the corresponding N-methyldithiocarbamate salt (equation 2.26). [33]

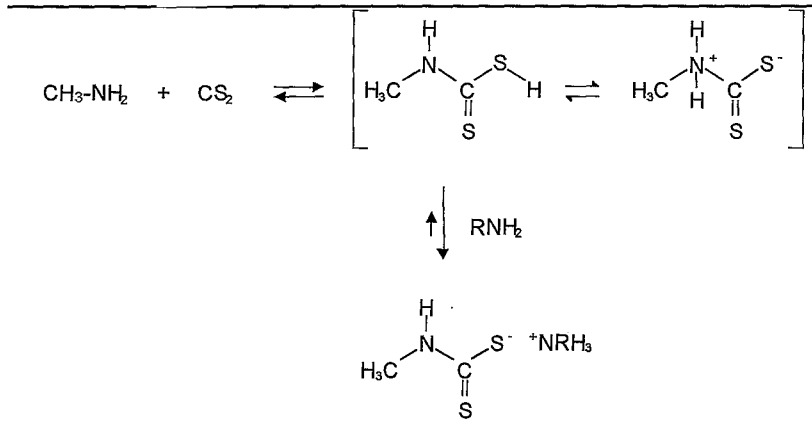

(2.26)

N-Methyldithiocarbamates are not stable. In alkaline media they decompose at elevated temperatures to form methyl isothiocyanate, a hydrosulphide anion, and traces of elemental sulphur (equation 2.27). [34]

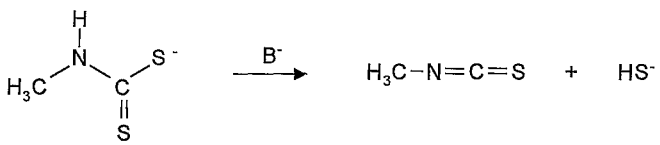

(2.27)

N-Methyldithiocarbamates are also sensitive to oxidation. [18] The first oxidation product is a methyl thiuram disulphide (equation 2.28), which is further oxidized by air to methyl isothiocyanate (equation 2.29). [34]

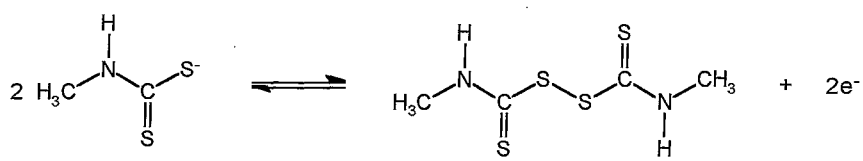

(2.28)

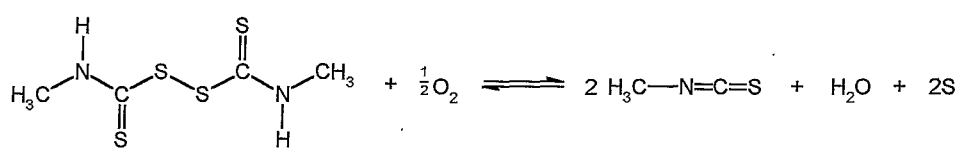

(2.29)

In acidic, the non-catalyzed decomposition of the dithiocarbamate anion occurs by means of a proton transfer from nitrogen to sulphur. This decomposition results in the formation of methyl isothiocyanate and H_2S (equations 2.30 and 2.31). [34], [35]

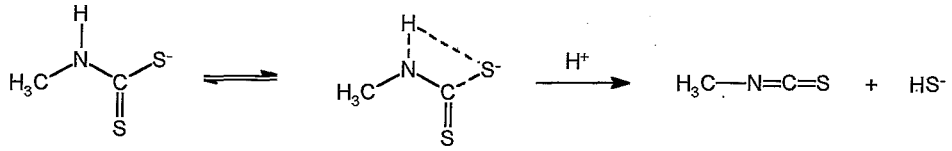

(2.30)

$$HS^- + H^+ \rightarrow H_2S \qquad (2.31)$$

The main impurity formed during the formation of N-methyldithiocarbamate, is N,N'-dimethylthiourea. This is formed when methyl isothiocyanate, the decomposition product of N-methyldithiocarbamate, reacts with unreacted methylamine (equation 2.32). [31]

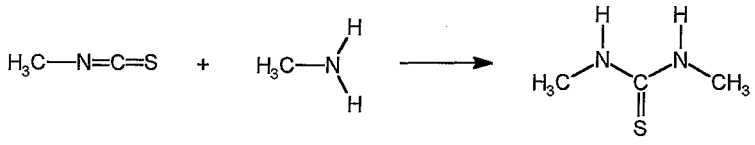

(2.32)

2.6.1.1 N,N-diisopropylethylamine (DIPEA) as auxiliary base for the synthesis of MTSC

Hünig's base (DIPEA) can be used in most applications that require a hindered tertiary amine as a proton acceptor. This makes it an excellent base for the preparation of the N-methyldithiocarbamate intermediate to MTSC. The low nucleophilicity of DIPEA ensures that it does not react with either reagent or intermediates to form undesirable byproducts, which could result in lower yields. [36]

Some properties of DIPEA include: [37]

- proton specific, "non-nucleophilic" base,
- auxiliary reagent in organic synthesis,
- proton acceptor/scavenger,

- replaces triethylamine and dimethylaniline as proton acceptors,
- low nucleophilicity,
- low self alkylation,
- low water solubility (0.4 % w/w),
- recyclable,
- increases process efficiency, and
- reduces process cost.

Recovery of DIPEA from reaction media is relatively straightforward because of its low solubility in water. It can simply be extracted from water-immiscible organic reaction media as its salt in the aqueous phase. The aqueous phase is then treated with sodium hydroxide and the DIPEA is separated to be reused (equation 2.33). DIPEA can also be recovered using azeotropic distillation. After cooling, the azeotrope separates as DIPEA of 99.8% purity and a water phase containing 0.4% DIPEA (equation 2.34).[36]

pH < 5

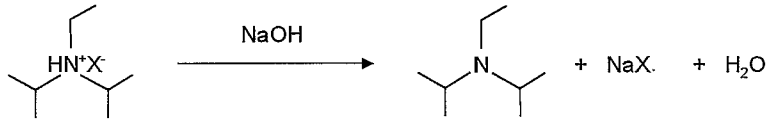

(2.33)

Soluble in aqueous phase

Separates from aqueous phase

pH > 9

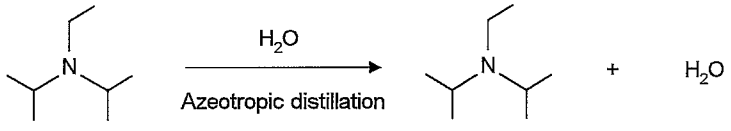

(2.34)

Present as free base

Separates from water on cooling

2.6.2 The hydrazinolysis of N-methyldithiocarbamate to MTSC

4-Methyl-3-thiosemicarbazide is formed during the reaction of N-methyldithiocarbamate and hydrazine hydrate. [38] Hydrazine is a very strong base in aqueous media. Methyl isothiocyanate is presumably formed *in situ* by the base catalyzed decomposition of the N-methyldithiocarbamate (equation 2.35). Hydrazine hydrate then reacts with methyl isothiocyanate to form MTSC (equation 2.36). [39]

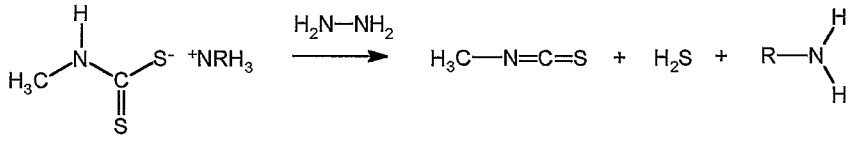

(2.35)

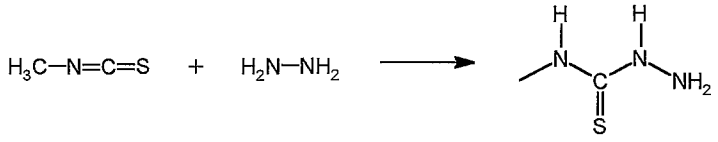

(2.36)

CHAPTER 3

Experimental

3.1 Materials

3.1.1 Reagents for the synthesis of 4-methyl-3-thiosemicarbazide (MTSC)

All reagents used during the synthesis of MTSC are listed in Table 3.1. Also included in Table 3.1 are the suppliers of the reagents and their respective grades.

TABLE 3.1: Reagents for the synthesis of MTSC

Chemical	Formula	Supplier	Grade / Purity
Methylamine	CH_3NH_2	Karbochem	Industrial
N,N-Diisopropyl-ethylamine	$[(CH_3)_2CH]_2NCH_2CH_3$	Whyte Chemicals	>98%
Carbon disulfide	CS_2	Karbochem	Industrial
Hydrazine monohydrate	$N_2H_4{\cdot}H_2O$	Elf Atochem	>98%

3.1.2 Reagents for analysis of MTSC

The reagents used as analytical standards as well as mobile phase for high performance liquid chromatography (HPLC) are listed in Table 3.2.

TABLE 3.2: Reagents for HPLC analysis

Chemical	Formula	Supplier	Grade / Purity
4-Methyl-3-thiosemicarbazide	$CH_3NHCSNHNH_2$	Aldrich	99%
Thiocarbohydrazide	$(NH_2NH)_2CS$	Aldrich	>98%
N,N'-Dimethylthiourea	$(CH_3NH)_2CS$	Aldrich	>98%
Acetonitrile	CH_3CN	BDH	Analytical
Deionized water	H_2O	BDH	-
Phosphoric acid	H_3PO_4	Aldrich	85%

3.2 Experimental procedures

3.2.1 Synthesis of N,N-diisopropylethylammonium N-methyl-dithiocarbamate (DIPEADTC)

Methylamine (40%; 1 mole) and N,N-diisopropylethylamine (DIPEA) (1.1 moles) were charged to a 1L reactor equipped with a reflux condenser and a stirrer (Figure 3.1). CS_2 (1 mole) was added dropwise with stirring during 30 minutes. The reaction temperature was maintained below 30°C by external cooling during the addition of CS_2. The mixture was stirred for an additional 3h after which distillate (60g) from a previous batch was added. The N-methyldithiocarbamate anion (DTC^-) concentration of the mixture was determined UV spectrophotometrically. Water was then added to obtain a DTC^- concentration of 24%.

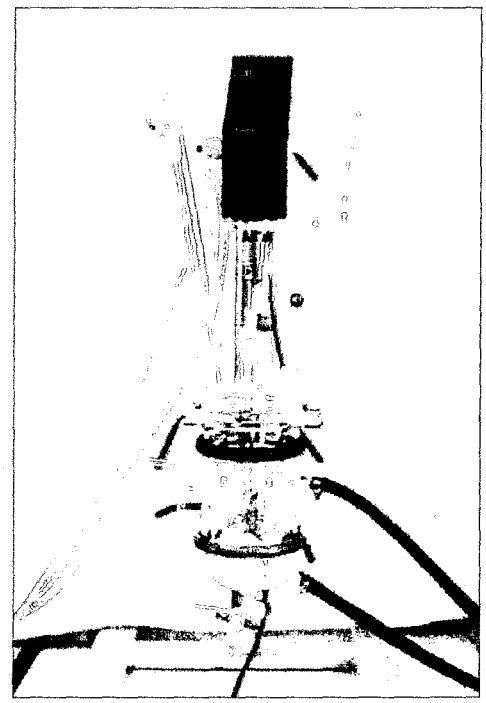

Figure 3.1: Reactor alignment for the synthesis of DIPEADTC

3.2.2 The hydrazinolysis of DIPEADTC to MTSC

Hydrazine hydrate (1.2 moles) was added to the DIPEADTC mixture in the glass reactor equipped with a reflux condenser, H_2S scrubber and stirrer (Figure 3.2). The reaction mixture was heated to 89°C and maintained at 89-92°C under reflux conditions for 2 hours and 20 minutes. The DIPEA was then removed using azeotropic distillation (Figure 3.3). The reaction was completed when the reaction temperature rose above 95°C. The reaction mixture was cooled to 15°C while stirring. The MTSC crystals were separated from the filtrate using vacuum filtration and the crystals were dried in a vacuum oven at 60°C for three hours to yield MTSC, a light yellow product.

The flow diagram and mass balance for both reaction steps are described in Figures 3.4 and Tables 3.3 and 3.4 respectively.

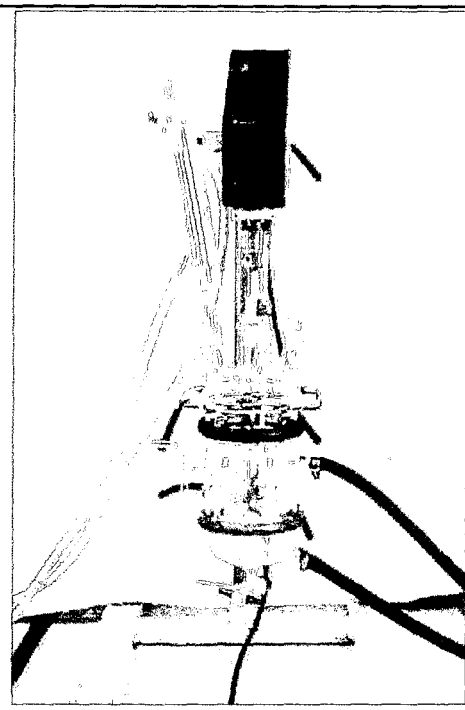

Figure 3.2: Reactor alignment for the hydrazinolysis of DIPEADTC to MTSC – reflux conditions.

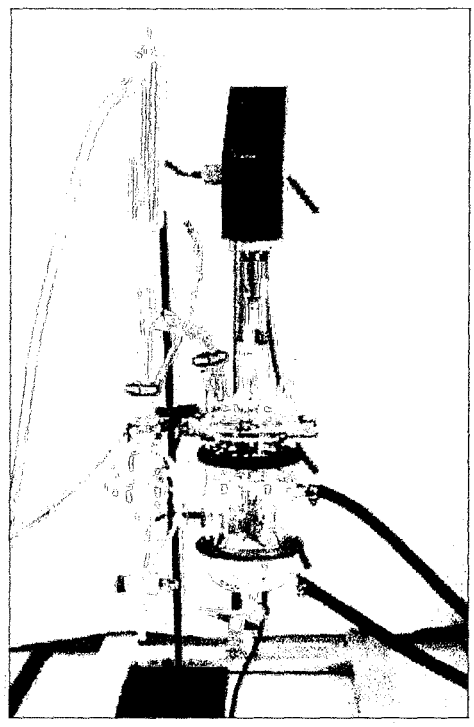

Figure 3.3: Reactor alignment for the hydrazinolysis of DIPEADTC to MTSC – DIPEA recovery.

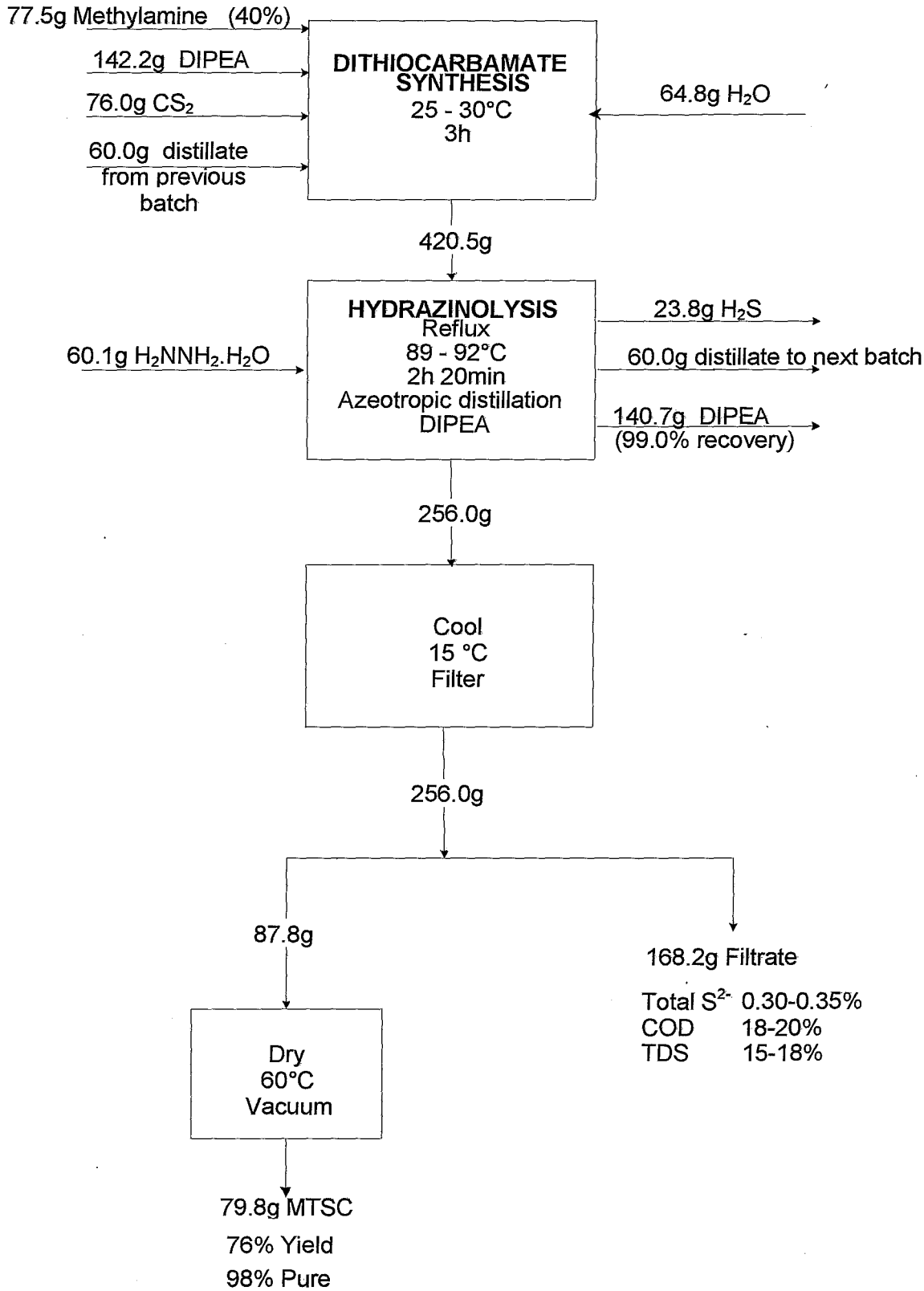

Figure 3.4: Flow diagram for the synthesis of MTSC

Table 3.3: Mass balance for the synthesis of MTSC using DIPEA as base.

MASS BALANCE		Scale	142.4g	DIPEA							
Stream ID	Name of stream	In(g)	Out (g)	AI%	DelHR (kW)	UNIT	Mass Acc. (g)	Density (g/cm3)	Opertion description	Mole Ratio	Unit Ratio
1	CS_2	76.0		100.0%		MTSC	76.0		Charge CS_2 to reactor	1	0.9719
2	Methylamine	77.7		40.0%		R	153.7		Charge methylamine to reactor	1	0.9930
3	DIPEA	142.2		100.0%		E	295.8		Charge DIPEA to reactor	1.1	1.8181
4	Distillate	60.0				A	355.8		Charge Distillate to reactor		0.7673
5	Water	64.8		100.0%		C	420.6	1055	Charge water to reactor	3.60	0.8286
6	$H_2NNH_2.H_20$	60.1		64.0%		T	480.7	936	Charge Hydrazine to reactor	1.2	0.7685
7	H_2S		23.8	100.0%		O	456.9		Burn H_2S in gas burner to (SO_2) or scrub		0.3043
8	DIPEA+H_2O DISTILLATE		200.8			R	256.2	1093	Remove & Condensate DIPEA and water		2.5672
	Mother liquor		256.2	33.7%			0.0				3.2759
	Water/effluent										
	Effluent + mother liq										
	Mother liquor	256.2		33.7%		Liq./Solid	256.18				3.2759
9	Filtrate		168.39	4.9%			87.8		Remove filtrate from mother liq. via buchner filtration		2.1533
10	MTSC CAKE (wet)		87.789	89.1%		Sep.	0.0		Filtrate mother liq. and remove MTSC cake		1.1226

Table 3.4: Stream compositions.

STREAM COMPOSITIONS																					
STREAM ID	*1*	*%M/M*	*2*	*%M/M*	*3*	*%M/M*	*4*	*%M/M*	*5*	*%M/M*	*6*	*%M/M*	*7*	*%M/M*	*8*	*%M/M*	*9*	*%M/M*	*10*	*%M/M*	Mother liq
STREAM COMP.	BATCH	(g/g)	BATCH	(g/g)	BATCH	(g/g)	BATCH	(g/g)	BATCH	(g/g)	BATCH	(g/g)	BATCH	(g/Kg)	BATCH	(g/g)	BATCH	(g/g)	BATCH	(g/g)	BATCH
WATER	0.0	0.0%	46.6	60.0%	0.0	0.0%	54.0	90.0%	64.8	100.0%	0.0	0.0%	0.0	0.0%	60.0	29.9%	157.4	93.5%	8.0	9.1%	165.4
DIPEA	0.0	0.0%	0.0	0.0%	142.2	100.0%	4.8	7.9%	0.0	0.0%	0.0	0.0%	0.0	0.0%	140.8	70.1%	0.0	0.0%	0.0	0.0%	0.0
MTSC	0.0	0.0%	0.0	0.0%	0.0	0.0%	0.0	0.0%	0.0	0.0%	0.0	0.0%	0.0	0.0%	0.0	0.0%	8.2	4.9%	78.2	89.1%	86.4
CS_2	76.0	100.0%	0.0	0.0%	0.0	0.0%	0.0	0.0%	0.0	0.0%	0.0	0.0%	0.0	0.0%	0.0	0.0%	0.0	0.0%	0.0	0.0%	0.0
Methylamine	0.0	0.0%	31.1	40.0%	0.0	0.0%	0.0	0.0%	0.0	0.0%	0.0	0.0%	0.0	0.0%	0.0	0.0%	0.0	0.0%	0.0	0.0%	0.0
$H_2NNH_2.H_20$	0.0	0.0%	0.0	0.0%	0.0	0.0%	0.0	0.0%	0.0	0.0%	60.1	100.0%	0.0	0.0%	0.0	0.0%	0.0	0.0%	0.0	0.0%	0.0
H_2S	0.0	0.0%	0.0	0.0%	0.0	0.0%	1.2	2.1%	0.0	0.0%	0.0	0.0%	23.8	100.0%	0.0	0.0%	0.0	0.0%	0.0	0.0%	0.0
DIPEADTC	0.0	0.0%	0.0	0.0%	0.0	0.0%	0.0	0.0%	0.0	0.0%	0.0	0.0%	0.0	0.0%	0.0	0.0%	0.0	0.0%	0.0	0.0%	0.0
TCH	0.0	0.0%	0.0	0.0%	0.0	0.0%	0.0	0.0%	0.0	0.0%	0.0	0.0%	0.0	0.0%	0.0	0.0%	1.8	1.1%	1.4	1.5%	3.2
DMTU	0.0	0.0%	0.0	0.0%	0.0	0.0%	0.0	0.0%	0.0	0.0%	0.0	0.0%	0.0	0.0%	0.0	0.0%	1.0	0.6%	0.2	0.3%	1.2
TOTAL	**76.0**	**100.0%**	**77.7**	**100.0%**	**142.2**	**100.0%**	**60.0**	**100.0%**	**64.8**	**100.0%**	**60.1**	**100.0%**	**23.8**	**100.0%**	**200.8**	**100.0%**	**168.4**	**100.0%**	**87.8**	**100.0%**	**256.2**

3.3 Analytical methods

3.3.1 High performance liquid chromatography [40]

Standard preparation

MTSC (0.1000 g), TCH (0.0100 g), and DMTU (0.0100 g) were accurately weighed into a 250 mL volumetric flask and made up to the mark with mobile phase.

Sample preparation

Approximately 0.1000 g of the sample is weighed accurately into a 250 mL volumetric flask and made up to the mark with mobile phase.

Instrument operating conditions

Instrument:	Alliance supplied by Waters
Detector:	2487 UV detector
Wave length:	240 nm
Flow rate:	1.0 mL / min
Mobile phase:	1615 mL deionized water + 112 mL acetonitrile + 30g H_3PO_4
Column:	Hibar LiChrosorb RP18
Injection volume:	10 µL

3.3.2 Ultraviolet spectrometry [40]

Approximately 140 mg of the DIPEADTC solution was weighed accurately into a 100mL volumetric flask. The sample was diluted to the mark with a buffer solution of 0.01 M Na_2HPO_4. Into another 100 mL volumetric flask, exactly 1mL of the above mentioned solution was measured, and diluted to the mark with the same buffer solution. The ultraviolet absorption of the final dilution

was measured at 281 nm, using deionized water as reference. The N-methyldithiocarbamate anion concentration was calculated by the following equation:

$$\%DTC^{-} = \frac{A \times 10000}{BM}$$

With *A* the absorption at 281 nm,
B the slope of the calibration curve, and
M the sample mass in milligrams.

3.3.3 Determination of chemical oxygen demand (COD)[41] in MTSC filtrate

Reagents

1. $K_2Cr_2O_7$ (0.25 N)
2. Sulphuric acid reagent (8.92 g Ag_2SO_4 in 1L H_2SO_4)
3. Standardized ferrous ammonium sulphide (0.25 N)
4. Ferroin indicator solution ($FeSO_4 \cdot 7H_2O$ (0.695 g) and 1,10-phenanthroline monohydrate (1.485 g)) was dissolved in water and diluted to 100 mL.
5. $HgSO_4$

Procedure

MTSC filtrate (50 mL) was pipetted into a 250 mL round bottom flask. Water (50 mL) was used for a blank determination. $K_2Cr_2O_7$ (25 mL) was added to the MTSC filtrate sample. H_2SO_4 (40 mL) was added while cooling the mixture after which it was refluxed for 2 hours. The mixture was cooled to room temperature, and 5 drops of ferroin indicator were added. The mixture was titrated with the ferrous ammonium sulphide solution until the colour of the mixture changed from blue-green to reddish brown.

The COD (in parts per million) was calculated using the following equation:

$$COD = \frac{(A-B)N}{V} \times 8000$$

With *A* the volume of $Fe(NH_4)_2(SO_4)_2$ solution used for the blank,
B the volume of $Fe(NH_4)_2(SO_4)_2$ solution used for the sample,
N the normality of $Fe(NH_4)_2(SO_4)_2$, and
V the volume of the sample.

3.3.4 Determination of total dissolved solids (TDS) in MTSC filtrate

Approximately 25 mL of the MTSC filtrate was measured into an evaporating dish. The sample was then evaporated in a vacuum oven for 24 hours at 105°C. The sample was removed from the oven, cooled, and weighed. The TDS (in parts per million) was then calculated using the following equation:

$$TDS = \frac{(W_1 - W_2)}{V} \times 10^6$$

With W_1 the weight of the evaporating dish and the dry sample,
W_2 the weight of the clean, dry, and empty evaporating dish, and
V the volume of the filtrate sample.

3.3.5 Gravimetric determination of total sulphur content in MTSC filtrate

Reagents

1. Bromine/Freon solution (a mixture of 200 mL bromine and 300 mL Freon, $CHCl_3$, CH_2Cl_2, CCl_4, or HCl).
2. Concentrated nitric acid.
3. Concentrated hydrochloric acid.
4. Barium chloride solution (100 g/L).
5. Ammonium hydroxide (250g/L).
6. Methyl red indicator solution (1 g/L in ethanol).

Procedure

A mass of MTSC filtrate (0.2000 – 2.0000 g) was weighed into a 250 mL Phillips beaker and 20 mL of the bromine/Freon mixture was added. The mixture was stirred and left to stand for 10 minutes, before 5mL concentrated nitric acid and 15 mL concentrated hydrochloric acid were added. The mixture was stirred and left for a further 5 minutes after which it was slowly evaporated until all the liquid had evaporated. A further 10 mL of concentrated hydrochloric acid was added and the evaporation process was repeated. After cooling, a further 10 mL concentrated hydrochloric acid and 50 mL deionized water were added. The mixture was heated until it started to boil, and filtered. The filtrate was diluted with water to 400 mL and approximately 0.2 mL methyl red indicator solution was added. The mixture was then titrated with the ammonium hydroxide solution until a permanent orange colour was observed. Approximately 0.5 mL ammonium hydroxide (25% solution) was added in excess. The mixture was heated to 90°C and 15 mL hot barium chloride solution was added.

The mixture was titrated with concentrated hydrochloric acid until the solution turned pink. An excess of 2 mL concentrated hydrochloric acid was added,

and the mixture was heated to the boiling point. It was then allowed to stand overnight. The resulting precipitate was filtered, using ashless filter paper, and washed with small volumes of water until no more chlorides were present in the filtrate. The filter paper with the precipitate was transferred to a porcelain crucible and ignited at 900°C in a furnace. The crucible was removed from the furnace, cooled, and weighed to determine the mass of barium sulphate.

The total sulphur contents was calculated by the following equation:

$$\%S = \frac{A-B}{M} \times 0.1374 \times 100$$

With *A* the mass of barium sulphate,
B the mass of the blank determination,
M the mass of the MTSC filtrate sample, and
0.1374 the factor for the conversion of $BaSO_4$ to sulphur.

3.3.6 Mass spectrometry

The mass spectrometry was recorded on a VG 70-70 E mass spectrometer. Figure 3.5 shows the mass spectrum of MTSC. Table 3.5 contains the interpretation of the mass spectrum of MTSC.

3.3.7 Infrared spectroscopy

Infrared spectroscopy was recorded on a Nicolet Magna-IR® 550 Series II spectrophotometer. The sample was prepared as a finely dispersed solid suspended in a potassium bromide pellet. Figure 3.6 shows the infrared spectrum of MTSC and Table 3.6 contains the interpretation of the spectrum.[42]

TABLE 3.5: Interpretation of mass spectrum of MTSC

Molecular mass	Fragment
105	Molecular ion peak - $[MTSC]^{+\bullet}$
74	$^{+}CH_4$-N=C=S
32	$[H_2N\text{-}NH_2]^{+\bullet}$
28	$[N_2]^{+\bullet}$

TABLE 3.6: Interpretation of the IR spectrum of MTSC

ν (cm^{-1})	Functional group
1275	C=S
920-1100	C-N stretch vibration
2950 and 2975	C-H stretch vibration
1375 and 1460	C-H bend vibration
3350 and 3300	N-H stretch vibration of primary amine
1610 and 1650	N-H bend vibration of primary amine
3150	N-H stretch vibration of secondary amine
600-800	N-H bend vibration of secondary amine

3.3.8 NMR spectrometry[43]

Proton and ^{13}C (proton decoupled) NMR were recorded using a Varian Gemini 300 broad band NMR spectrometer at 300.075 MHz and 75.462 MHz respectively. Tetramethylsilane was used as internal reference in both proton and ^{13}C NMR spectroscopy, and deuteriated dimethyl sulfoxide (DMSO-d_6) was used as solvent. Figures 3.7 and 3.8 show the proton and ^{13}C (proton decoupled) NMR spectra of MTSC respectively. Tables 3.7 and 3.8 contain

the interpretation of the proton and ^{13}C (proton decoupled) NMR spectra respectively.

TABLE 3.7: Interpretation of the proton NMR spectrum of MTSC

δ_H in ppm	Multiplicity	Functional group	Coupling constant J
8.475	Triplet	NH	None recorded
7.743	Quartet	NH	3.22 Hz
4.372	Doublet	NH_2	None recorded
2.875	Doublet	CH_3	4.67 Hz

TABLE 3.8: Interpretation of the ^{13}C (proton decoupled) NMR spectrum of MTSC

δ_C in ppm	Multiplicity	Functional group
183.022	Singlet	C=S
39.498	Multiplet	DMSO-d_6 (solvent)
30.476	Singlet	CH_3

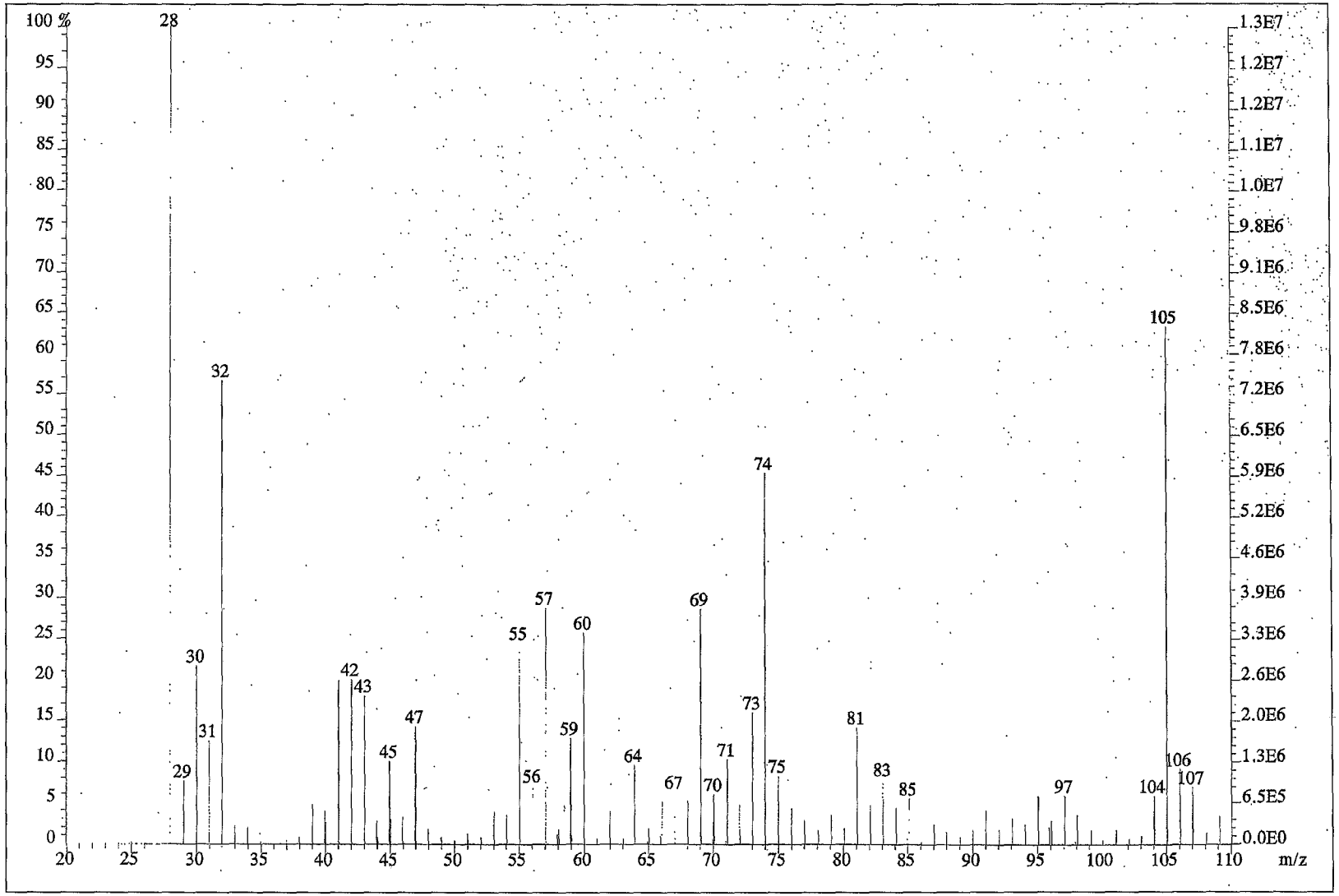

Figure 3.5: Mass spectrum of MTSC

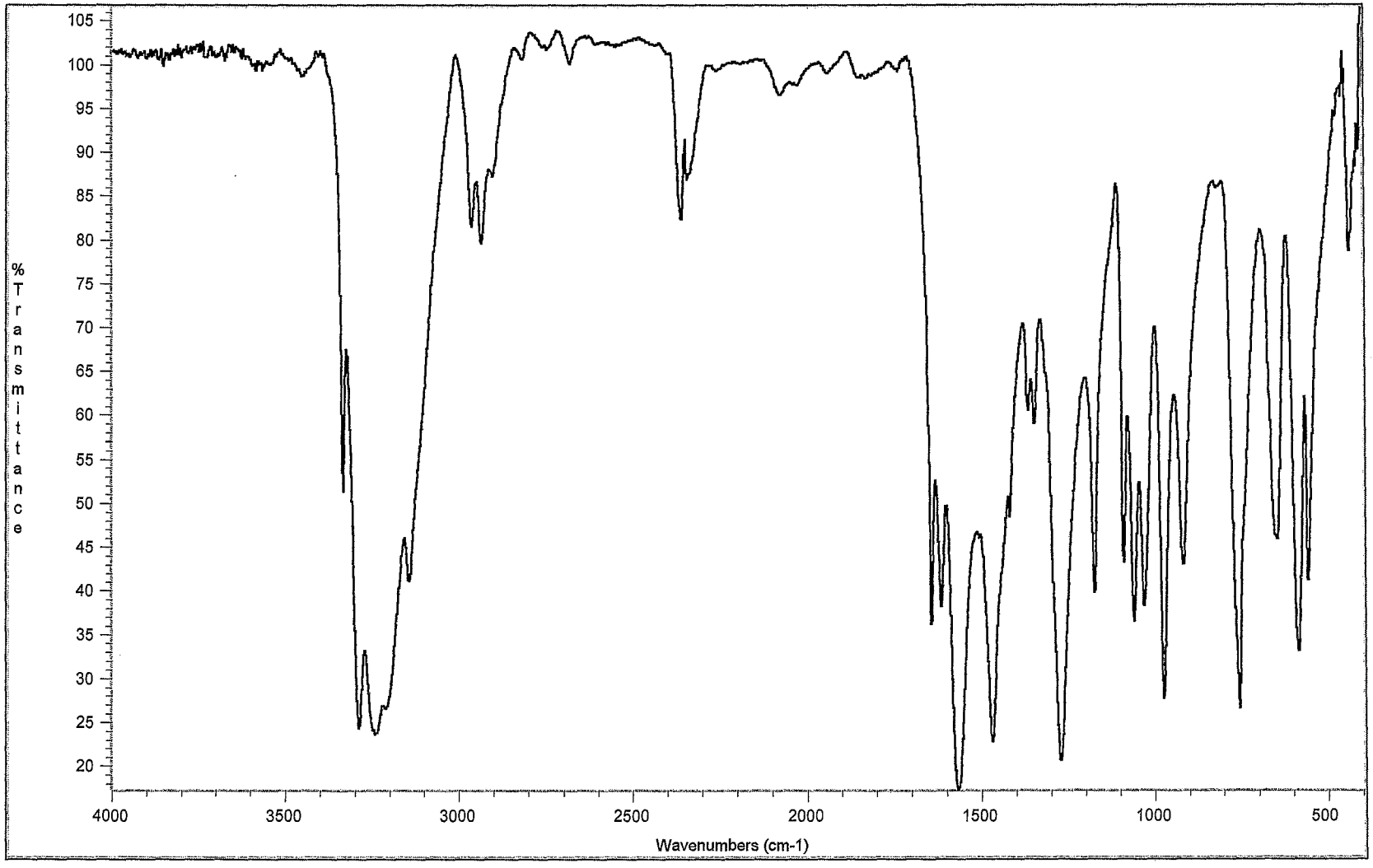

Figure 3.6: Infrared spectrum of MTSC

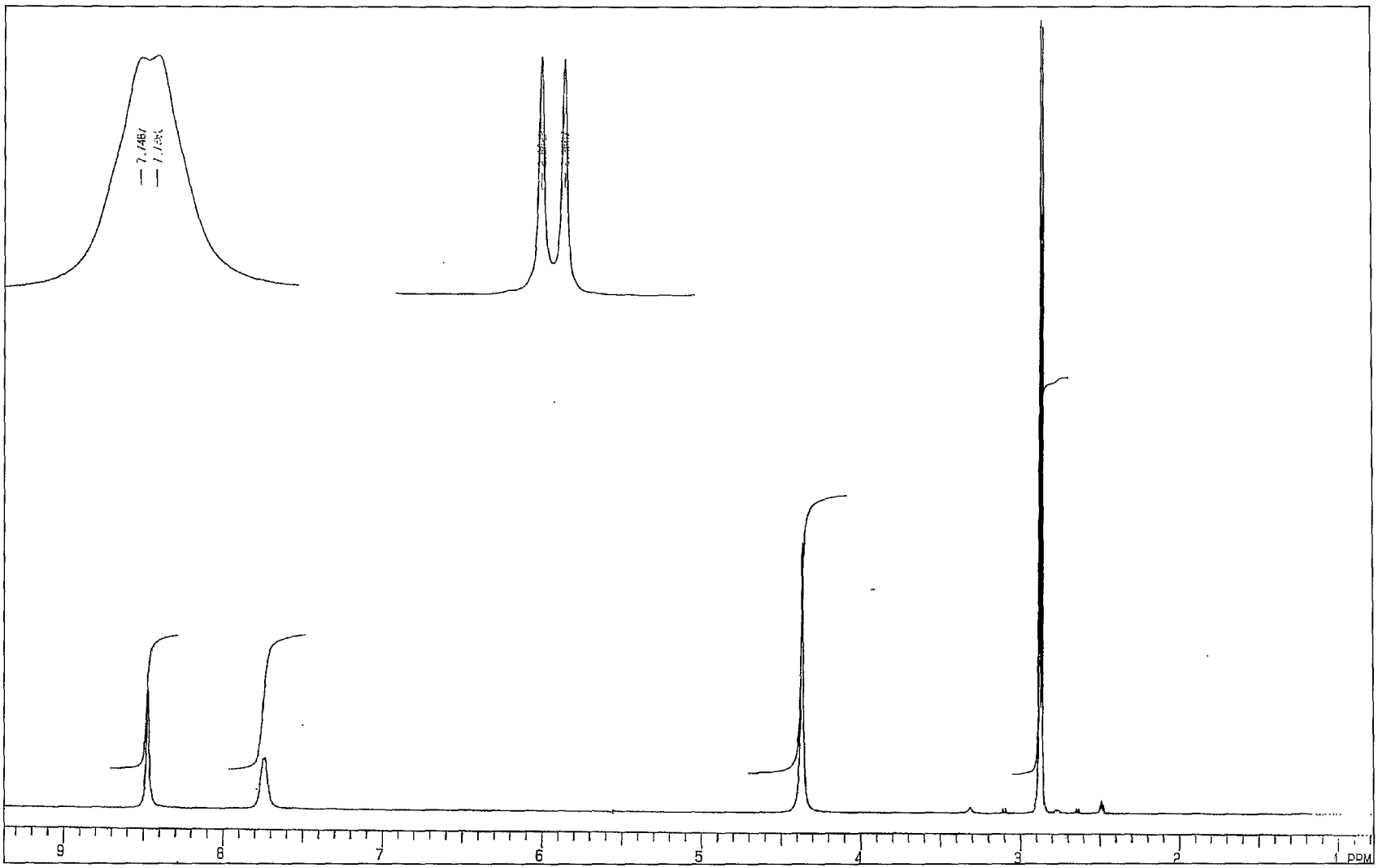

Figure 3.7: Proton NMR spectrum of MTSC

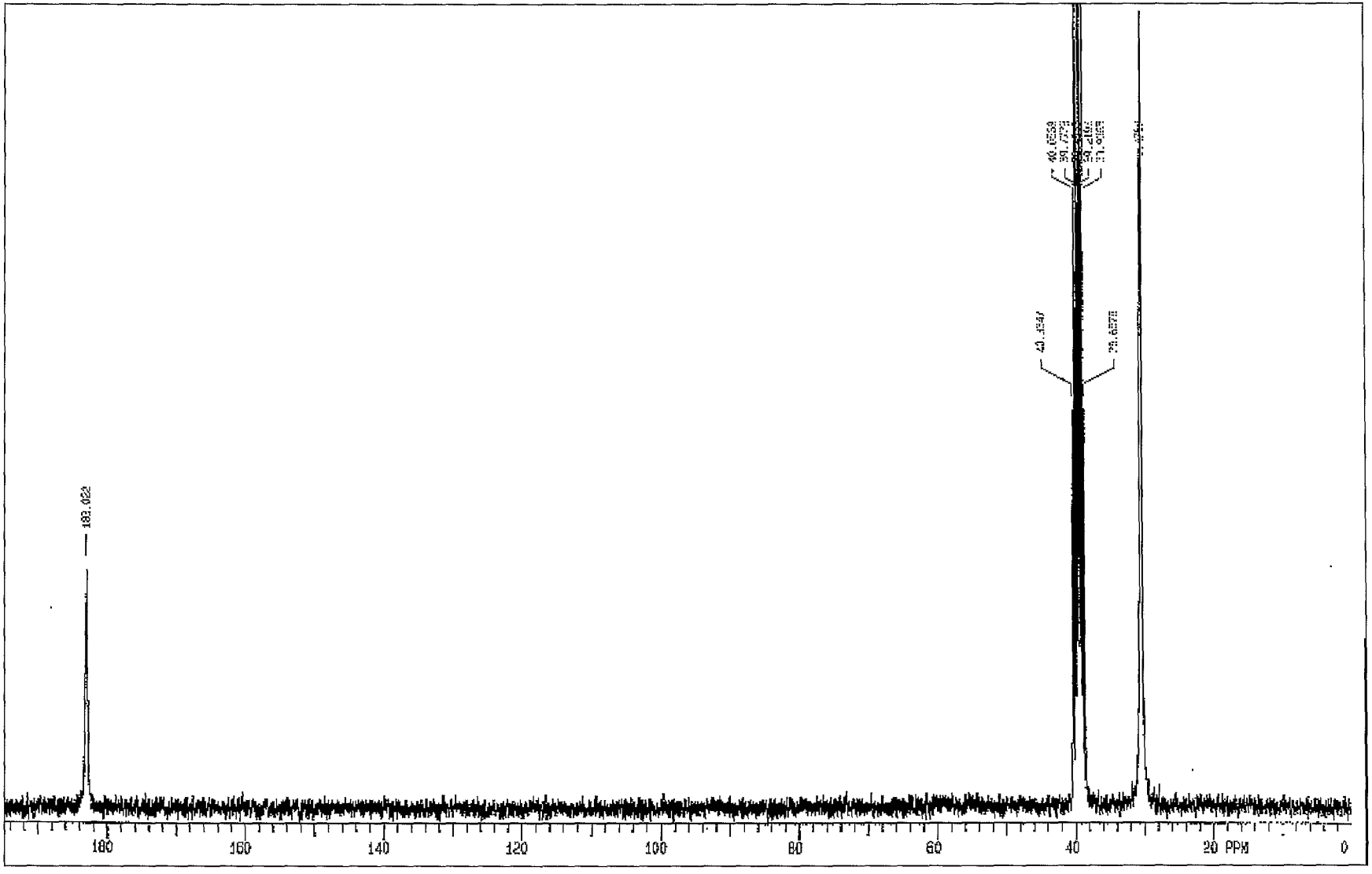

Figure 3.8: ^{13}C NMR spectrum of MTSC

CHAPTER 4.

The Synthesis of 4-Methyl-3-thiosemicarbazide (MTSC)

Experimental results and discussion

4.1 Objective

In the search for an alternative base to ammonium hydroxide, two tertiary amines namely triethylamine (TEA) and N,N-diisopropylethylamine (DIPEA) were identified as potential bases for the synthesis of the N-methyldithiocarbamate intermediate to MTSC.

The objective of this study is to compare TEA and DIPEA as bases for the synthesis of the N-methyldithiocarbamate intermediate with regard to MTSC yield and purity, waste volumes and quality, and eventual recovery of the base. Another objective is to minimize the formation of the by-product N,N'-dimethylthiourea (DMTU) during the synthesis of N,N-diisopropyl-ethylammonium N-methyldithiocarbamate (DIPEADTC). The stability of DIPEADTC at different temperatures also had to be determined to establish its stability after prolonged storage.

Another very important objective of this study is the optimization of the hydrazinolysis of DIPEADTC to MTSC with regards to MTSC yield and purity and the suppression of the formation of the by-product thiocarbohydrazide (TCH).

4.2 The synthesis of N,N-diisopropylethylammonium methyldithiocarbamate (DIPEADTC)

4.2.1 Evaluating the reaction time of the DIPEADTC formation step

Three solutions of DIPEADTC were prepared as described in §3.2.1. After CS_2 addition the three reaction mixtures were stirred for 2½ h, 3h and 13h respectively. Hydrazine hydrate (1.2 mole equivalents) was added to each reaction mixture and the hydrazinolysis reactions were completed as described in § 3.2.2.

TABLE 4.1: Reaction time for the synthesis of the dithiocarbamate

Time (h)	MTSC yield (%)
2.5	78
3	83
Overnight (13h)	86

The preferred reaction time for the synthesis of DIPEADTC was determined to be three hours. More favourable MTSC yields were obtained by extending the reaction times, but such extended reaction times are not feasible on plant scale.

4.2.2 Evaluation of the order of reagent addition during the DIPEADTC formation step

The reason for this investigation was to minimize the formation of the byproduct N,N'-dimethylthiourea (DMTU). The following addition options were investigated:

a. CS_2 (1 mole) was added to methylamine (1 mole), and then DIPEA (1.05 moles) was added.
b. methylamine (1 mole) was added to a mixture of DIPEA (1.05 moles) and CS_2 (1 mole).
c. CS_2 (1 mole) was added to a mixture of DIPEA (1.05 moles) and methylamine (1 mole).

During all the reactions the temperature was kept below 30°C. The results are summarized in Table 4.2.

TABLE 4.2: Summary of results - order of reagent addition during the DIPEADTC formation step

Addition option	Reaction time*	DIPEADTC yield (%)	%DMTU
a	2.75h	93.0	0.866
b	4.5h	93.0	0.516
c	3.5h	93.0	0.322

* Reaction time after reagent addition.

To minimize the formation of DMTU it is preferred to add CS_2 to a mixture of methylamine and DIPEA. The use of stoichiometric amounts of methylamine and CS_2 lowers the DMTU formation to less than 1% in all three options.

4.2.3 Stability of the DIPEADTC salt

In order to determine the stability of the DIPEADTC mixture on storage after preparation, its stability at different temperatures had to be measured.

4.2.3.1 Stability of solid DIPEADTC salt

A sample of solid DIPEADTC was prepared as described in § 3.2.1, without the addition of water/distillate, to yield a suspension of DIPEADTC crystals in

water. The suspension was cooled to 5°C, filtered, and washed with cold ethanol. The crystals were dried overnight (±13h) at room temperature under vacuum. The N-methyldithiocarbamate anion (DTC^-) concentration was determined using the UV analytical method described in §3.3.2. The sample was analyzed twice a week for three weeks. It was observed that the sample decomposed at a rate of 1.03% per day.

4.2.3.2 Stability of the DIPEADTC salt solution diluted with water

A sample of DIPEADTC was prepared, and diluted with water to a solution with an N-methyldithiocarbamate anion concentration of 25-26% (w/w). This solution was divided into five equal portions. Two of the portions were kept at room temperature - one in contact with sunlight, and the other one in the cupboard, in the dark. The other three portions were kept in reactors equipped with reflux condensers and heated to 50, 70, and 90°C, respectively. The following results were obtained:

TABLE 4.3: Stability of the DIPEADTC salt solution

Temperature (°C)	Time (hours)	Rate of decomposition (%/h)
25 (light)	360	0.007
25 (cupboard)	360	0.005
50	77	0.252
70	24	0.973
90	24	1.350

From the results in Table 4.3 it is evident that significant decomposition of the DIPEADTC solution occurred at 70°C and at 90°C, while the DIPEADTC solution may be stored at room temperature for one week without any significant decomposition.

4.2.3.3 Stability of the DIPEADTC salt solution diluted with distillate

A sample of DIPEADTC was prepared as before, and diluted with distillate of a previous experiment to a solution of 25-26% (w/w) N-methyldithiocarbamate anion concentration. This solution was kept at 70°C for 25.5h. The decomposition of the DIPEADTC and the formation of DMTU were monitored. The results are summarized in Table 4.4 and Figure 4.1.

TABLE 4.4: Stability of DIPEADTC solution diluted with distillate at 70°C

Time (h)	% DTC-	% DMTU	CS_2 Accountability
0	28.079	0.025	1
0.5	28.444	0.021	1.01
2	27.936	0.021	0.99
3	28.351	0.028	1.01
4	27.934	0.028	0.99
23.5	26.412	0.103	0.94
24.5	26.824	0.11	0.96
25.5	26.797	0.114	0.96

The rate of decomposition of DIPEADTC in distillate at 70°C was determined as 0.179 %/h. It is five times more stable than DIPEADTC diluted with water. The DIPEADTC is thus much more stable at 70°C when diluted with distillate. The rate of formation of DMTU during the decomposition of the DIPEADTC solution diluted with distillate at 70°C was determined to be 0.035 %/h.

The CS_2 accountability after 25.5 h at 70°C was only 96%. This may be explained by the decomposition of the DIPEADTC to methylamine, DIPEA and CS_2 and the subsequent loss of CS_2 to the atmosphere due to its low boiling point (46°C).

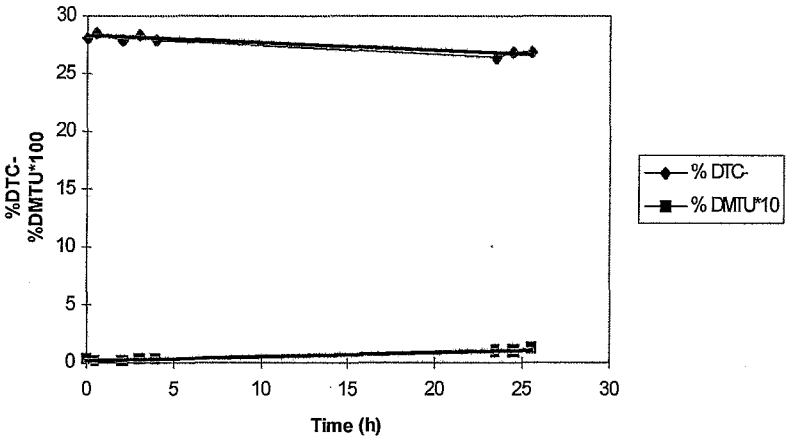

Figure 4.1: Stability of DIPEADTC diluted with distillate at 70°C

Another sample of DIPEADTC was prepared, and diluted with distillate to a solution of 25-26% (w/w) N-methyldithiocarbamate anion concentration. This solution was kept at 25°C for 6 weeks. The decomposition of the DIPEADTC was monitored as usual, and it was observed that the solution remained stable for the entire period.

This increased stability of the DIPEADTC salt solution when diluted with distillate could be contributed to the presence of DIPEA in the distillate (see §4.5). The reaction of CS_2 with DIPEA and methylamine is an equilibrium reaction (equation 4.1). The increased excess of DIPEA in the reaction mixture forces the reaction to the right hand side of the equilibrium, therefore favouring DIPEADTC formation.

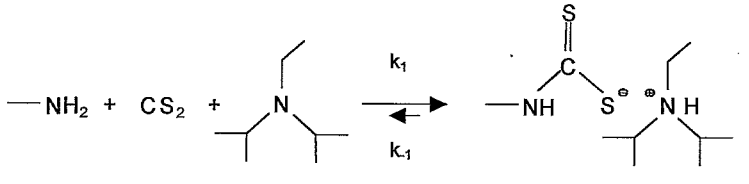

(4.1)

4.2.4 Kinetic evaluation of the DIPEADTC formation

Methylamine (2.75 moles of a 45% solution) and DIPEA (2.63 moles) were charged to a 1.5 L reactor. CS_2 (2.5 moles) was added over a period of 30 minutes while stirring. The temperature was controlled at 28°C with external cooling. The reaction mixture was analyzed for N-methyldithiocarbamate anion concentration at regular intervals. The results are summarized in Table 4.5 and Figure 4.2.

TABLE 4.5: Progress of the DIPEADTC reaction at 28°C

Time (min)	Moles DIPEADTC	$\ln(f_\infty - f_t)$
0	0.000	0.41
15	0.630	-0.14
30	0.959	-0.61
45	1.099	-0.91
60	1.217	-1.26
75	1.275	-1.49
120	1.361	-1.98
140	1.358	-1.95
160	1.357	-1.94

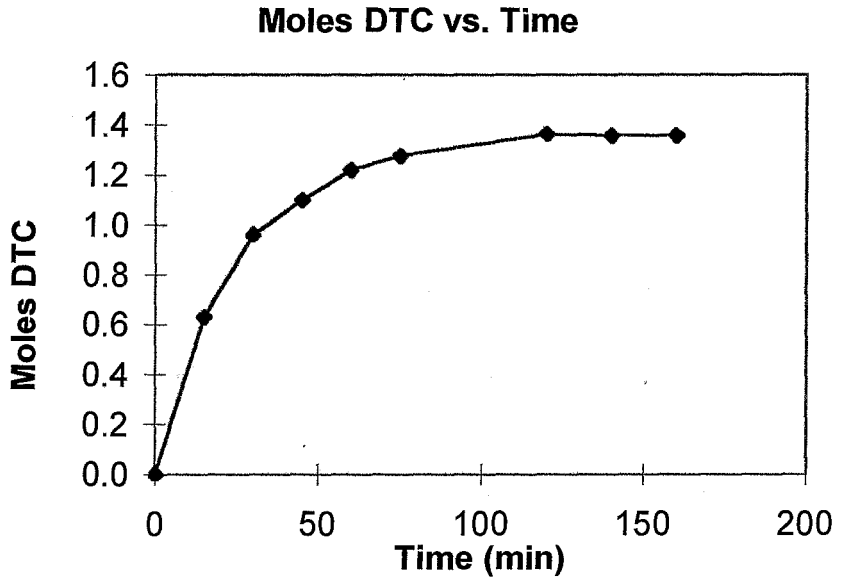

Figure 4.2: Plot of DIPEADTC formation over time at 28°C

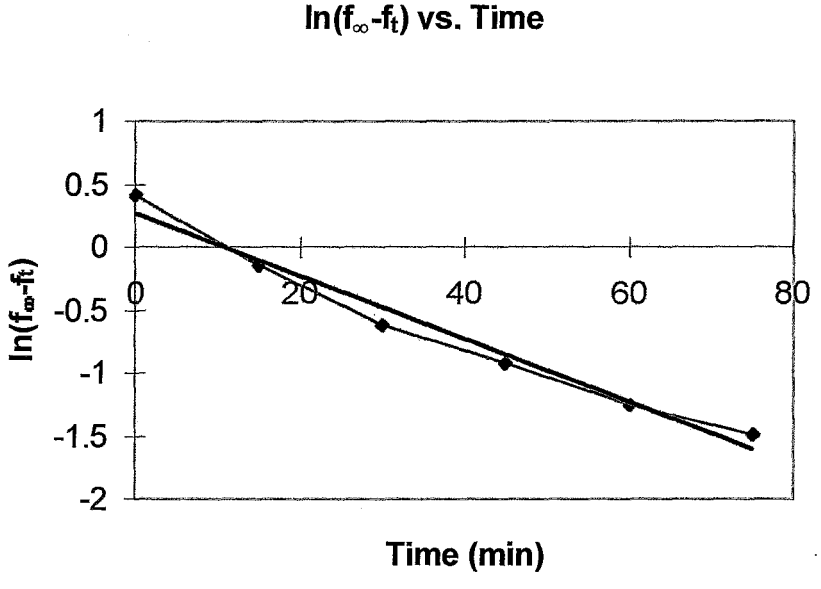

Figure 4.3: Plot of $\ln(f_\infty - f_t)$ vs. Time at 28°C

$\mathrm{Ln}(f_\infty - f_t)$ versus time was plotted (Figure 4.3) and a straight line with a slope of -0.025039 was obtained. The correlation coefficient of this line was

0.989033. The formation of DIPEADTC fits a first order model well. The slope of the straight line gives the value of $-k_{obs}$.

Thus, $k_{obs1} = 0.025039$.

The process was repeated at 22°C, and the results are summarized in Table 4.6 and Figure 4.4.

TABLE 4.6: Progress of the DIPEADTC reaction at 22°C

Time (min)	DIPEADTC moles	$Ln(f_\infty - f_t)$
0	0.000	0.41
30	0.799	-0.35
45	1.059	-0.82
70	1.291	-1.57
105	1.434	-2.72
135	1.467	-3.40
175	1.466	-3.40
195	1.466	-3.38

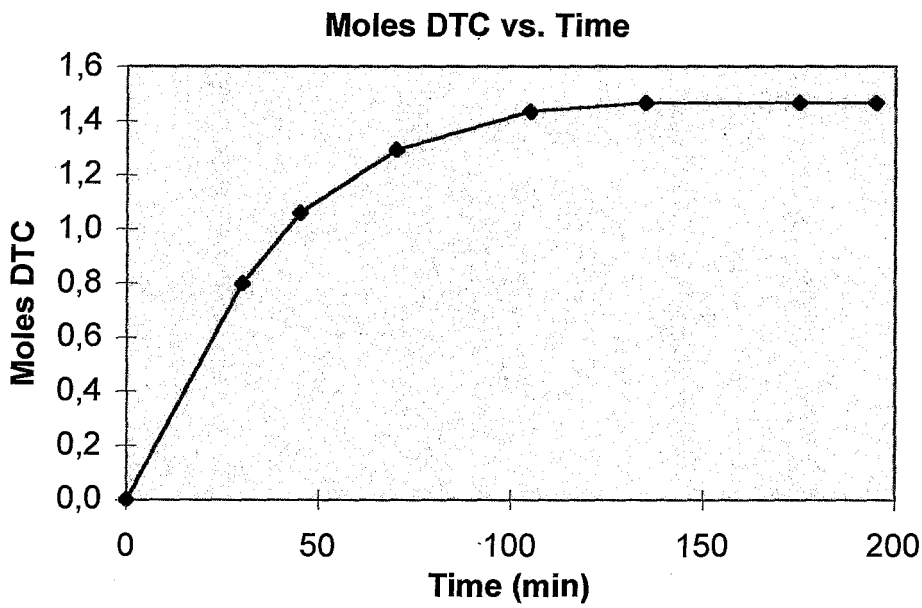

Figure 4.4: Plot of DIPEADTC formation over time at 22°C

Ln(f_∞-f_t) versus time was plotted (Figure 4.5) and a straight line with a slope of -0.029048 was obtained. The correlation coefficient of this line was 0.998644. The value of *k* was determined as:

$$k_{obs2} = 0.029048$$

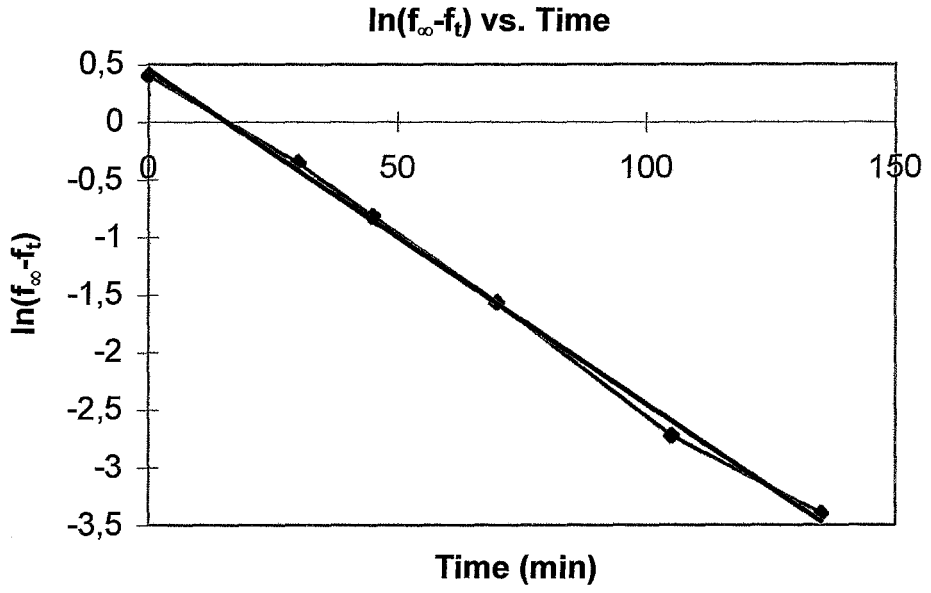

Figure 4.5: Plot of ln(f_∞-f_t) vs. Time at 22°C

For reaction (4.1) the following equation applies:

$$k_{obs} = k_1 - k_{-1} \qquad [4.1]$$

Using the Arrhenius equation [44], the activation energy, E_a, and the pre-exponential factor, *A*, could be calculated.

$$k_{obs} = Ae^{-E_a/RT} \qquad [4.2]$$

where R = 8.314 J K^{-1} mol^{-1}, and

T is the temperature in K

From the relationship k_{obs1}/k_{obs2}, using equation [4.2], the activation energy may be calculated as:

$$E_a = R\ln(\frac{k_{obs1}}{k_{obs2}})\left[\frac{T_1T_2}{T_1 - T_2}\right] \qquad [4.3]$$

$$= -18.273 \text{ kJ mol}^{-1}$$

Substituting this value into equation [4.2] for either k_1 or k_2, gives:

$$A = 1.688 \times 10^{-5}$$

4.3 Hydrazinolysis of DIPEADTC to MTSC

4.3.1 Evaluation of the order of reagent addition during the hydrazinolysis of DIPEADTC to MTSC

The reasons for this investigation were to maximize the yield of MTSC, and to minimize the formation of thiocarbohydrazide (TCH). Another important reason for this investigation was to ensure control over the H_2S release from the reaction to the scrubber system.

The DIPEADTC solution was prepared by the addition of 1.5 moles of CS_2 to a mixture of 1.5 moles of methylamine and 1.6 moles of DIPEA while stirring and controlling the temperature below 25°C. After CS_2 addition, the mixture was stirred for a further 3 hours.

The following combinations of reagent addition for hydrazine were investigated:

a. The DIPEADTC mixture was preheated to 75°C and 1.8 moles of hydrazine hydrate, which was pre-heated to 90°C, was added dropwise to the DIPEADTC mixture during 1h.

b. Hydrazine hydrate (1.8 moles) was heated to 90°C and the DIPEADTC mixture at 25°C was added dropwise during 1-2h.

c. Hydrazine hydrate (1.8 moles) was added all at once to the DIPEADTC mixture at 25°C and the mixture was then heated to 86°C.

d. 20-25% of both the DIPEADTC mixture and the hydrazine hydrate were charged to the reactor, and heated to 86°C. The remaining reagents were then added simultaneously to the reaction mixture during 1.5 hours.

The results of the investigation are summarized in Table 4.7.

Addition option (a) gave a lower yield of MTSC than the other three options. This was due to the decomposition of the DIPEADTC at 75°C.

There was no significant difference in the yield of MTSC between options (b) and (c), but the main difference was the contribution of TCH. Option (b) yielded a product with a TCH content of more than 5%, while option (c) yielded a product containing less than 3% TCH.

TABLE 4.7: Summary of results - order of reagent addition during the hydrazinolysis of DIPEADTC to MTSC

Addition option	MTSC yield (%)	%MTSC	%TCH	%DMTU
a	66.4	94.1	5.16	0.71
a	63.4	95.5	3.6	0.92
b	77.1	93.7	5.87	0.47
b	77.7	93.6	5.7	0.73
c	80.1	96.4	2.68	0.90
c	79.6	96.1	2.83	1.06
c	75.6	96.1	2.65	1.2
d	70.7	93.4	5.51	1.08
d	69.3	94.0	5.11	0.86
d	71.6	94.4	4.44	1.16

Options (b) and (d) would be ideal for controlling the H_2S release, but the TCH content from these two operations is higher. The purity of MTSC is very important to produce BTDA of high purity. For this reason options (b) and (d) were found to be less preferable.

The best option for preparing MTSC, from a purity point of view, is thus option (c).

4.3.2 Effect of hydrazine hydrate on the formation of TCH

An excess of 20% hydrazine hydrate was used in the laboratory synthesis of MTSC. This resulted in a TCH content of 3-5% in the final product. To determine the effect of the hydrazine hydrate mole ratio on the formation of TCH in the final product, six laboratory experiments were done - three of them with a hydrazine hydrate excess of 10%, and three with no excess at all. The results are summarized in Table 4.8.

There was no difference in the yield of MTSC when using either a 10% or no excess of hydrazine hydrate. However, the TCH contributions vary considerably in the various MTSC samples. The TCH content in MTSC could be reduced to almost 1% when using no excess of hydrazine hydrate.

TABLE 4.8: Effect of hydrazine hydrate mole ratio

	1	2	3	4	5	6
Excess hydrazine	10%	10%	10%	0%	0%	0%
Reaction time	2.5h	2.75h	2.75h	3h	3h	3.25h
DIPEA recovered	99.8%	99.3%	98.8%	98.8%	98.3%	98.5%
MTSC yield (%)	80	79	78	79	79	78
MTSC purity (%)	94.2	95.0	95.2	94.5	95.6	92.1
%TCH	4.60	4.36	4.07	3.16	1.08	1.42
%DMTU	1.08	1.29	1.43	2.34	3.36	6.45

4.3.3 Stability of MTSC in different media

The purpose of this study was to determine the stability of MTSC in water, filtrate, water in the presence of 20% excess hydrazine hydrate, and filtrate in the presence of 20% excess hydrazine hydrate. The experiments of MTSC in the presence of 20% excess hydrazine hydrate were done to confirm that TCH is formed by the reaction of free CS_2 and hydrazine hydrate, and not by the reaction of MTSC with hydrazine hydrate.

4.3.3.1 Stability of MTSC in water at 92°C

MTSC (100g) of known purity was added to 150g of water and heated to 92°C for 5h. The mass of recovered solids was 91.9g. It was analyzed, together with the filtrate, to determine the MTSC, DMTU, and TCH content. The results are summarized in Tables 4.9 and 4.10.

TABLE 4.9: Results – stability and distribution of MTSC in water at 92°C

Mass recovered (g)			Mass in filtrate (g)			Total (g)
MTSC	TCH	DMTU	MTSC	TCH	DMTU	
88.10	3.68	0.10	6.63	1.60	0.22	100.33

These results were compared to the composition of the sample before the stability test was conducted.

TABLE 4.10: Comparison – stability and distribution of MTSC in water at 92°C

	MTSC (g)	TCH (g)	DMTU (g)	Total (g)
Before	94.49	5.13	0.38	100.00
After	94.73	5.28	0.32	100.33

No significant changes in the composition of the MTSC were found. Thus, MTSC remains stable in water at 92°C for 5h.

4.3.3.2 Stability of MTSC in filtrate at 92°C

MTSC (100g) of known purity was added to 150g of filtrate with known composition, and heated to 92°C for 5h. The recovered product was analyzed together with the filtrate. The results are summarized in Tables 4.11 and 4.12.

TABLE 4.11: Results – stability and distribution of MTSC in filtrate at 92°C

Mass recovered (g)			Mass in filtrate (g)			Total (g)
MTSC	TCH	DMTU	MTSC	TCH	DMTU	
92.15	3.84	0.21	1.93	1.08	0.42	99.64

TABLE 4.12: Comparison – stability and distribution of MTSC in filtrate at 92°C

	MTSC (g)	TCH (g)	DMTU (g)	Total (g)
Before	94.28	5.02	0.70	100.00
After	94.08	4.92	0.64	99.64

All solids were accounted for. There was no significant difference in the composition of the sample after the stability test was completed. MTSC remained stable at 92°C in the filtrate for 5h.

4.3.3.3 Stability of MTSC in water in the presence of 20% excess hydrazine hydrate at 92°C

MTSC (105g) of known purity was added to a mixture of 140g of water and 10g of hydrazine hydrate and heated to 92°C for 5h. The recovered solids as well as the filtrate were analyzed. The results are summarized in Tables 4.13 and 4.14.

TABLE 4.13: Results – stability and distribution of MTSC in water and hydrazine hydrate at 92°C

Mass recovered (g)			Mass in filtrate (g)			Total
MTSC	TCH	DMTU	MTSC	TCH	DMTU	
90.78	2.42	1.36	7.63	1.36	0.91	104.50

TABLE 4.14: Comparison – stability and distribution of MTSC in water and hydrazine hydrate at 92°C

	MTSC (g)	TCH (g)	DMTU (g)	Total (g)
Before	98.81	3.78	2.31	104.90
After	98.41	3.82	2.27	104.50

There was no increase in TCH contents during 5h. It can thus be concluded that MTSC is stable in water and 20% excess hydrazine hydrate for 5h at 92°C. TCH is thus not formed by the reaction of MTSC and hydrazine hydrate.

4.3.3.4 Stability of MTSC in filtrate and 20% excess hydrazine hydrate at 92°C

MTSC (105g) of known purity was added to a mixture of 140g of filtrate and 10g of hydrazine hydrate and kept at 92°C for 4h. The results are summarized in Table 4.15 and Figure 4.6.

TABLE 4.15: Progress of the reaction of MTSC with filtrate and hydrazine hydrate at 92°C

Time (min)	Moles MTSC	Moles TCH	Moles DMTU	Total moles
0	0.941	0.046	0.012	1.000
30	0.934	0.048	0.013	0.995
75	0.962	0.057	0.017	1.037
105	0.960	0.057	0.019	1.036
135	0.967	0.057	0.020	1.044
150	0.953	0.057	0.020	1.030
195	0.955	0.055	0.024	1.034
225	0.943	0.052	0.025	1.020

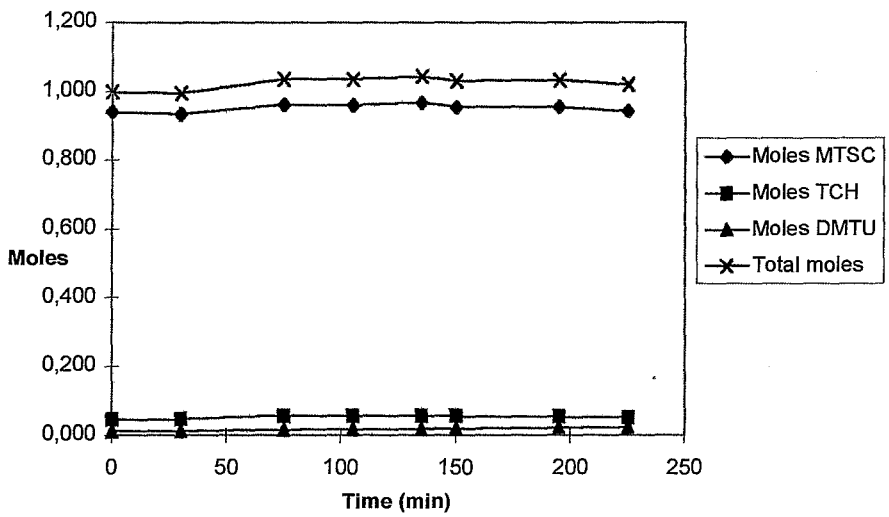

Figure 4.6: Reaction progress of MTSC in filtrate and hydrazine

The difference in total moles may be contributed to the unreacted DIPEADTC in the filtrate before the experiment was conducted. The DIPEADTC content of the filtrate before the experiment was 0.083 mole. From these results it could be concluded that MTSC remains stable in the filtrate in the presence of 20% excess hydrazine hydrate at 92°C. It is again evident that TCH is not formed by the reaction of MTSC with hydrazine hydrate.

4.3.4 Progress of the hydrazinolysis of DIPEADTC to MTSC.

The objective of this investigation was to monitor the hydrazinolysis reaction in terms of the consumption of DIPEADTC and the subsequent formation of MTSC, TCH, and DMTU. This information was also used to account for CS_2 usage and losses during the hydrazinolysis of DIPEADTC to MTSC.

CS_2 (1.5 moles) was added to a mixture of methylamine (1.5 moles) and DIPEA (1.575 moles) while keeping the temperature below 30°C. The mixture was then stirred overnight (13h). Hydrazine hydrate (1.575 moles) was added to the DIPEADTC mixture. The mixture was heated to 86°C. The reaction mixture was sampled every 20 min and analyzed for %DTC^-, %MTSC, %TCH, and %DMTU. The results are summarized in Table 4.16 and Figure 4.7.

TABLE 4.16: Progress of the hydrazinolysis of DIPEADTC to MTSC.

Time (min)	Moles DTC^-	Moles MTSC	Moles TCH	Moles DMTU	Total moles of product (MTSC+TCH+DMTU)	Total moles
0	1.430	0.024	0.000	0.007	0.031	1.460
20	1.102	0.320	0.003	0.007	0.330	1.431
40	0.847	0.550	0.008	0.007	0.565	1.411
60	0.674	0.717	0.013	0.008	0.739	1.413
80	0.483	0.899	0.023	0.010	0.931	1.414
100	0.340	1.013	0.031	0.011	1.056	1.397
120	0.235	1.116	0.044	0.013	1.173	1.407
140	0.176	1.171	0.054	0.016	1.241	1.417
180	0.137	1.183	0.062	0.022	1.267	1.404
200	0.109	1.181	0.061	0.024	1.266	1.375
260	0.103	1.211	0.057	0.032	1.301	1.404

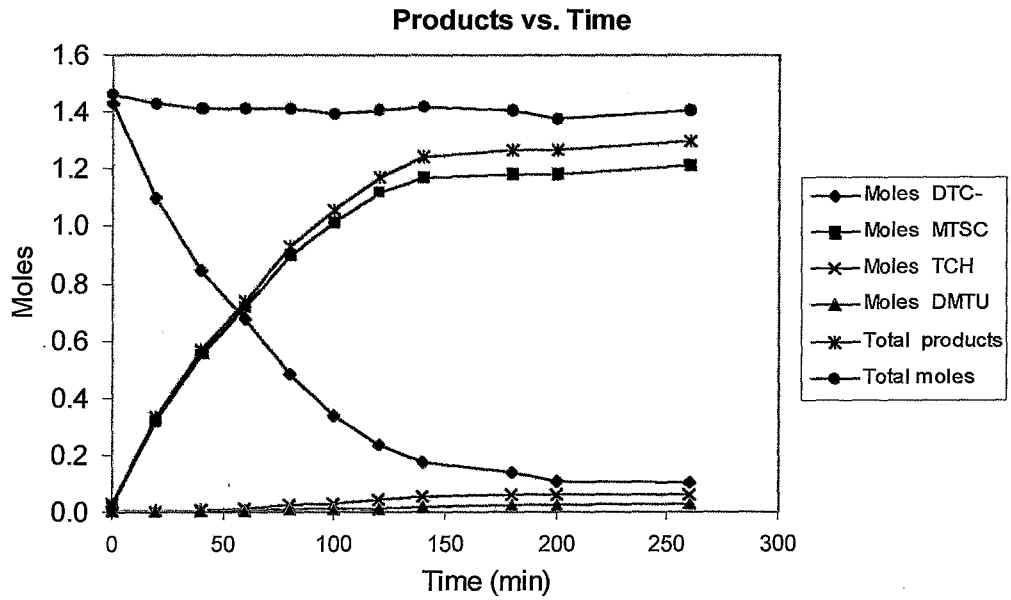

Figure 4.7: Reaction progress of the hydrazinolysis of DIPEADTC to MTSC

It is evident that some CS_2 is lost during the hydrazinolysis of DIPEADTC to MTSC. Only 93% of the CS_2 is accounted for. The loss of CS_2 is due to the thermal decomposition of DIPEADTC to methylamine, DIPEA and CS_2. Because of its low boiling point CS_2 is then lost to the atmosphere. Figure 4.7 describes the reaction progress of the hydrazinolysis reaction. Evidence of the decomposition of DIPEADTC can be seen after 180 – 200 min reaction time.

4.4 Comparing DIPEA and TEA as alternatives to NH_4OH as base for the synthesis of the N-methyldithiocarbamate intermediate

Triethylamine (TEA) and N,N-diisopropylethylamine (DIPEA) were compared to NH_4OH as alternative bases for the synthesis of the N-methyldithiocarbamate intermediate with regards to MTSC yield, purity, and effluent profiles. These comparisons are summarized in Tables 4.17 and 4.18.

TABLE 4.17: Comparing experimental results employing NH_4OH, TEA, and DIPEA as bases

	NH_4OH	**TEA**	**DIPEA**
MTSC yield (%)	65-70	78-80	78-80
Purity (%)	93-94	93-95	96-98
Base recovery (%)	-	90	99
Mass of effluent (kg/kg)	3.5	1.3	1.1

Both methods employing TEA and DIPEA as base, produced approximately three and half times less effluent than the NH_4OH method on laboratory scale. This implies that both methods would be more cost effective with regards to waste disposal.

TABLE 4.18: Effluent analysis of NH_4OH-, TEA-, and DIPEA-based methods

	NH_4OH	**TEA**	**DIPEA**
Total S	12 % (w/w)	8-11 % (w/w)	7-9 % (w/w)
Total S^{2-}	2000 ppm	5000 ppm	3000 ppm
Chemical oxygen demand (COD)	150 000 ppm	240 000 ppm	240 000 ppm
Total dissolved solids (TDS)	12	20	16

The effluent generated, employing both the TEA- and DIPEA-based methods, had higher COD levels than those of the NH_4OH-based method. The reason for this is that the effluent being formed during the TEA- and DIPEA-based methods is much more concentrated than that of the NH_4OH method.

4.5 The effect of recycling of the distillate on the recovery of DIPEA

DIPEA is recovered from the reaction mixture using azeotropic distillation during the hydrazinolysis step. The azeotrope separates with cooling into two layers. The organic layer (upper layer) is DIPEA of 98% purity and the aqueous layer or distillate contains 10% DIPEA. Because the solubility of DIPEA in water is only 0.39% (w/w), it is predicted that DIPEA may be present in the distillate as a salt formed by the reaction of DIPEA and H_2S (equation 4.2).

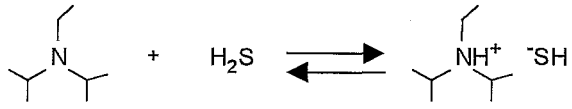

(4.2)

This hypothesis was evaluated by preparing a mixture of 200 mL water and 200mL DIPEA, resulting in a mixture containing two layers of equal volume (the upper layer being DIPEA). Gaseous H_2S was then purged through this mixture. During this procedure the total volume of the mixture remained the same. However, the volume of the aqueous layer increased to 280 mL, while the volume of the DIPEA layer decreased to 120 mL. The two layers were then separated and the DIPEA layer was analyzed and found to contain 99.6% DIPEA. Sodium hydroxide (0.6 moles, 25% solution) was added to the aqueous layer, resulting in the formation of a DIPEA layer of 80 mL. From this result it can be concluded that DIPEA does react with H_2S to form a water soluble salt.

By recycling the distillate to the DIPEADTC formation step, other than discarding it along with the effluent, may result in the reduction of process effluent. It is also believed that the recycling of the distillate to the DIPEADTC formation reaction may enhance the recovery of DIPEA during the hydrazinolysis of DIPEADTC to MTSC. The reason for this is that recycling of

the distillate will decrease the losses of DIPEA due to the reaction of DIPEA with H_2S, and the high solubility in water of the subsequent salt.

TABLE 4.19: Recycling of distillate to DIPEADTC formation step.

	MTSC yield (%)	MTSC purity (%)	DIPEA recovery (%)
Without recycle	80.7	95.2	91
With recycle	79.6	96.2	99

From the results in Table 4.19 it is evident that there was no significant difference in isolated yield or purity of MTSC when recycling the overhead aqueous phase. There was however a significant difference in the amount of DIPEA recovered during distillation. This proves that the recycling of the distillate does indeed enhance the recovery of DIPEA.

According to the effluent profiles of both the TEA- and DIPEA-based methods in Table 4.20, a gradual increase of chemical oxygen demand (COD), total dissolved solids (TDS) and total sulphur occurs in the effluent after recycling the distillate three times employing TEA as base. Using DIPEA however, no significant increases of COD, TDS or total sulphur were observed after three recycles.

The solubility of TEA in water is 5.5% (w/w) and it is highly toxic to fish and micro-organisms. This will result in excessive costs to dispose of the effluent. The solubility of DIPEA in water is only 0.39% (w/w). This proves once again that DIPEA is the prefered alternative to ammonium hydroxide as base for the preparation of the N-methyldithiocarbamate intermediate to MTSC.

TABLE 4.20: Effluent profiles of the TEA- and DIPEA-based methods after three recycles

TEA			
Type	**TDS**	**COD**	**Total S**
Fresh	11.9% (w/w)	165 000 ppm	7.2% (w/w)
Recycle #1	17.3% (w/w)	239 000 ppm	9.6% (w/w)
Recycle #2	19.4% (w/w)	255 000 ppm	9.6% (w/w)
Recycle #3	21.3% (w/w)	261 000 ppm	10.8% (w/w)
DIPEA			
Type	**TDS**	**COD**	**Total S**
Fresh	15.6% (w/w)	206 000 ppm	7.7% (w/w)
Recycle #1	16.8% (w/w)	238 000 ppm	8.9% (w/w)
Recycle #2	15.5% (w/w)	210 000 ppm	7.9% (w/w)
Recycle #3	15.6% (w/w)	205 000 ppm	8.0% (w/w)

4.6 Effluent treatment[45]

Approximately 2 kg of effluent is generated for each kilogram of MTSC employing DIPEA as base. This effluent has very high COD levels (240 000 ppm). In order for the effluent to be acceptable for disposal to a water treatment plant, the COD level must be reduced significantly. The treatment of MTSC effluent entails cooling it to 0°C for 4 days, filtering off the crystals (containing 83.3% MTSC) that formed and oxidizing the remaining filtrate with oxygen for five hours at 120°C and 7 bar pressure (Figure 4.8). Cooling and filtering the effluent reduces the COD level of the filtrate to 12200 ppm. The oxidation of the remaining filtrate resulted in a further reduction of the COD level to 4000 ppm.

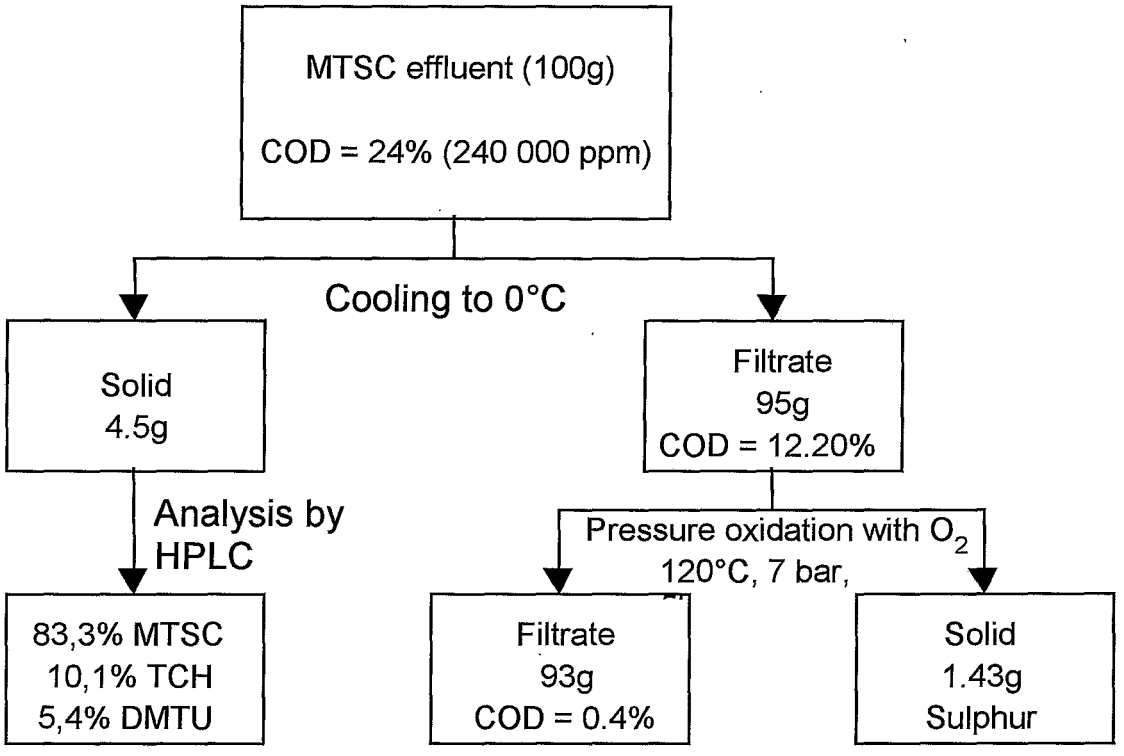

Figure 4.8: MTSC effluent treatment

4.7 Scale up to mini plant (50 L scale)

Six mini plant runs were executed to confirm the laboratory results on a larger scale. Another reason for these mini plant runs was to test the necessity of using a decanter to separate the distillate from the DIPEA before recycling both the DIPEA and distillate to the next run. In other words, could the distillate not be added to the reaction mixture together with the DIPEA instead of adding it after the CS_2 reaction was completed?

Another question that had to be addressed was that of the CS_2 addition being a simple titration. In other words, is the reaction completed immediately after the addition of CS_2? The results from these six mini plant runs are summarized in Table 4.21.

TABLE 4.21: Summary of mini plant results

	MP1 (start-up)	MP2	MP3	MP4	MP5	MP6
Reaction time after CS_2 addition	0,5 h	0,5 h	overnight (13h)	overnight (13h)	3h	3h
Order of addition of overhead water.	-	Before CS_2	Before CS_2	After CS_2	After CS_2	After CS_2
% Recovery of DIPEA	87.3	100.0	93.3	90.1	100.0	96.0
% Crude MTSC yield	65.5	53.6	78.3	80.1	79.6	75.6
% Purity	80.3	76.4	93.0	96.4	96.1	96.1
% TCH	18.7	22.6	4.28	2.68	2.83	2.65
% DMTU	0.96	0.92	0.87	0.90	1.06	1.20

From runs 1, 2, and 3 it could be concluded that the addition of CS_2 was not a simple titration. From runs 1 and 2 it was evident that the CS_2 reaction was incomplete. The high TCH content in runs 1 and 2 resulted from unreacted CS_2, in the dithiocarbamate formation step, which reacted with hydrazine hydrate during the hydrazinolysis of the DIPEADTC to MTSC.

The TCH content of run 4 was significantly lower than that of run 3. This implied the importance of a decanter for separating the distillate from the recovered DIPEA before recycling the DIPEA to the next batch. The H_2S in the distillate consumed CS_2 to form the salt of trithiocarbonic acid,[15] thus acting as a CS_2 carrier during the DIPEADTC formation step. This resulted in increased levels of TCH in the final product.

The results obtained from runs 5 and 6 proved that the laboratory results could be reproduced successfully in the mini plant.

4.8 Optimization of the hydrazinolysis of DIPEADTC to MTSC

The next step in the study of the synthesis of MTSC using DIPEA as base, was the optimization of the hydrazinolysis of DIPEADTC to MTSC. This subject is discussed in detail in Chapter 5.

CHAPTER 5

Factorial Design of the Hydrazinolysis of DIPEADTC to MTSC

5.1 Introduction to experimental design

The classical research method of changing one variable at a time, gives important information but is inefficient. The one-variable-at-a-time method is seemingly successful and simple, but it is a poor strategy that will often lead to totally erroneous conclusions. This method can only be used if the variables are independent of each other. Unfortunately, in most cases the variables are independent only in the sense that they can be adjusted independently. When they exert their influence on a chemical system, the level of a variable may have an effect on the influences of other variables.

Statistical design can never substitute chemical reason or knowledge, but it can provide a chemist with useful tools to:[46]

- determine the significance of a factor on the outcome of an experiment,
- predict results in future experiments, and
- rapidly determine the optimum experimental conditions.

An advantage of statistically designed experiments is that relatively few experiments are needed to obtain the desired information.

A chemical synthesis can often be described as the functional relationship

Result = *f* (experimental conditions) [5.1]

This means that one or more measurable results are influenced by a number of experimental factors controlled by the experimenter.

There is a need to determine:

- how these factors influence the results, or
- which combination of the factor settings will give the best results.

5.2 Historical development of experimental design

The late Sir Ronald A. Fisher was the innovator in the use of statistical methods in experimental design in the early 1930's. He developed and first used the analysis of variance as the primary method of statistical analysis in experimental design. While Fisher was clearly the pioneer in this field, there have been many other significant contributors, including F. Yates, O. Kemthorne, W. G. Cochran, R. H. Meyers, J. S. Hunter , and G. E. P. Box, to name a few.[47]

Many of the early applications in experimental design methods were used in the biological and agricultural sciences. However, the first industrial applications of experimental design appeared in the1930's in the British textile and wool industries. After World War II, experimental design methods were introduced to the chemical and process industries in the United States and Western Europe.

In recent years there has been a revival of interest in experimental design, because of increased competitiveness in the industrial sector.

5.3 Sorting a few variables from many

Many variables may affect the outcome of a chemical analysis or synthesis. Some examples include time, temperature, concentration of reagents, order of reagent addition, pH, pressure, stirring rate, catalyst, solvent, sampling methods and operator performance. The chemist's knowledge and intuition may eliminate many of these variables, but a considerable number may remain, which may be sorted by means of normal probability plotting. [48], [49]

Three factors were identified for the factorial optimization of the hydrazinolysis of DIPEADTC to MTSC. They were the DTC^- concentration (factor A), the excess of hydrazine hydrate used to perform the reaction (factor B), and the time the reaction was kept at 70°C before the DIPEA was recovered (factor C). The reason for including factor C was to ensure that the H_2S formed during the reaction could be removed, for safety reasons, before removing the DIPEA.

5.4 The 2^3 factorial design of the hydrazinolysis of DIPEADTC to MTSC

In a factorial design, each factor (variable) is investigated at pre-determined fixed values. For example, in a two level factorial experiment, each factor is investigated at two values. For continuous variables (pH, temperature, concentration, etc.) one value will be a low value and one will be the high value, and for discrete variables (catalyst type, solvent type, etc.) the two values will represent two alternatives. A full factorial design will contain all the possible settings of the variables. A factorial design at two levels with k settings will require 2^k experiments. Each result obtained from the experiments in a factorial design is used in combination with the other results to determine the average response, all the main effects and all the interaction effects of the chosen variables.

5.4.1 Design and representation of the 2^3 factorial design

A full two level factorial design with three factors will require eight experimental runs. The levels of the three factors A, B, and C at their individual low and high settings are represented by (-1) and (+1) respectively. These are the coded values of the variables. [46] Figure 5.1 illustrates what the design looks like.

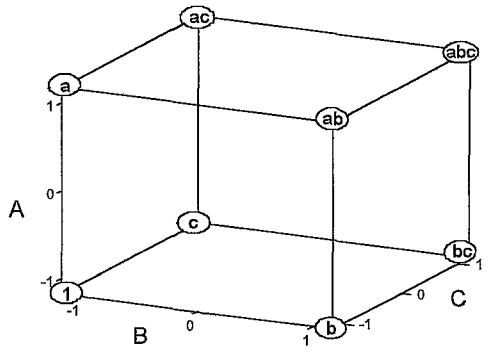

Figure 5.1: Cube plot of factors without the responses

The coded values for each factor were obtained by equation [5.2] and are summarized in Table 5.1.

$$\chi_i = \frac{(x_i - x_c)}{s_x} \qquad [5.2]$$

Where χ_i = coded value of variable x_i

x_i = natural value of variable x_i

x_c = natural value of x_i at the design centre

s_x = step size in x_i

TABLE 5.1: Coded values of factors

Factor	-1	0	1
A: DTC^- concentration	19%	22%	25%
B: Hydrazine hydrate excess	0%	10%	20%
C: Time @ 70°C	1h	1.75h	2.5h

The factorial design is represented in the form of a sign table as illustrated in Table 5.2. Before actually carrying out the experimental runs, it is important to determine a randomized sequence of runs. The statistical validity of a factorial design is dependent on randomization and the assumption that all the runs are carried out identically, except for the factor setting [50]. Three responses were identified for the optimization of the hydrazinolysis of DIPEADTC to MTSC. They were the isolated yield of MTSC based on CS_2, the purity of the MTSC, and the TCH contents of the MTSC.

TABLE 5.2: Design matrix for three factors at two levels

Run no.	A	B	C	Label	Responses		
					%Yield	%Purity	%TCH
1	-1	-1	-1	1	59.8	97.93	1.71
2	1	-1	-1	a	64.1	97.40	2.15
3	-1	1	-1	b	64.3	97.97	1.75
4	1	1	-1	ab	69.2	97.47	2.36
5	-1	-1	1	c	54.8	97.79	2.09
6	1	-1	1	ac	65.7	96.46	3.03
7	-1	1	1	bc	58.1	98.02	1.73
8	1	1	1	abc	66.3	95.64	4.12

5.4.2 Calculating the effects of the factors

In a 2^3 factorial design there are seven degrees of freedom. Three degrees of freedom are associated with the main effects of A, B, and C. Four degrees of

freedom are associated with the effect of the interactions AB, AC, BC, and ABC.

5.4.2.1 Main Effects

The main effect of A is calculated as the average of the four runs where A is at the high level ($\bar{y}_{A+}$) minus the average of the four runs where A is at the low level ($\bar{y}_{A-}$),[48] or

$$A = \bar{y}_{A+} - \bar{y}_{A-} \qquad [5.3]$$

Thus

$$Eff_A = \frac{a + ab + ac + abc}{4} - \frac{(1) + b + c + bc}{4} \qquad [5.4]$$

The effects of B and C are calculated in a similar fashion.

$$Eff_B = \frac{abc + ab + bc + b}{4} - \frac{ac + a + c + (1)}{4} \qquad [5.5]$$

and

$$Eff_C = \frac{abc + ac + bc + c}{4} - \frac{ab + a + b + (1)}{4} \qquad [5.6]$$

5.4.2.2 Interaction effects

The two-factor interaction effect of AB can be calculated as one half of the difference between the average A effect at the two levels of B.

Mathematically,[51]

B	Average A effect	
High (+)	$\frac{[(abc-bc)+(ab-b)]}{2}$	[5.7]
Low (-)	$\frac{[(ac-a)+(a-(1))]}{2}$	[5.8]
Difference	$\frac{[abc-bc+ab-b-ac+c-a+(1)]}{2}$	[5.9]

Since the effect of the AB interaction is one half of this difference,

$$Eff_{AB} = \frac{abc+ab+c+(1)}{4} - \frac{bc+b+ac+a}{4} \qquad [5.10]$$

Similarly, the effects of the AC and BC interactions are,

$$Eff_{AC} = \frac{abc+ac+b+(1)}{4} - \frac{ab+a+bc+c}{4} \qquad [5.11]$$

and

$$Eff_{BC} = \frac{abc+bc+a+(1)}{4} - \frac{ab+b+ac+c}{4} \qquad [5.12]$$

The effect of the ABC interaction is defined as the average difference between the AB interaction for the two different levels of C.[51] Thus,

$$Eff_{ABC} = \frac{abc+a+b+c}{4} - \frac{ab+ac+bc+(1)}{4} \qquad [5.13]$$

The effects of the factors are summarized in Table5.3.

TABLE 5.3: Summary of main and interaction effects

Source of Variance	Effect		
	Yield response	Purity response	TCH response
A	7.075	-1.185	1.095
B	3.375	-0.120	0.245
C	-3.125	-0.715	0.750
AB	-0.525	-0.255	0.405
AC	2.475	-0.670	0.570
BC	-1.425	-0.175	0.120
ABC	-0.825	-0.270	0.320

These effects can then be plotted on normal probability paper in order of increasing magnitude, from most negative to most positive. Effects that can be contributed to random error will essentially be plotted on a straight line. Those effects, which are not on the straight line, are significant and deserve further investigation.

In order to obtain a full design matrix for a 2^3 factorial design, an identity column, **I**, must be added. This column contains only (+1) elements. The full design matrix is given in Table 5.4.

5.4.3 Interpretation of effects

The value calculated for an effect does not indicate the significance of an effect. It is particularly difficult to determine if small effects are real or simply the result of random experimental error.

The most convenient method for determining the significance of factors is by means of a normal probability plot. However, the most reliable method for determining the significance of factors is by means of centre point replicates.

This method entails completing a number of experiments at the design centre to obtain an independent estimate of the experimental error variance.

Table 5.4 contains the full design matrix and responses of the factorial design of the hydrazinolysis reaction with six centre points.

TABLE 5.4: Design matrix with centre points

Run	Factor levels								Responses		
No.	I	A	B	C	AB	AC	BC	ABC	%Yield	%Purity	%TCH
1	1	-1	-1	-1	1	1	1	-1	59.8	97.93	1.71
2	1	1	-1	-1	-1	-1	1	1	64.1	97.40	2.15
3	1	-1	1	-1	-1	1	-1	1	64.3	97.97	1.75
4	1	1	1	-1	1	-1	-1	-1	69.2	97.47	2.36
5	1	-1	-1	1	1	-1	-1	1	54.8	97.79	2.09
6	1	1	-1	1	-1	1	-1	-1	65.7	96.46	3.03
7	1	-1	1	1	-1	-1	1	-1	58.1	98.02	1.73
8	1	1	1	1	1	1	1	1	66.3	95.64	4.12
9	1	0	0	0	0	0	0	0	64.3	97.64	2.03
10	1	0	0	0	0	0	0	0	62.2	97.70	1.99
11	1	0	0	0	0	0	0	0	65.1	97.11	2.63
12	1	0	0	0	0	0	0	0	62.0	97.71	2.06
13	1	0	0	0	0	0	0	0	62.4	97.60	2.15
14	1	0	0	0	0	0	0	0	63.8	97.52	2.19

The standard deviations of the replicate centre point experiments were:[48]

$$s_1 = \sqrt{\frac{\sum(\bar{y} - y_i)^2}{N_0 - 1}} \qquad [5.14]$$

= 1.432 for the yield response,

= 0.2516 for the purity response, and

= 0.2628 for the TCH response.

Where N_0 = the number of replicates at the design centre.

The error of variance was then calculated as:

s_1^2 = 2.050 for the yield response,
= 0.06328 for the purity response, and
= 0.06909 for the TCH response.

The error of variance obtained from the centre point experiments was used in the analysis of variance (ANOVA) evaluation of the significance of the individual effects. The ANOVA's for each response are summarized in Tables 5.5, 5.6, and 5.7.

The sum of squares (SS) of each effect was obtained by the following equations:[47]

Main effects: $$SS = \frac{(\sum a_i y_i)^2}{N} \quad [5.15]$$

Interaction effects: $$SS = \frac{(\sum a_i b_i y_i)^2}{N} \quad [5.16]$$

Where N = the number of treatment combinations (in this case N = 8)

The mean squares (MS) were calculated by dividing the sum of squares by the number of degrees of freedom of each effect.[47] In an unreplicated design the degrees of freedom for each effect is one. The design of the MTSC formation reaction was an unreplicated design. Thus:

$$SS = MS \quad [5.17]$$

TABLE 5.5: ANOVA using centre points - Yield

Source of variance	Degrees of freedom	SS	MS	F-Ratio
A	1	100.111	100.111	48.835
B	1	22.7813	22.7813	11.113
C	1	19.5313	19.5313	9.5274
AB	1	0.55125	0.55125	0.2689
AC	1	12.2513	12.2513	5.9762
BC	1	4.06125	4.06125	1.9811
ABC	1	1.36125	1.36125	0.664
	Centre points		2.050	

From the F-tables (Appendix A) it was found that F^{crit} = 7.71 for 1 and four degrees of freedom for the upper 5% of the points (P = 0.05). The calculated F-ratio's in Table 5.5 were compared to F^{crit}, and it was evident that effects A, B and C were highly significant.

TABLE 5.6: ANOVA using centre points - Purity

Source of variance	Degrees of freedom	SS	MS	F-Ratio
A	1	2.80845	2.80845	44.379
B	1	0.0288	0.0288	0.4551
C	1	1.02245	1.02245	16.157
AB	1	0.13005	0.13005	2.055
AC	1	0.8978	0.8978	14.187
BC	1	0.06125	0.06125	0.9679
ABC	1	0.1458	0.1458	2.3039
	Centre points		0.06328	

The F-ratio's were compared with F^{crit} = 7.71 for 1 and four degrees of freedom for the upper 5% of the points (P = 0.05), and it was observed that A, C, and AC had significant effects on the purity of MTSC.

TABLE 5.7: ANOVA using centre points - TCH

Source of variance	Degrees of freedom	SS	MS	F-Ratio
A	1	2.39805	2.39805	34.71
B	1	0.12005	0.12005	1.7377
C	1	1.125	1.125	16.284
AB	1	0.32805	0.32805	4.7483
AC	1	0.6498	0.6498	9.4055
BC	1	0.0288	0.0288	0.4169
ABC	1	0.2048	0.2048	2.9644
	Centre points		0.0690875	

By comparing the F-ratio's from Table 5.7 with that of $F^{crit} = 7.71$ for 1 and four degrees of freedom for the upper 5% of the points (P = 0.05), it was observed that A, C, and AC had significant effects on the formation of TCH.

5.5 Response surface methods

A response surface model gives an exact description of the relationship between the experimental variables and the response. The technique is extremely useful in analysis and interpreting mechanistic aspects of a system. This is particularly important in developmental work where new products or methods are designed.

5.5.1 Regression methods

These methods entail using mathematical equations to describe the response surface in the region where the optimum is to be found.

It can be assumed that the response can be modelled as

$$y = f(A,B,C) + \varepsilon \qquad [5.18]$$

where ε is the residual in each run, that is, the difference between the value of $f(A,B,C)$ and y.[52]

The prediction equation that defines any response surface can be described as

$$y = b_0 + \sum_{i=1}^{k} b_i x_i + \sum_{i=1}^{k} b_{ii} x_i^2 + \sum_{i=1}^{k-1} \sum_{j=i+1}^{k} b_{ij} x_i x_j + \varepsilon \qquad [5.19]$$

where k is the number of variables and the x_i's are the experimental factors. This means that for a 2^3 factorial design:[47]

$$y = b_0 + b_1 x_1 + b_2 x_2 + b_3 x_3 + b_{11} x_1^2 + b_{22} x_2^2 + b_{33} x_3^2 + b_{12} x_1 x_2 + b_{13} x_1 x_3 + b_{23} x_2 x_3 + b_{123} x_1 x_2 x_3$$

[5.20]

The x_i's represent the coded forms of the variables (see equation 5.2). The use of coded variables simplifies calculations considerably, but natural variables allow easier visualization of the optimization process.

5.5.1.1 Second order 2^3 design

In order to determine the second order equation,

$$y = \beta_0 + \beta_1 x_1 + \beta_2 x_2 + \beta_3 x_3 + \beta_{11} x_1^2 + \beta_{22} x_2^2 + \beta_{33} x_3^2 + \beta_{12} x_1 x_2 + \beta_{13} x_1 x_3 + \beta_{23} x_2 x_3 \ , \qquad [5.21]$$

a central composite design must be completed.[46] This means that a further two experiments at the star points, -α and +α, must be added for each

variable. The central composite design must be both a rotatable and uniform precision design. To ensure rotatability, α must be equal to the fourth root of the number of factorial experiments in the design. To ensure uniform precision, a fixed number of factorial (N_c), axial (N_a), and centre (N_0) points are required.[46] The values of α and the number of points required for 2 – 6 factors are summarized in Table 5.8.

TABLE 5.8: Rotatable and uniform precision central composite designs

Factors (f)	$N_c = 2^f$	$N_a = 2f$	N_0	α
2	4	4	5	1.414
3	8	6	6	1.682
4	16	8	7	2.000
5	32	10	10	2.378
6	64	12	15	2.828

TABLE 5.9: Extra trials forming the composite design

Run	Factor levels							Response		
No.	I	x_1	x_2	x_3	x_1^2	x_2^2	x_3^2	%Yield	%Purity	%TCH
15	1	-1.682	0	0	2.828	0	0	58.5	98.07	1.65
16	1	1.682	0	0	2.828	0	0	64.7	95.77	4.09
17	1	0	-1.682	0	0	2.828	0	58.2	97.63	1.93
18	1	0	1.682	0	0	2.828	0	63.9	97.61	2.20
19	1	0	0	-1.682	0	0	2.828	66.5	97.69	2.06
20	1	0	0	1.682	0	0	2.828	62.0	97.11	2.76

The method of Least Squares [53] was used to calculate estimates for the yield model parameters for the second order model. Substitution of the parameters into equation [5.21] resulted in equation [5.22] to describe the yield model.

$$y = 63.28 + 2.84x_1 + 1.69x_2 - 1.47x_3 - 0.28x_1x_2 + 1.24x_1x_3 - 0.71x_2x_3 - 0.49x_1^2 - 0.68x_2^2 + 0.45x_3^2 \quad [5.22]$$

The purity model was described by the following equation:

$$y = 97.545 - 0.631x_1 - 0.038x_2 - 0.281x_3 - 0.127x_1x_2 - 0.335x_1x_3 - 0.087x_2x_3 - 0.214x_1^2 + 0.034x_2^2 - 0.044x_3^2 \quad [5.23]$$

The TCH model was described by the following equation:

$$y = 2.178 + 0.621x_1 + 0.105x_2 + 0.306x_3 + 0.203x_1x_2 + 0.285x_1x_3 + 0.060x_2x_3 + 0.255x_1^2 - 0.060x_2^2 + 0.063x_3^2 \quad [5.24]$$

5.5.1.2 Validation of the second order model

Tables 5.10, 5.11, and 5.12 show the residuals calculated using equations [5.22], [5.23], and [5.24] respectively.

The second independent estimate of the experimental error [46] was obtained by

$$s_2^2 = \frac{\sum e_i^2 - \sum (y_{0i} - \bar{y}_0)^2}{(N-p)-(N_0-1)} \quad [5.25]$$

where N is the total number of experiments performed,

p is the number of parameters in the response surface model, and

N_0 is the number of centre point runs.

Thus:

s_2^2 = 3.6341 for the yield model,

= 0.09811 for the purity model, and

= 0.1333 for the TCH model.

TABLE 5.10: Residuals from the second order equation – yield model

Run no.	y^{obs}	y^{pred}	$e = (y^{obs} - y^{pred})$	e^2
1	59.8	59.80	0.00	0.00
2	64.1	63.52	0.58	0.34
3	64.3	65.12	-0.82	0.67
4	69.2	67.80	1.40	1.96
5	54.8	55.80	-1.00	1.00
6	65.7	64.48	1.22	1.49
7	58.1	58.28	-0.18	0.03
8	66.3	65.92	0.38	0.14
9	64.3	63.28	1.02	1.04
10	62.2	63.28	-1.08	1.17
11	65.1	63.28	1.82	3.31
12	62.0	63.28	-1.28	1.64
13	62.4	63.28	-0.88	0.77
14	63.8	63.28	0.52	0.27
15	58.5	57.12	1.38	1.91
16	64.7	66.67	-1.97	3.88
17	58.2	58.51	-0.31	0.10
18	63.9	64.20	-0.30	0.09
19	66.5	67.11	-0.61	0.37
20	62.0	62.17	-0.17	0.03

Calculating the $F^{Lack\ of\ fit}$ gave: [46]

$$F^{Lof} = \frac{s_2^{\,2}}{s_1^{\,2}} \qquad [5.26]$$

= 1.7727 for the yield model,

= 1.5503 for the purity model, and

= 1.9299 for the TCH model.

TABLE 5.11: Residuals from the second order equation – purity model

Run no.	y^{obs}	y^{pred}	$e = (y^{obs} - y^{pred})$	e^2
1	97.93	97.722	0.208	0.043
2	97.40	97.384	0.016	0.000
3	97.97	98.074	-0.104	0.011
4	97.47	97.228	0.242	0.059
5	97.79	98.004	-0.214	0.046
6	96.46	96.326	0.134	0.018
7	98.02	98.008	0.012	0.000
8	95.64	95.822	-0.182	0.033
9	97.64	97.545	0.095	0.009
10	97.70	97.545	0.155	0.024
11	97.11	97.545	-0.435	0.189
12	97.71	97.545	0.165	0.027
13	97.60	97.545	0.055	0.003
14	97.52	97.545	-0.025	0.001
15	98.07	98.001	0.069	0.005
16	95.77	95.878	-0.108	0.012
17	97.63	97.705	-0.075	0.006
18	97.61	97.577	0.033	0.001
19	97.69	97.893	-0.203	0.041
20	97.11	96.948	0.162	0.026

From the F-tables it was found that $F_{(5,5)} = 5.05$ at $P = 0.05$. Since $F^{Lof} < F^{crit}$ it was concluded that the second order models were adequate descriptions of the response surfaces in all three cases. Normal probability plots of the residuals (Figures 5.2, 5.3 and 5.4) showed that they were good fits, and plots of the residuals against predicted responses (Figure 5.5, 5.6 and 5.7) confirmed that.

TABLE 5.12: Residuals from the second order equation – TCH model

Run no.	y^{obs}	y^{pred}	$e = (y^{obs} - y^{pred})$	e^2
1	1.71	1.952	-0.242	0.059
2	2.15	2.218	-0.068	0.005
3	1.75	1.636	0.114	0.013
4	2.36	2.714	-0.354	0.125
5	2.09	1.874	0.216	0.047
6	3.03	3.28	-0.250	0.063
7	1.73	1.798	-0.068	0.005
8	4.12	4.016	0.104	0.011
9	2.03	2.178	-0.148	0.022
10	1.99	2.178	-0.188	0.035
11	2.63	2.178	0.452	0.204
12	2.06	2.178	-0.118	0.014
13	2.15	2.178	-0.028	0.001
14	2.19	2.178	0.012	0.000
15	1.65	1.855	-0.205	0.042
16	4.09	3.944	0.146	0.021
17	1.93	1.832	0.098	0.010
18	2.2	2.185	0.015	0.000
19	2.06	1.842	0.218	0.048
20	2.76	2.871	-0.111	0.012

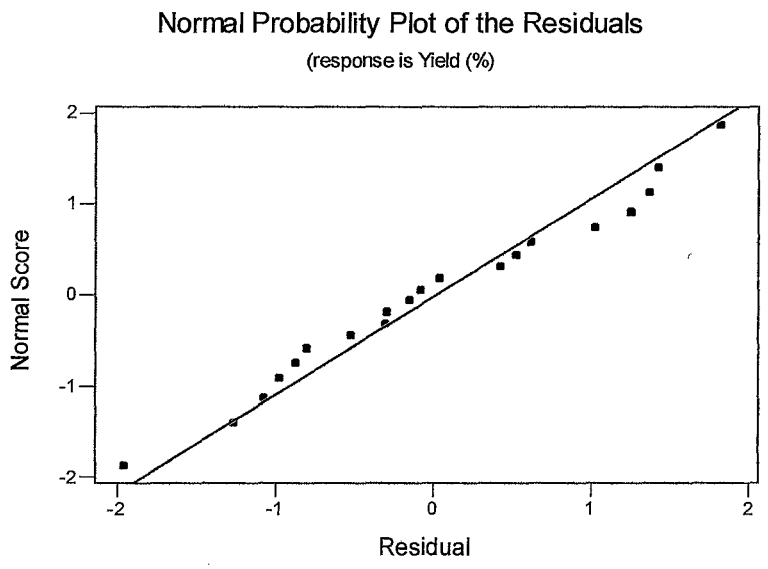

Figure 5.2: Normal probability plot of residuals for the yield response

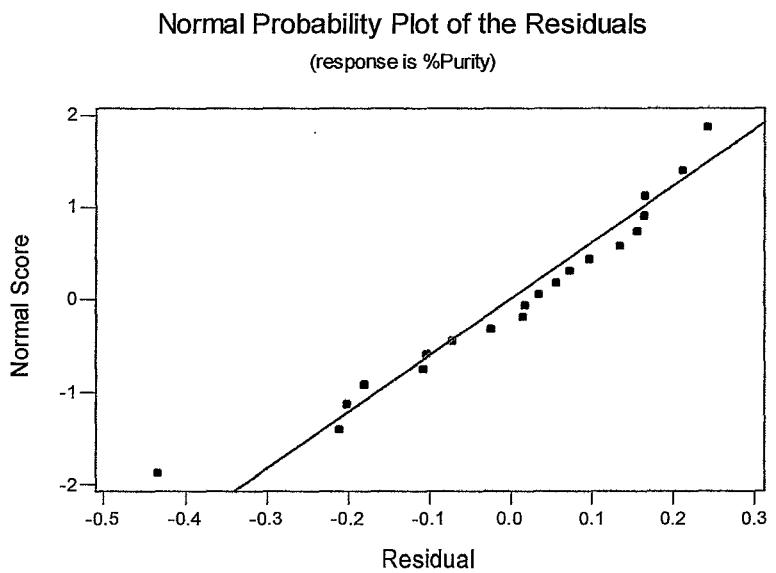

Figure 5.3: Normal probability plot of residuals for the purity response

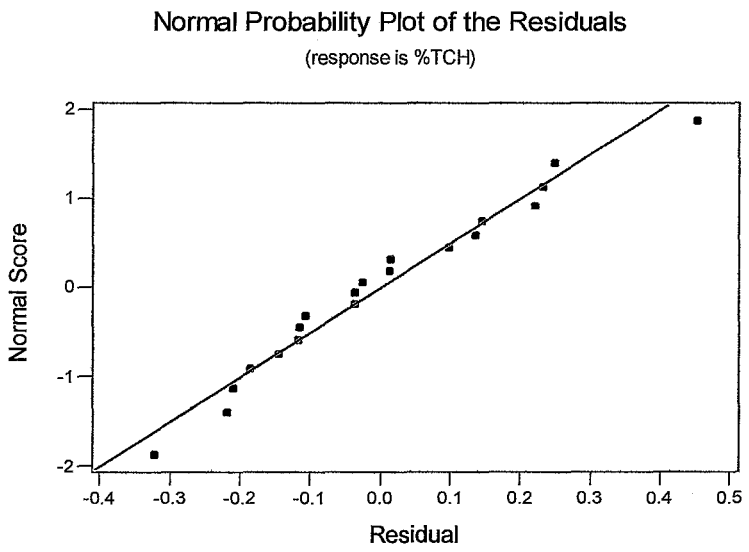

Figure 5.4: Normal probability plot of residuals for the TCH response

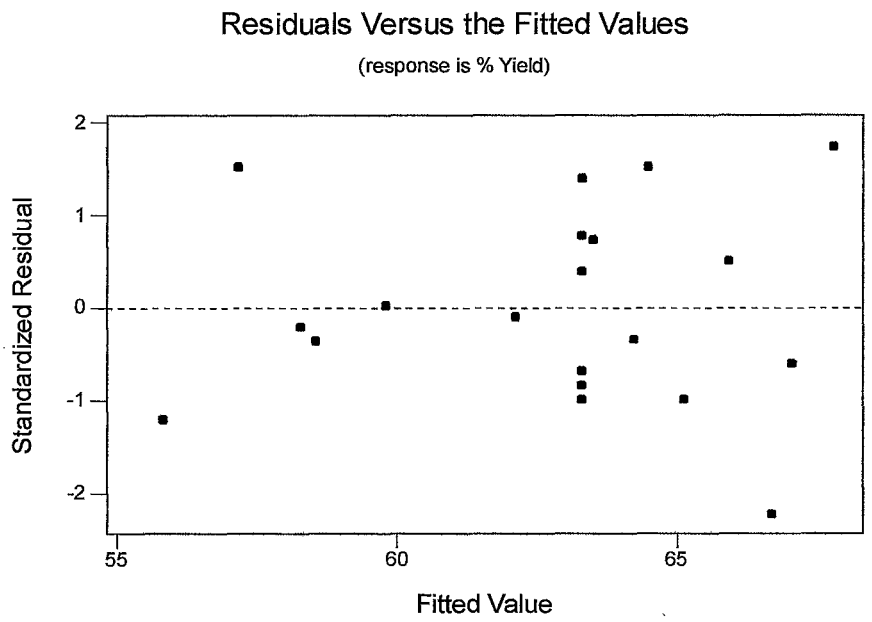

Figure 5.5: Plot of residuals versus predicted responses for the yield response

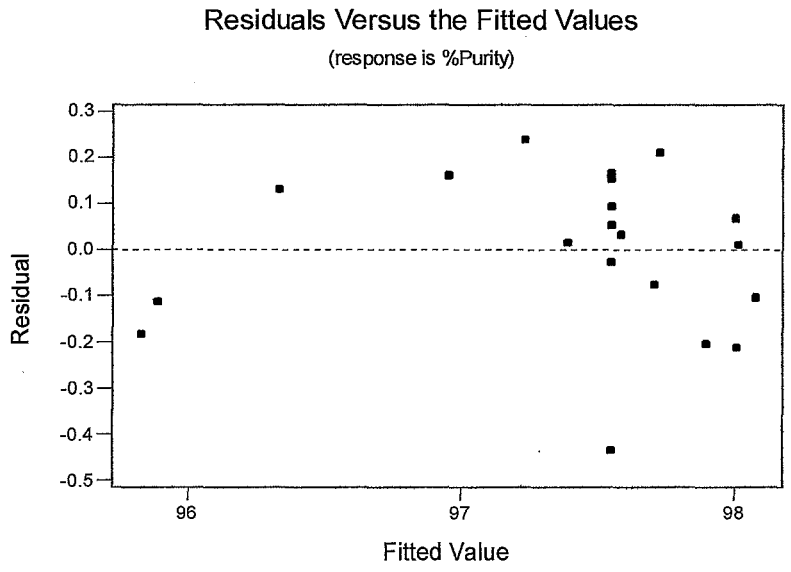

Figure 5.6: Plot of residuals versus predicted responses for purity response

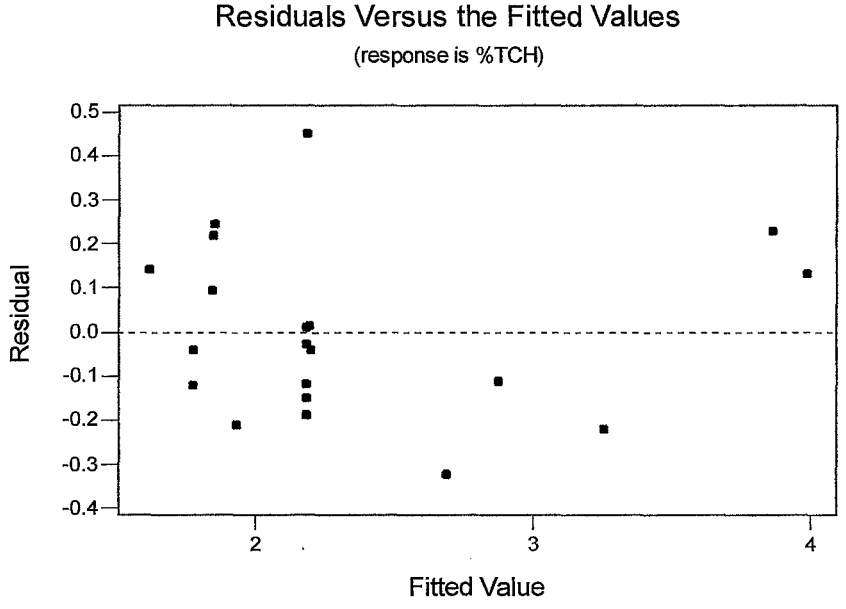

Figure 5.7: Plot of residuals versus predicted responses for the TCH response

From equations [5.22], [5.23], and [5.24] the following response surfaces were derived:

The yield model:

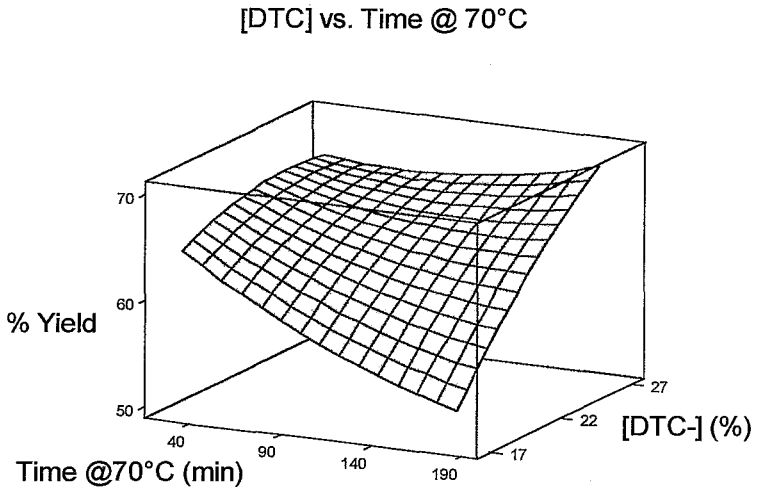

Figure 5.8: Response surface of [DTC] versus Hydrazine excess for the yield model

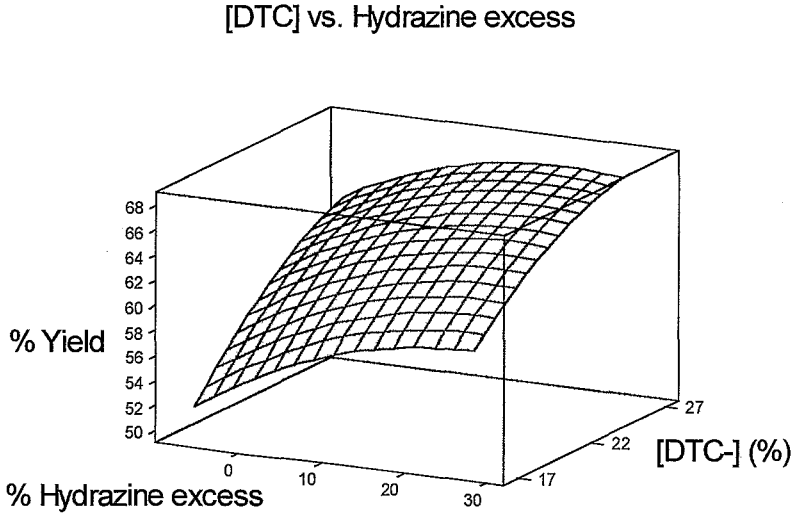

Figure 5.9: Response surface of [DTC] versus Time @ 70°C for the yield model

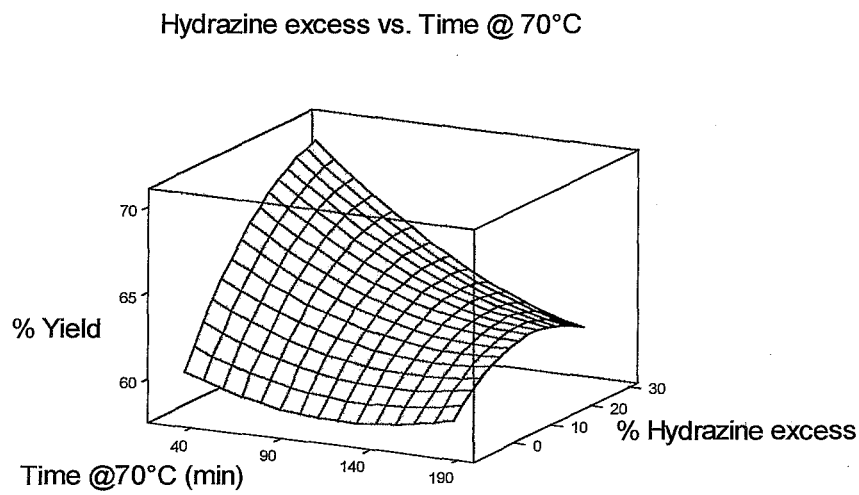

Figure 5.10: Response surface of hydrazine excess versus Time @ 70°C for the yield model

The purity model:

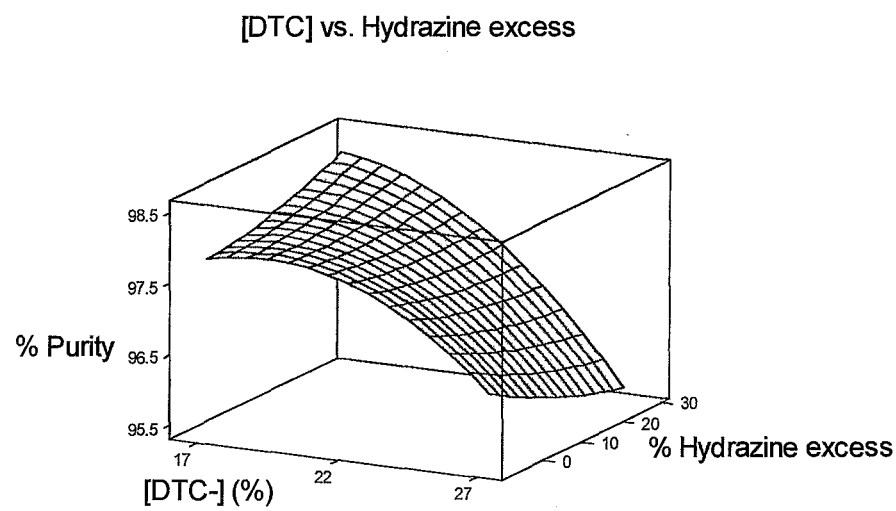

Figure 5.11: Response surface of [DTC] versus Hydrazine excess for the purity model

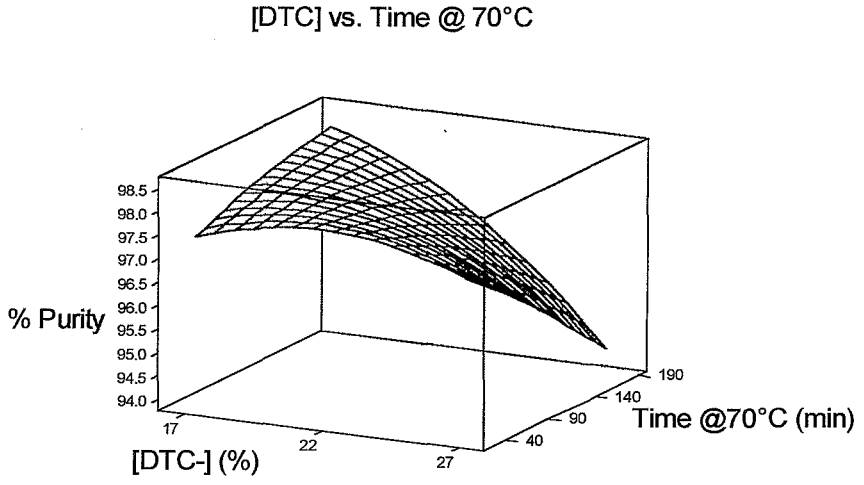

Figure 5.12: Response surface of [DTC] versus Time @ 70°C for the purity model

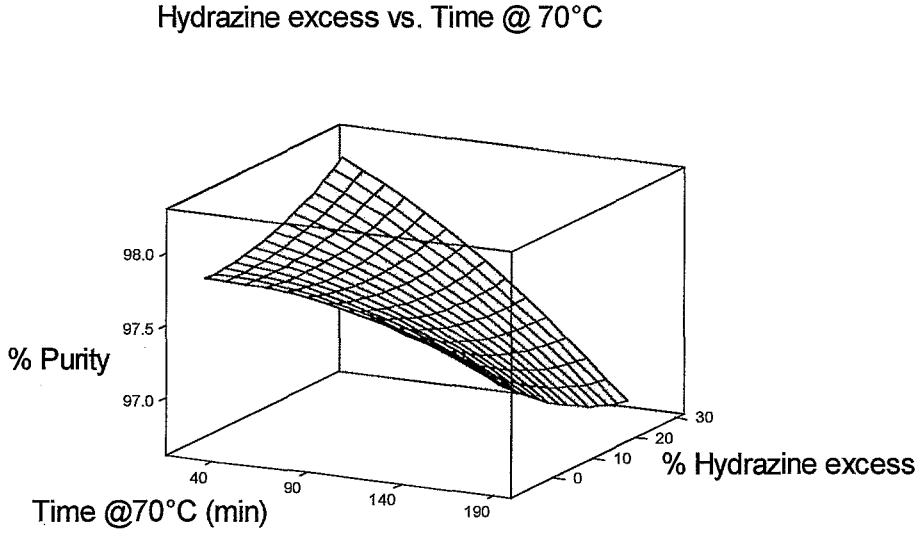

Figure 5.13: Response surface of hydrazine excess versus Time @ 70°C for the purity model

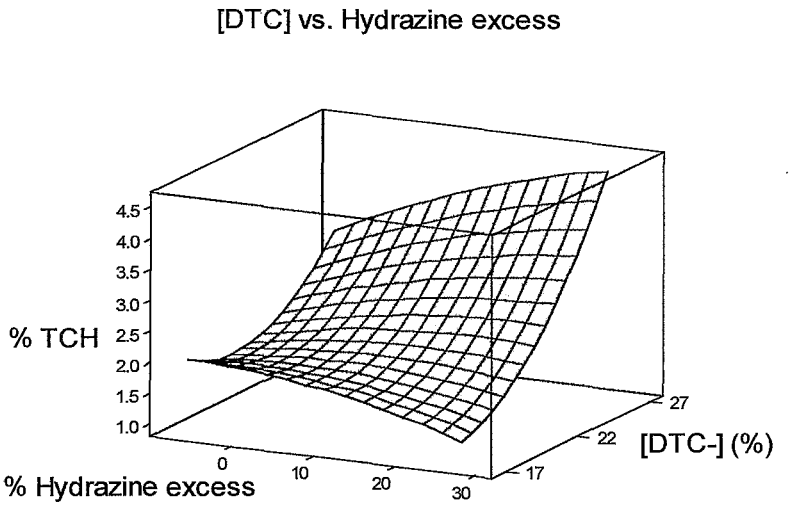

Figure 5.14: Response surface of [DTC] versus Hydrazine excess of the TCH model

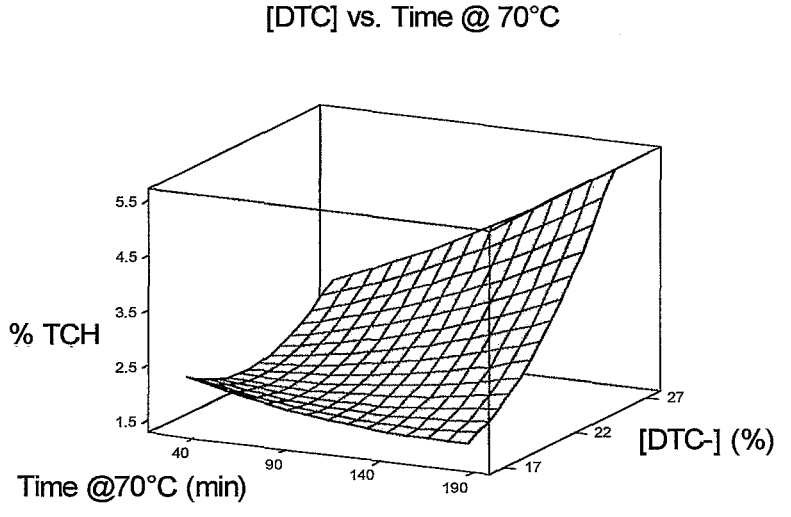

Figure 5.15: Response surface of [DTC] versus Time @ 70°C of the TCH model

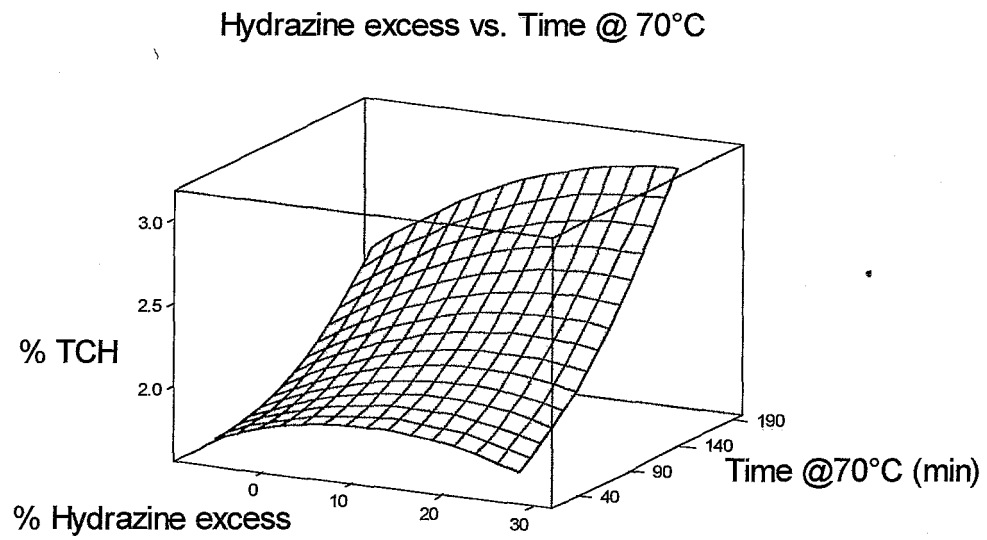

Figure 5.16: Response surface of hydrazine excess versus Time @ 70°C of the TCH model

5.5.1.3 Analysis of the fitted response surface

The stationary points were obtained by partial differentiation of equations [5.22], [5.23], and [5.24] with respect to each of the variables, and solving the resulting three equations using matrix calculations. The optimum solutions were then converted from the coded values back to the actual values using equation [5.2].

Maximum yield was achieved when a 20.6% excess hydrazine hydrate was added to a 28.3% DTC^- solution, and the mixture was kept at 70°C for 1.5 hours, before removing the DIPEA. This stationary point however was outside the design range and was therefore not an accurate estimate of the optimum.

The optimum purity was achieved when a 2.8% shortage of hydrazine hydrate was added to a DIPEADTC solution with an N-methyldithiocarbamate anion

(DTC$^-$) concentration of 21.4%, and the mixture was kept at 70°C for 54 minutes before removing the DIPEA.

The minimum TCH formation was achieved when a 2.5% excess hydrazine hydrate was added to a 18.8% DTC$^-$ solution, and the reaction mixture was kept at 70°C for 2 hours before removing the DIPEA.

5.5.1.4 Confirming the purity model

From the results of the factorial design it is evident that MTSC yield must be sacrificed for purity and vice versa.

The purity of MTSC is an important factor to produce BTDA of high purity. The purity model was therefore chosen as the most important model.

One laboratory experiment and one mini plant run were completed to confirm the results of the purity model.

The runs were completed with the factors set at:
a. 21.4% DTC$^-$ concentration,
b. –2.79% excess $H_2NNH_2 \cdot H_2O$, and
c. 54 min at 70°C before heating the mixture to 85-92°C.

The following results were obtained:

TABLE 5.13: MTSC - predicted results and actual results

	MTSC yield (%)	%MTSC	%TCH	%DMTU
Predicted	60.8	97.79	1.77	-
Lab run	63.5	98.32	1.43	0.25
Mini plant run	66.0	97.79	1.94	0.23

From the results in Table 5.13 it was concluded that the purity model obtained from the factorial design, was accurate for both the laboratory and the mini plant.

When running the experiment at the stationary point of the purity model the effluent to product ratio was 4:1.

5.5.1.5 Conclusive remarks

From the above factorial design the following conclusions could be made:

- All three factors investigated influence the yield of MTSC significantly. Higher DTC^- concentration, increased hydrazine hydrate excess, and shorter reaction time will increase the yield of MTSC. The second order model fitted to the data gave an excellent fit and could be used to analyse the response surface within the domain of the investigation.
- Only the DTC^- concentration and the time the reaction is kept at 70°C influence the purity of MTSC. Lowering the DTC^- concentration and reducing the time at 70°C will increase the purity of MTSC. This clearly points to the formation of TCH as a result of the decomposition of DIPEADTC to liberate CS_2 in the equilibrium reaction (equation 4.1). A higher DTC^- concentration will force the reaction to the left, and an extended reaction time will increase the formation of TCH as the equilibrium is disturbed by removing CS_2 from the reaction with hydrazine hydrate.

Although the results from the factorial design may be used to find an optimum yield and purity, this optimum will only be valid under the conditions specified in the design.

5.6 The 2^3 factorial design of the hydrazinolysis of DIPEADTC to MTSC in excess DIPEA

The factorial design described in §5.5 proved that MTSC of high quality could be produced. However, the effluent to product ratio was 4:1 - the same as the method using ammonia as base. The MTSC yield was also not improved significantly when using DIPEA as base instead of ammonia. Another set of conditions had to be found in order to obtain a better optimum.

From the results in §4.2.3.3 it was concluded that the DIPEADTC salt could be stabilized at higher temperatures by running the hydrazinolysis reaction in a 10% excess DIPEA.

Four experiments were completed using the following procedure:

Hydrazine hydrate (1.458 moles, 2.79% shortage) was added to 1.5 moles of a 25% DTC^- solution. The reaction mixture was heated to 86°C under reflux conditions for 2 - 2.25 h. The DIPEA was recovered and the product isolated. The following results were obtained:

TABLE 5.14: Summary of results – hydrazinolysis in an excess DIPEA.

Run	Isolated yield (%)	% MTSC	% TCH	% DMTU
1	65.9	97.93	1.73	0.34
2	70.7	98.15	1.58	0.26
3	67.2	97.88	1.72	0.37
4	67.9	98.06	1.58	0.36

From these results it was evident that the optimum of the purity model may be shifted by working with higher DTC^- concentrations in an excess DIPEA.

There were no significant improvements in MTSC yield or purity. The effluent / product ratio however, could be reduced to 2.5 : 1 as opposed to the 4 : 1

ratio obtained when using a 21.4% DTC^- solution as indicated by the purity model in §5.5.1.4.

5.6.1. Screening Experiments

5.6.1.1. The effect of DTC^- concentration on the yield and purity of MTSC

Hydrazine hydrate (1.458 moles) was added to a 21%, 25%, and 28% DTC^- solution. The reaction mixtures were heated to 86°C under reflux conditions for 2.25h, after which the DIPEA was recovered and the MTSC isolated. The following results were obtained:

TABLE 5.15: Effect of DTC^- concentration on the yield and purity of MTSC

Run	%DTC^-	MTSC yield (%)	%MTSC	%TCH	%DMTU
1	21.4	68.6	97.60	1.34	1.06
2	25.0	70.7	98.15	1.58	0.26
3	25.0	67.9	98.06	1.58	0.36
4	28.0	68.3	97.36	2.30	0.35

From Table 5.15 it was evident that the concentration of the DIPEADTC solution had no significant effect on the yield of MTSC. The concentration of the DIPEADTC solution, however, did have some effect on the formation of TCH.

5.6.1.2. The effect of reaction time under reflux conditions on the yield and purity of MTSC

Three reactions were completed by the addition of hydrazine hydrate (1.458 moles) to a 25% DTC^- solution. The reaction mixtures were heated to 86°C

under reflux conditions for 1h, 2h, and 2.25h. The DIPEA was then recovered and the MTSC isolated. The results are summarized in Table 5.16.

TABLE 5.16: Effect of the reaction time under reflux conditions on the yield and purity of MTSC

Run	Reaction time (h)	MTSC yield (%)	%MTSC	%TCH	%DMTU
1	2	65.9	97.93	1.73	0.34
2	2.25	67.9	98.06	1.58	0.36
3	1	60.2	97.79	1.94	0.28

The reaction time under reflux conditions had no significant effect on the formation of either TCH or DMTU. It did, however, have an effect on the yield of MTSC.

5.6.1.3. The effect of hydrazine hydrate excess on the yield and purity of MTSC

Two reactions were completed by the addition of hydrazine hydrate at a 2.8% shortage, and 10% excess respectively to a 25% DTC^- solution. The reaction mixtures were heated to 86°C under reflux conditions for 2h. The DIPEA was then recovered and the MTSC isolated. The following results were obtained:

TABLE 5.17: Effect of hydrazine hydrate excess on the yield and purity of MTSC

Run	Hydrazine excess (%)	MTSC yield (%)	%MTSC	%TCH	%DMTU
1	-2.8	65.9	97.93	1.73	0.34
2	10	73.0	97.79	1.88	0.33

The excess of hydrazine hydrate used in the hydrazinolysis reaction had no significant effect on the formation of TCH, but it did have a significant effect on the yield of MTSC.

5.6.2. Factorial design of the hydrazinolysis reaction in an excess DIPEA

The optimization of the hydrazinolysis reaction entailed a 3 factor central composite design. The following factors were identified:

a. The concentration of the DIPEADTC solution,
b. the excess hydrazine hydrate, and
c. the time the reaction mixture is kept under reflux conditions before removing the DIPEA.

The coded values that will be used in the design were obtained as indicated in Table 5.18.

TABLE 5.18: Coded values of factors – hydrazinolysis in excess DIPEA

Factor	-1.682	-1	0	1	1.682
a	18%	20%	23%	26%	28%
b	-6.8%	0%	10%	20%	26.8%
c	40 min	1h	1.5h	2h	2h 20 min

The results of the 20 design experiments are summarized in Table 5.19.

The error of variance was calculated as:

s_1^2 = 7.131 for the yield response, and
= 0.02759 for the purity response.

TABLE 5.19: Results of central composite design of hydrazinolysis in excess DIPEA.

Run No.	Factor levels				Responses	
	I	A	B	C	%Yield	%Purity
1	1	-1	-1	-1	68.4	98.91
2	1	1	-1	-1	70	96.49
3	1	-1	1	-1	67.3	98.54
4	1	1	1	-1	71.9	96.72
5	1	-1	-1	1	65.4	98.72
6	1	1	-1	1	65.1	97.87
7	1	-1	1	1	70.8	98.45
8	1	1	1	1	72.9	97.38
9	1	0	0	0	64	97.83
10	1	0	0	0	68.9	98.27
11	1	0	0	0	69.6	98.21
12	1	0	0	0	70.2	98.19
13	1	0	0	0	69.9	98.22
14	1	0	0	0	65.2	98.26
15	1	-1.682	0	0	62.1	98.75
16	1	1.682	0	0	71.1	96.04
17	1	0	-1.682	0	67.8	98.37
18	1	0	1.682	0	74.5	97.97
19	1	0	0	-1.682	66.8	98.37
20	1	0	0	1.682	67.8	98.18

The ANOVA for each response are summarized in Tables 5.20 and 5.21.

The method of Least Squares was used to calculate estimates for the yield model parameters for the second order model. The yield model was described by the following equation:

$$y = 67.947 + 1.694x_1 + 1.850x_2 - 0.126x_3 + 0.675x_1x_2 - 0.55x_1x_3 - 1.55x_2x_3 - 0.356x_1^2 + 1.252x_2^2 - 0.109x_3^2 \quad [5.27]$$

The purity model was described by the following equation:

$$y = 98.165 - 0.785x_1 - 0.115x_2 + 0.105x_3 + 0.0475x_1x_2 + 0.29x_1x_3 - 0.0775x_2x_3 - 0.282x_1^2 - 0.00789x_2^2 + 0.0292x_3^2 \quad [5.28]$$

TABLE 5.20: ANOVA using centre points - Yield

Source of variance	Degrees of freedom	SS	MS	F-Ratio
A	1	38060.41	38060.41	5337.566
B	1	8	8	1.121915
C	1	24.5	24.5	3.435864
AB	1	1.445	1.445	0.202646
AC	1	3.645	3.645	0.511172
BC	1	2.42	2.42	0.339379
ABC	1	19.22	19.22	2.6954
	Centre points		7.130667	

From the F-tables it was found that F^{crit} = 7.71 for 1 and four degrees of freedom for the upper 5% of the points (P = 0.05). The calculated F-ratio's in Table 5.20 were compared to F^{crit}, and it was evident that the effect of A was highly significant.

TABLE 5.21: ANOVA using centre points - Purity

Source of variance	Degrees of freedom	SS	MS	F-Ratio
A	1	76651.79	76651.786	2778581
B	1	4.7432	4.7432	171.9381
C	1	0.10125	0.10125	3.670251
AB	1	0.3872	0.3872	14.03577
AC	1	0.01805	0.01805	0.654302
BC	1	0.6728	0.6728	24.38859
ABC	1	0.04805	0.04805	1.741783
	Centre points		0.0275867	

The F-ratio's were compared with F^{crit} = 7.71 for 1 and four degrees of freedom for the upper 5% of the points (P = 0.05), and it was observed that A, B, AB and BC had significant effects on the purity of MTSC.

5.6.3 Validation of the second order model

Tables 5.22 and 5.23 show the residuals calculated using equations [5.27] and [5.28] respectively.

The second independent estimate of the experimental error was calculated as:

s_2^2 = 2.485 for the yield model, and
= 0.06985 for the purity model.

Calculating the $F^{Lack\ of\ fit}$ gave:

F^{Lof} = 0.35 for the yield model, and
= 2.53 for the purity model.

From the F-tables it was found that $F_{(5,5)} = 5.05$ at $P = 0.05$. Since $F^{Lof} < F^{crit}$ it was concluded that the second order models are adequate descriptions of the response surfaces in both cases. Normal probability plots of the residuals (Figures 5.17 and 5.18) showed that they were good fits, and plots of the residuals against predicted responses (Figure 5.19 and 5.20) confirmed that.

TABLE 5.22: Residuals from the second order equation – yield model in excess DIPEA

Run no.	y^{obs}	y^{pred}	$e = (y^{obs} - y^{pred})$	e^2
1	68.4	66.99	1.41	1.98
2	70.0	70.13	-0.13	0.02
3	67.3	66.24	1.06	1.12
4	71.9	72.08	-0.18	0.03
5	65.4	64.74	0.66	0.44
6	65.1	65.68	-0.58	0.33
7	70.8	70.19	0.61	0.37
8	72.9	73.83	-0.93	0.86
9	64.0	67.95	-3.95	15.58
10	68.9	67.95	0.95	0.91
11	69.6	67.95	1.65	2.73
12	70.2	67.95	2.25	5.07
13	69.9	67.95	1.95	3.81
14	65.2	67.95	-2.75	7.55
15	62.1	64.09	-1.99	3.96
16	71.1	69.79	1.31	1.72
17	67.8	68.38	-0.58	0.33
18	74.5	74.60	-0.10	0.01
19	66.8	67.85	-1.05	1.11
20	67.8	67.43	0.37	0.14

TABLE 5.23: Residuals from the second order equation – purity model in excess DIPEA

Run no.	y^{obs}	y^{pred}	$e = (y^{obs} - y^{pred})$	e^2
1	98.91	98.959	-0.049	0.002
2	96.49	96.714	-0.224	0.050
3	98.54	98.789	-0.249	0.062
4	96.72	96.734	-0.014	0.000
5	98.72	98.745	-0.025	0.001
6	97.87	97.660	0.210	0.044
7	98.45	98.264	0.186	0.034
8	97.38	97.370	0.010	0.000
9	97.83	98.165	-0.335	0.112
10	98.27	98.165	0.105	0.011
11	98.21	98.165	0.045	0.002
12	98.19	98.165	0.025	0.001
13	98.22	98.165	0.055	0.003
14	98.26	98.165	0.095	0.009
15	98.75	98.688	0.062	0.004
16	96.04	96.048	-0.008	0.000
17	98.37	98.336	0.034	0.001
18	97.97	97.949	0.021	0.000
19	98.37	98.070	0.300	0.090
20	98.18	98.425	-0.245	0.060

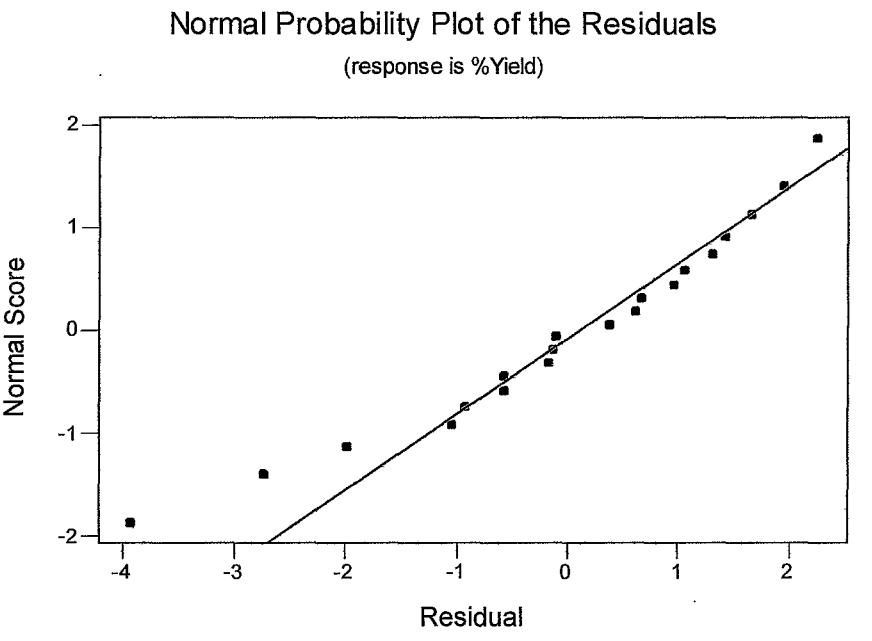

Figure 5.17: Normal probability plot of residuals for the yield response in excess DIPEA

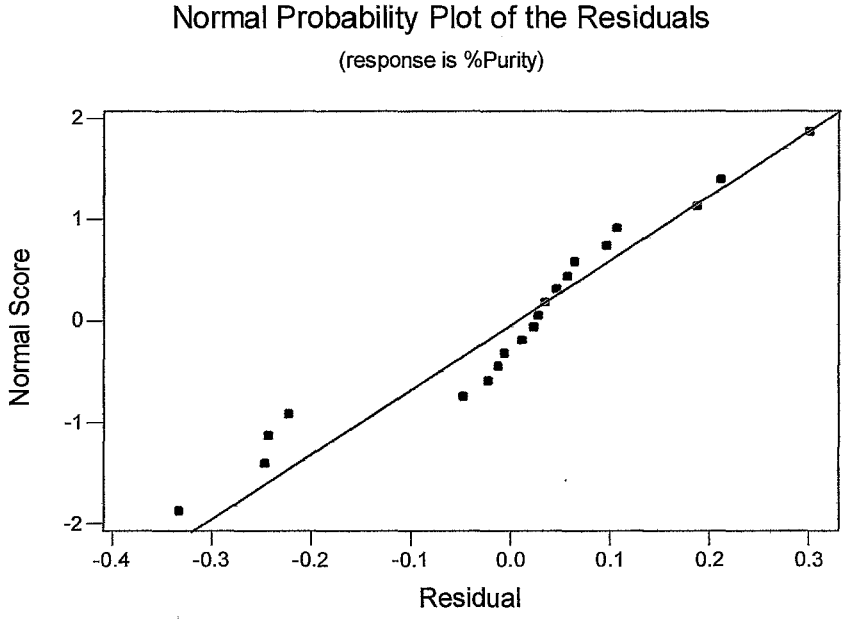

Figure 5.18: Normal probability plot of residuals for the purity response in excess DIPEA

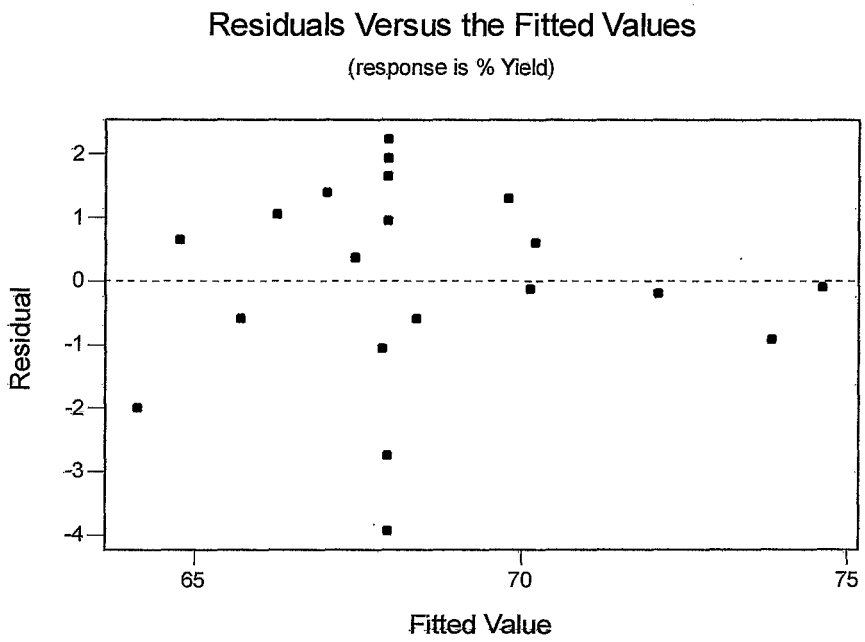

Figure 5.19: Plot of residuals versus predicted responses for the yield response in excess DIPEA

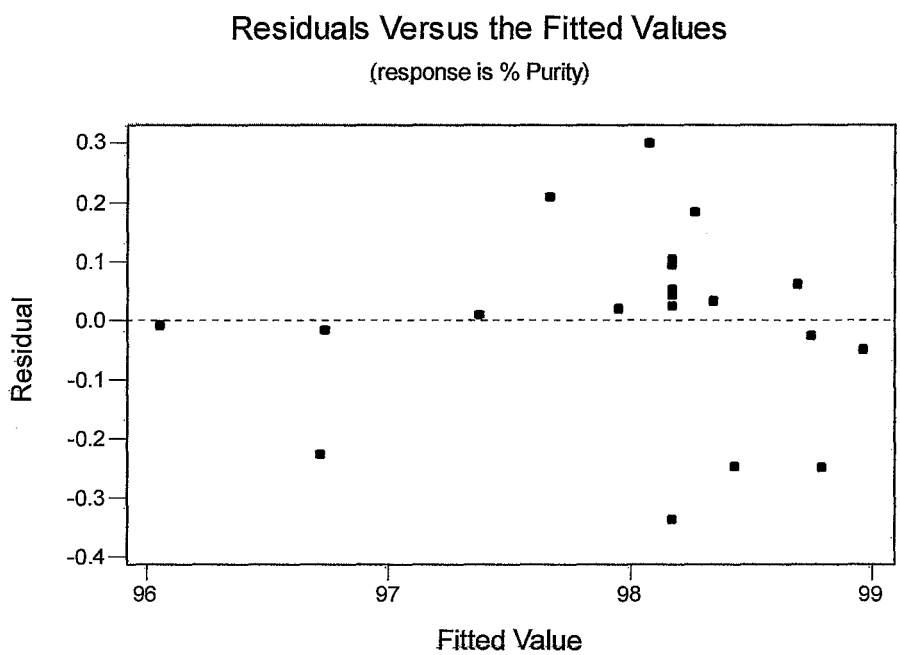

Figure 5.20: Plot of residuals versus predicted responses for the purity response in excess DIPEA

From equations [5.27] and [5.28] the following response surfaces were derived:

The yield model:

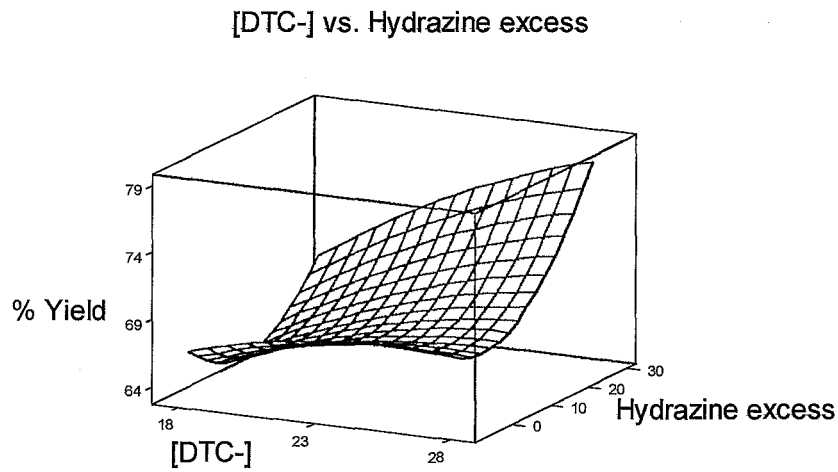

Figure 5.21: Response surface of [DTC] versus Hydrazine excess for the yield model in excess DIPEA

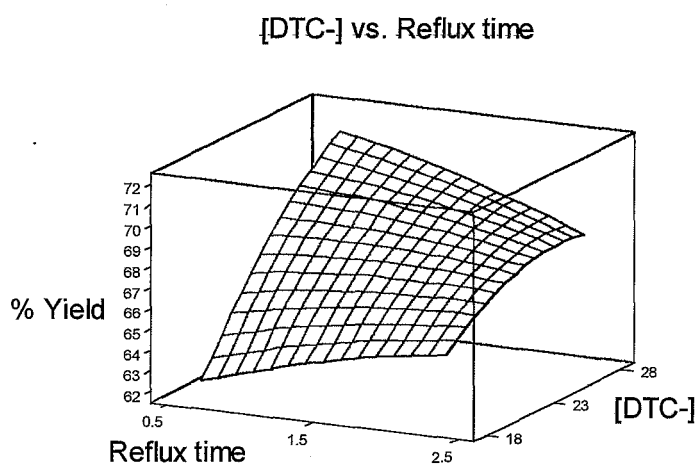

Figure 5.22: Response surface of [DTC] versus Time @ 70°C for the yield model in excess DIPEA

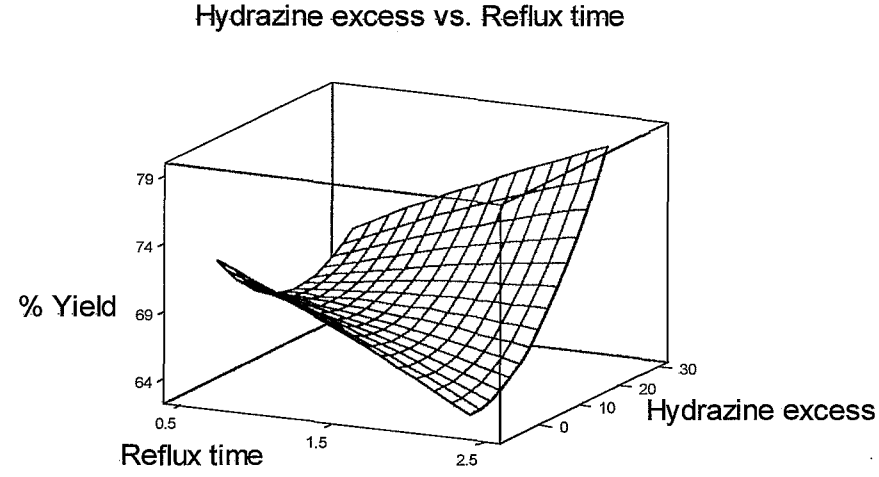

Figure 5.23: Response surface of hydrazine excess versus Time @ 70°C for the yield model in excess DIPEA

The purity model:

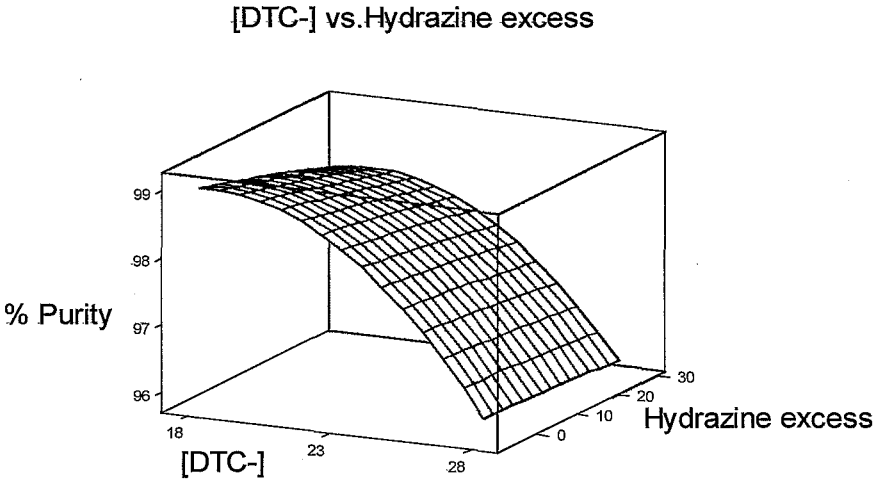

Figure 5.24: Response surface of [DTC-] versus Hydrazine excess for the purity model in excess DIPEA

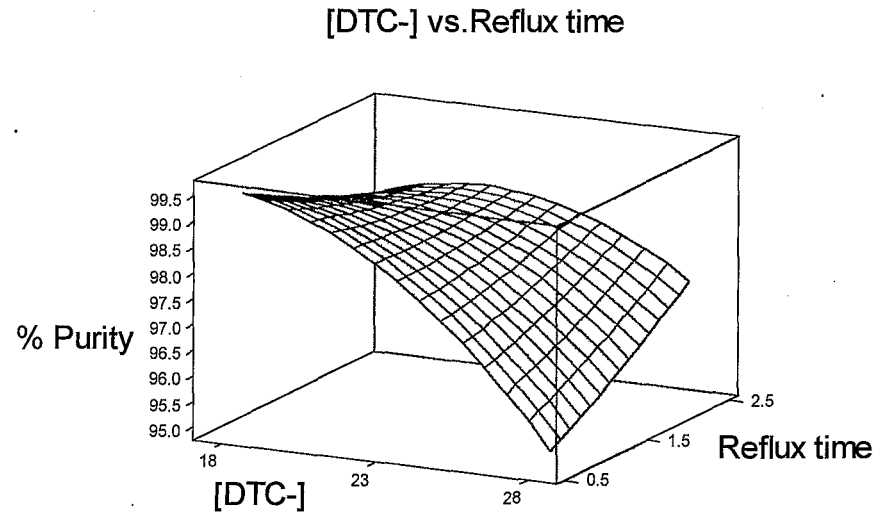

Figure 5.25: Response surface of [DTC⁻] versus Time @ 70°C for the purity model in excess DIPEA

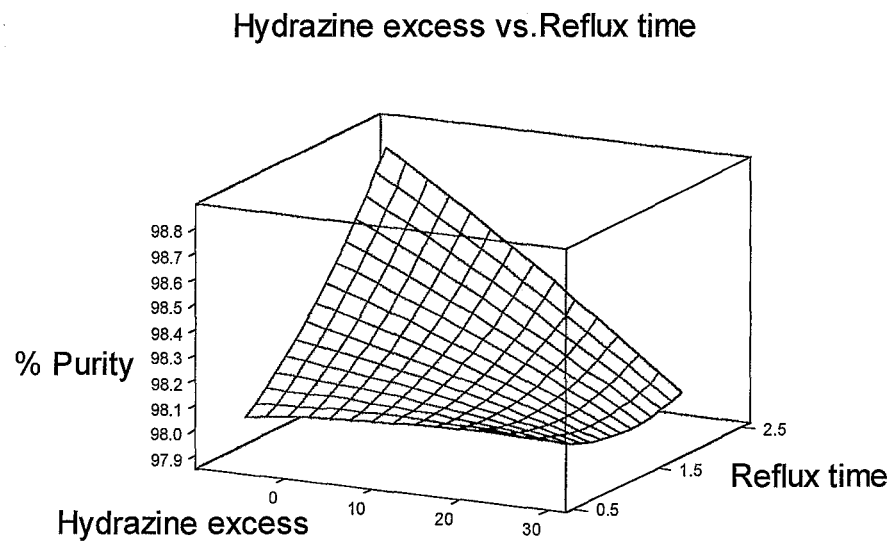

Figure 5.26: Response surface of hydrazine excess versus Time @ 70°C for the purity model in excess DIPEA

5.6.4 Analysis of the fitted response surface

The optimum conditions for both the yield model and the purity model were determined to be the following:

Yield model:
91.41% DTC^- concentration
63.9 % excess hydrazine
-8.4 h under reflux conditions

Purity model:
14.46 % DTC^- concentration
91.6 % shortage hydrazine
0.9 h under reflux conditions

These optimum conditions were situated outside the design and were not only meaningless, but totally unrealistic. Another method of optimization was employed using the data from the design experiments. This method entailed optimizing both responses at the same time.

5.6.4.1 Multiple Response Optimization

Both responses were maximized within the range of the design by using the multiple response optimizer of Minitab™ Statistical Software. The following optimum was obtained:

Optimal Solution:

$[DTC^-]$ = 21.9%
Hydrazine excess = -6.3%
Reflux time = 1h

Predicted Responses:

% Yield = 70.35

% Purity = 98.51

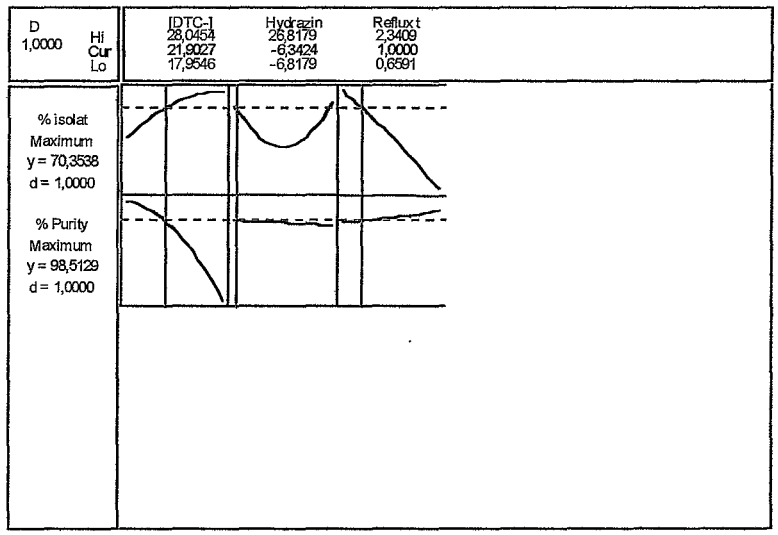

Figure 5.27: Multiple response optimizer – optimum yield and purity.

Because waste minimization is also very important, hydrazinolysis of the DIPEADTC to MTSC must be completed at the highest possible DTC^- concentration without sacrificing too much purity. By moving the red vertical lines on the above graph the following conditions were identified to yield the least volume of effluent while the purity still remained higher than 98%:

Optimal Solution:

$[DTC^-]$ = 24.2%

Hydrazine excess = 20.2%

Reflux time = 2h 20min

Predicted Responses:

% Yield = 73.78

% Purity = 98.08

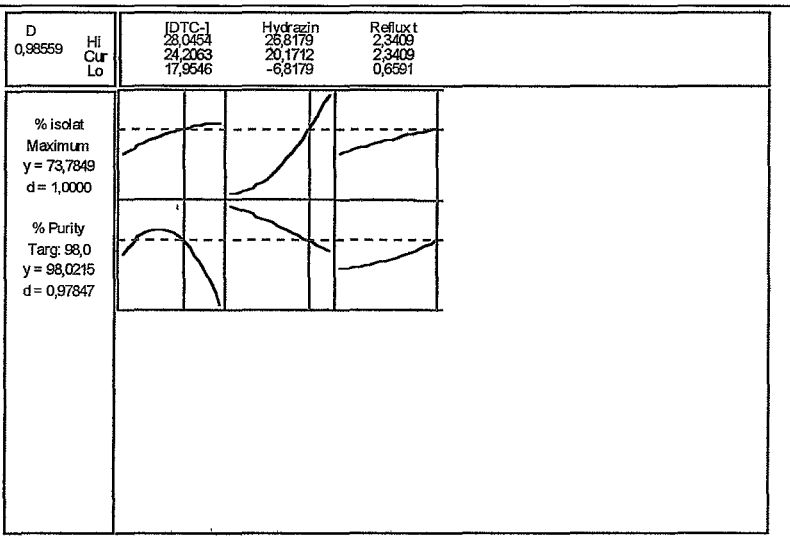

Figure 5.28: Multiple response optimizer – minimum waste.

5.6.5. Confirmation of optimum conditions

Experiments were completed using the above conditions. The following results were obtained:

TABLE 5.24: Confirmation of optimum

Run	Predicted responses		Actual observations	
	% Yield	% Purity	% Yield	% Purity
1	70.4	98.5	69.5	98.0
2	73.8	98.1	76.2	97.5

In both cases, the model derived from the F-design proved to be relatively accurate.

A waste / product ratio of approximately 2.1 : 1 was obtained at the optimum of this design.

5.7 Conclusive remarks

From the above factorial design in § 5.6 the following conclusion could be reached:

- Only DTC^- concentration influences the yield of MTSC significantly. Increased DTC^- concentrations will increase the yield of MTSC.
- The DTC^- concentration and the excess of hydrazine hydrate influence the purity of MTSC. Lowering the DTC^- concentration and reducing the hydrazine hydrate excess will increase the purity of MTSC.
- The waste / product ratio of 2.1 : 1 was obtained, proving that not only could better yield and purity of MTSC be obtained, but that the waste of the process could also be reduced by 50% when using DIPEA as base instead of ammonium hydroxide.

Once again, although the results from the factorial design may be used to find an optimum yield and purity, this optimum will only be valid under the conditions specified in the design. The second order model fitted to the data gave an excellent fit and could be used to analyse the response surface within the domain of the investigation.

CHAPTER 6.

Conclusion

Initial experiments indicated that there was no significant difference in the yield of MTSC between the TEA and the DIPEA-based methods. However, there was a difference in purity between the MTSC as derived from the TEA-based method and that of the DIPEA-based method. The purity of the MTSC as derived from the DIPEA-based method was much higher than that of the TEA-based method. Only 90% of the TEA could be recovered, while 99% of the DIPEA was recovered. The low recovery of TEA is due to its solubility in water (5.5%), therefore, unrecovered TEA ends up in the effluent stream, thereby, increasing the toxicity of the effluent, which results in higher cost of disposal.

DIPEA enhances the stability of the N-methyldithiocarbamate, thereby, making it ten times more stable at higher temperatures (70-90°C) than the TEA derived product.[40] The increased stability of the N-methyldithiocarbamate may be explained by the formation of a tightly associated ion pair, due to DIPEA being a proton specific, non-nucleophilic tertiary amine.[54] The use of sodium hydroxide, potassium hydroxide, and ammonium hydroxide as bases in the synthesis of N-methyldithiocarbamate results in the formation of solvent separated ion pairs, lowering the stability of the corresponding N-methyldithiocarbamate at higher temperatures. DIPEA is evidently an excellent alternative to NH_4OH as base for the synthesis of the N-methyldithiocarbamate intermediate to MTSC.

The formation of the byproduct, DMTU, during the DIPEADTC formation step was decreased by ensuring the absence of an excess of methylamine in the

reaction mixture. According to the results in Table 4.2 the order of addition of reagents during the DIPEADTC reaction had a significant effect on the formation of DMTU.

The order of addition of reagents during the hydrazinolysis of DIPEADTC to MTSC had a significant effect on the yield of MTSC as well as the formation of the byproduct, TCH (see Table 4.7). According to Table 4.8 the formation of TCH is proportional to the excess of hydrazine hydrate in the reaction mixture.

The stability tests proved that MTSC remained stable at higher temperatures in both water and filtrate under the specified conditions. The findings of the stability tests for both DIPEADTC and MTSC are summarized in Scheme 6.1.

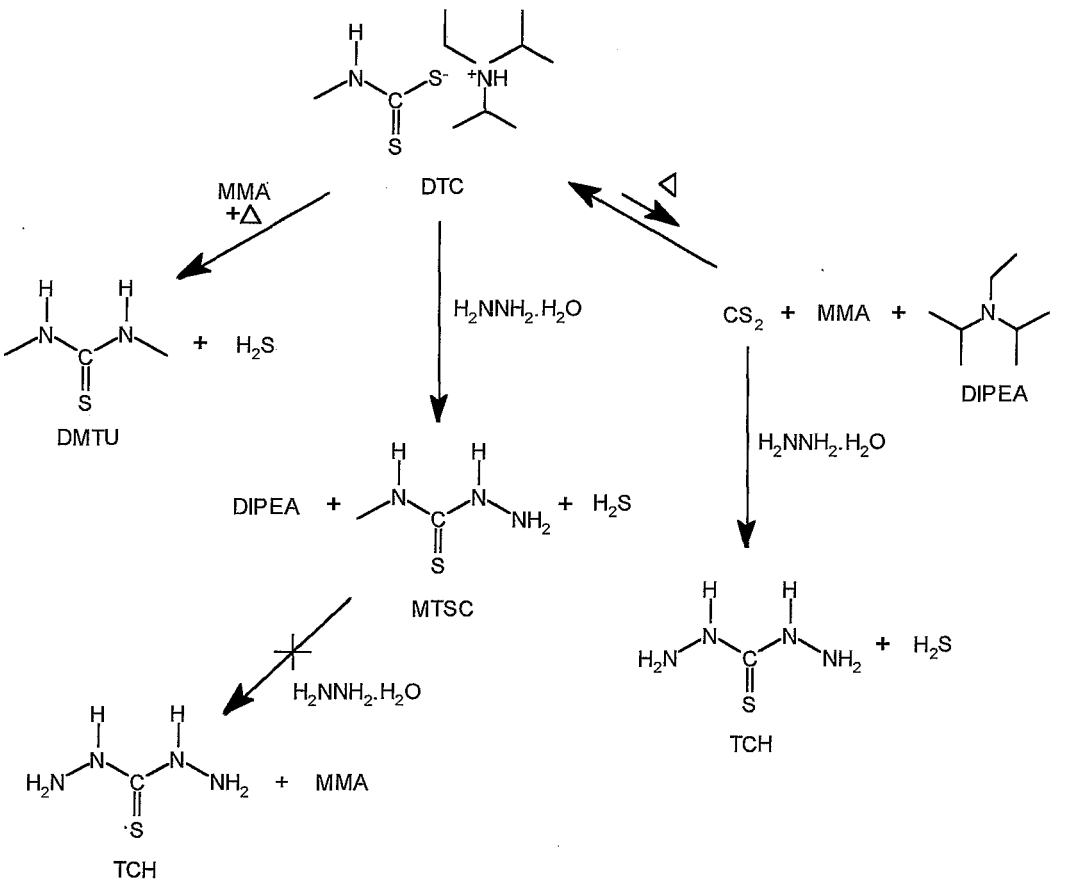

Scheme 6.1: Stability of DIPEADTC and MTSC

At elevated temperatures in the absence of excess methylamine, DIPEADTC decomposes to its starting materials at a slower rate than the sodium-, potassium- or ammonium derived dithiocarbamates. In excess methylamine at elevated temperatures DIPEADTC will react with methylamine to form the byproduct, DMTU. Hydrazine hydrate reacts with the CS_2 formed during the decomposition of DIPEADTC, to form the byproduct, TCH. From the stability tests of MTSC it is evident that hydrazine hydrate does not react with MTSC to form TCH.

The reaction of DIPEADTC with hydrazine hydrate was optimized for the specific set of conditions. From the results of the factorially designed experiments it was evident that MTSC yield had to be sacrificed in order to obtain MTSC of high quality. Running the hydrazinolysis reaction in a 10% excess DIPEA resulted in a higher MTSC yield while still maintaining MTSC purity of 98%.

In conclusion, it is possible to produce MTSC of sufficient purity, to produce BTDA of acceptable quality, when using DIPEA as base. The effluent generated during the synthesis of MTSC was reduced from four kilograms per kilogram of MTSC to two kilograms per kilogram MTSC when using DIPEA as opposed to ammonium hydroxide.

References

1. The Pesticide Manual (Tomlin, C. D. S., ***ed.***), 11th ed., Surrey: British Crop Protection Council, 1997, 1606p.
2. Kluge, R. L., Marshall, C. R., Siebert, M. W., Tebuthiuron as a Selective Herbicide for the Control of *Hakea gibbosa* (Proteaceae) in Mountain Fynbos Vegetation, *South African Forestry Journal*, 1987, 140: 35-38, March.
3. Coats, T. C., Presentation - Tebuthiuron Process Research: Technology Review, Dow, Midland, Michigan, 1993.
4. Dugmore, G., Technology Package: Production of BTDA – $POCl_3$ Technology, Dow AgroSciences, 1998.
5. McNeil, W. K., Stritzke, J. F., Basler, E., Absorption, Translocation, and Degradation of Tebuthiuron and Hexazinone in Woody Species, *Weed Science*, 1984, 32: 739-743.
6. Chang, S. S., Stritzke, Sorption, Movement, and Dissipation of Tebuthiuron in Soils, *Weed Science*, 1977, 25: 184-187.
7. Zimdahl,R. L., Fundamentals of Weed Science, Academic Press, San Diego, 1999, p 299-302.
8. Hatzios, K. K., Penner, D., Bell, D., Inhibition of Photosynthetic Electron Transport in Isolated Spinach Chloroplasts by two 1,3,4-Thiadiazolyl Derivatives, *Plant Physiology*, 1980, 65: 319-321.

9. Ashton, F. M., Crafts, A, S., Mode of Action of Herbicides, Wiley-Interscience, New York, 1973, p 34-57.

10. Corbett, J. R., Wright, K., Baillie, A. C., The Biochemical Mode of Action of Pesticides, 2nd ed., Academic Press, London, 1984, p 50-68.

11. Cremlyn, R. J. W., Agrochemicals: Preparation and Mode of Action, Wiley, London, 1991, p 41 – 43, p 239.

12. Roberts, T. R., (***ed.***), Metabolic Pathways of Agrochemicals: Part 1: Herbicides and Plant Growth Regulators, The Royal Society of Chemistry, Cambridge, 1998, p 770-772.

13. Smith, D. E., Carbon Disulphide, (*In* Kirk-Othmer, Encyclopedia of Chemical Technology, 4th ed., 1993, 5: 53-76).

14. Hofmann, W., Vulcanization and Vulcanizing Agents, Maclaren and Sons Ltd., London, 1967, p73-80.

15. Cremlyn, R. J., An Introduction to Organosulphur Chemistry, Wiley, Chichester, 1996, 250p.

16. Ohm, R. F., Rubber Chemicals, (*In* Kirk-Othmer, Encyclopedia of Chemical Technology, 4th ed., 1993, 21: 461).

17. Lay, M.D.S., Sauerhoff, M. W., Saunders, D. R., Carbon Disulfide, (*In* Ullmann's Encyclopedia of Industrial Chemistry, 5th ed., 1986, A5: 187).

18. Schubart, R., Dithiocarbamic Acid and Derivatives, (*In* Ullmann's Encyclopedia of Industrial Chemistry, 5th ed., 1986, A9: 5).

19. Roy, K. M., Xanthates, (*In* Ullmann's Encyclopedia of Industrial Chemistry, 5th ed., 1986, A28: 426).

20. Yarar, B., Flotation, (*In* Kirk-Othmer, Encyclopedia of Chemical Technology, 4th ed., 1993, 11: 93).

21. Ramachandra Rao, S., Xanthates and Related Compounds, Marcel Dekker Inc., New York, 1971, p41.

22. Romanowski, F., Klenk, H., Organic Thiocyanates and Isothiocyanates, (*In* Ullmann's Encyclopedia of Industrial Chemistry, 5th ed., 1995, A26: 754).

23. Joubert, R., Synthesis of Methyl Isothiocyanate and Trimercapto-s-triazine Trisodium Salt, Karbochem, Sasolburg, 1996, p8-10.

24. ANON, Selected Opportunities in Organosulfur Chemicals: A Brief Overview, Report to Karbochem, Arthur D. Little International, Inc., Brussels, 1996.

25. Jackman, D.E., Combs, G.W., Westphal, D. B., US patent 4940815, Mobay Chem. Corp., USA, 17 March 1989.

26. Aoyagi, E. I., US patent 4477459, Chevron Research Co., 16 October 1984.

27. Bright, D. A., EP patent 308225 A2, ICI Americas, Inc., USA, 22 March 1989.

28. Cramm, G., Kranz, E.,Hellrung, G., DE patent 2546096, Bayer A-G, 21 April 1977.

29. Steinacker, K., Adolphen, G., BR patent 7803218, Bayer A-G, 10 July 1979.

30. Barton, D. B., US patent 4237066, Mobay Chem. Corp., USA, 2 December 1980.

31. Schroeder, D.C., Thioureas, *Chemical Reviews*, 1955, 55: 189.

32. Thorn, G.D., Ludwig, R. A., The Dithiocarbamates and Related Compounds, Elsevier, Amsterdam, 1962, 292p.

33. Coucouvanis, D., The Chemistry of the Dithioacid and 1,1-Dithiolate Complexes, *Progress in Inorganic Chemistry*, 1970, 11:240.

34. Joris, S. J., Aspila, K. I., Chakrabarti, C. L., Decomposition of Monoalkyl Dithiocarbamates, *Analytical Chemistry*, 1970, 42(6): 648, May.

35. Miller, D. M., Latimer, R. A., The Kinetics of the Decomposition and Synthesis of some Dithiocarbamates, *Canadian Journal of Chemistry*, 1962, 40: 246-255.

36. Littlewood, P., Ketteman, C., Hindered Amine Bases for Fine Chemical Synthesis, *Speciality Chemicals*, 1995, p260, September/October.

37. ANON, Whyte Chemicals – Speciality Chemicals, Whyte Chemicals Product Catalogue, London, 1997, p5.

38. Schiessel, H. W., Hydrazine and its Derivatives, (*In* Kirk-Othmer, Encyclopedia of Chemical Technology, 4^{th} ed., 1993, 13: 573-574).

39. Jensen, K. A., Anthoni, U., Kägi, B., Larsen, C., Pedersen, C., Studies of Thioacids and their Derivatives: Thiosemicarbazides, *Acta Chemica Scandinavica*, 1968, 22: 16.

40. Herst, E.J., Study and Description of a process to manufacture 4-Methyl-3-Thiosemicarbazide via a Triethylammonium N-methyldithiocarbamate, Dow Chemical Company Internal Report, Midland, Michigan, 1995, p46.

41. ANON, Determination of Chemical Oxygen Demand, Government Gazette, South Africa, No. 2512, August 1969.

42. Nakanishi, K., Infrared Absorption Spectroscopy – Practical, Holden-Day, California, 1962, 232p.

43. Silverstein, R. M., Bassler, G. C., Morril, T. C., Spectrometric Identification of Organic Compounds – 5th Ed., Wiley and Sons, Inc., New York, 1991, p3-251.

44. Atkins, P. W., Physical Chemistry – 4th Ed., Oxford University Press, Oxford, 1990, p792.

45. Bennen, W., Clean up of MTSC Process Effluent, Department of Applied Science, Port Elizabeth Technicon, 1999, p11-27.

46. Carlson, R., Design and Optimization in Organic Synthesis, Elsevier, Amsterdam, 1992, 536p.

47. Montgomery, D. C., Design and analysis of experiments, 4th Edition, Wiley, New York, 1997, 603p.

48. Davies, L., Efficiency in Research, Development and Production, Royal Society of Chemistry, Cambridge, 1993, 180p.

49. Box, G. E. P., Hunter, W. S., Hunter, J. S., Statistics for Experimenters, Wiley, New York, 1979, p329.

50. Strange, R. S., Introduction to Experimental Design for Chemists, *Journal of Chemical Education*, 1990, 67(2): 113 – 115, February.

51. Myers, R. H., Montgomery, D. C., Response Surface Methodology, Wiley, New York, 1995, p94.

52. Van Ryswyk, H., Van Hecke, G. R., Attaining Optimal Conditions, *Journal of Chemical Education*, 1991, 68(10): 878 – 882, October.

53. Johnson, L. W., Riess, R. D., Arnold, J. T., Introduction to Linear Algebra, 3rd Edition, Addison-Wesley, Reading, Massachusetts, 1993, p196 – 210.

54. Wiechers, A., Manufacturing of MTSC by employing DIPEA as preferred proton acceptor during the initial *in situ* formation of methylaminodithiocarbamate, Internal Communication, Karbochem, 1 July 1997.

APPENDIX A

F-tables

F- distribution: Upper 5% Points (ν_1 degrees of freedom in numerator and ν_2 in denominator)

ν_2	ν_1=1	2	3	4	5	6	7	8	9	10	12	15	20	24	30	40	60	120	∞
1	161	200	216	225	230	234	237	239	241	242	244	246	248	249	250	251	252	253	254
2	18.5	19.0	19.2	19.2	19.3	19.3	19.4	19.4	19.4	19.4	19.4	19.4	19.4	19.5	19.5	19.5	19.5	19.5	19.5
3	10.10	9.55	9.28	9.12	9.01	8.94	8.89	8.85	8.81	8.79	8.74	8.70	8.66	8.64	8.62	8.59	8.57	8.55	8.53
4	7.71	6.94	6.59	6.39	6.26	6.16	6.09	6.04	6.00	5.96	5.91	5.86	5.80	5.77	5.75	5.72	5.69	5.66	5.63
5	6.61	5.79	5.41	5.19	5.05	4.95	4.88	4.82	4.77	4.74	4.68	4.62	4.56	4.53	4.50	4.46	4.43	4.40	4.36
6	5.99	5.14	4.76	4.53	4.39	4.28	4.21	4.15	4.10	4.06	4.00	3.94	3.87	3.84	3.81	3.77	3.74	3.70	3.67
7	5.59	4.74	4.35	4.12	3.97	3.87	3.79	3.73	3.68	3.64	3.57	3.51	3.44	3.41	3.38	3.34	3.30	3.27	3.23
8	5.32	4.46	4.07	3.84	3.69	3.58	3.50	3.44	3.39	3.35	3.28	3.22	3.15	3.12	3.08	3.04	3.01	2.97	2.93
9	5.12	4.26	3.86	3.63	3.48	3.37	3.29	3.23	3.18	3.14	3.07	3.01	2.94	2.90	2.86	2.83	2.79	2.75	2.71
10	4.96	4.10	3.71	3.48	3.33	3.22	3.14	3.07	3.02	2.98	2.91	2.85	2.77	2.74	2.70	2.66	2.62	2.58	2.54
11	4.84	3.98	3.59	3.36	3.20	3.09	3.01	2.95	2.90	2.85	2.79	2.72	2.65	2.61	2.57	2.53	2.49	2.45	2.40
12	4.75	3.89	3.49	3.26	3.11	3.00	2.91	2.85	2.80	2.75	2.69	2.62	2.54	2.51	2.47	2.43	2.38	2.34	2.30
13	4.67	3.81	3.41	3.18	3.03	2.92	2.83	2.77	2.71	2.67	2.60	2.53	2.46	2.42	2.38	2.34	2.30	2.25	2.21
14	4.60	3.74	3.34	3.11	2.96	2.85	2.76	2.70	2.65	2.60	2.53	2.46	2.39	2.35	2.31	2.27	2.22	2.18	2.13
15	4.54	3.68	3.29	3.06	2.90	2.79	2.71	2.64	2.59	2.54	2.48	2.40	2.33	2.29	2.25	2.20	2.16	2.11	2.07
16	4.49	3.63	3.24	3.01	2.85	2.74	2.66	2.59	2.54	2.49	2.42	2.35	2.28	2.24	2.19	2.15	2.11	2.06	2.01
17	4.45	3.59	3.20	2.96	2.81	2.70	2.61	2.55	2.49	2.45	2.38	2.31	2.23	2.19	2.15	2.10	2.06	2.01	1.96
18	4.41	3.55	3.16	2.93	2.77	2.66	2.58	2.51	2.46	2.41	2.34	2.27	2.19	2.15	2.11	2.06	2.02	1.97	1.92
19	4.38	3.52	3.13	2.90	2.74	2.63	2.54	2.48	2.42	2.38	2.31	2.23	2.16	2.11	2.07	2.03	1.98	1.93	1.88
20	4.35	3.49	3.10	2.87	2.71	2.60	2.51	2.45	2.39	2.35	2.28	2.20	2.12	2.08	2.04	1.99	1.95	1.90	1.84
21	4.32	3.47	3.07	2.84	2.68	2.57	2.49	2.42	2.37	2.32	2.25	2.18	2.10	2.05	2.01	1.96	1.92	1.87	1.81
22	4.30	3.44	3.05	2.82	2.66	2.55	2.46	2.40	2.34	2.30	2.23	2.15	2.07	2.03	1.98	1.94	1.89	1.84	1.78
23	4.28	3.42	3.03	2.80	2.64	2.53	2.44	2.37	2.32	2.27	2.20	2.13	2.05	2.01	1.96	1.91	1.86	1.81	1.76
24	4.26	3.40	3.01	2.78	2.62	2.51	2.42	2.36	2.30	2.25	2.18	2.11	2.03	1.98	1.94	1.89	1.84	1.79	1.73
25	4.24	3.39	2.99	2.76	2.60	2.49	2.40	2.34	2.28	2.24	2.16	2.09	2.01	1.96	1.92	1.87	1.82	1.77	1.71
28	4.20	3.34	2.95	2.71	2.56	2.45	2.36	2.29	2.24	2.19	2.12	2.04	1.96	1.91	1.87	1.82	1.77	1.71	1.65
30	4.17	3.32	2.92	2.69	2.53	2.42	2.33	2.27	2.21	2.16	2.09	2.01	1.93	1.89	1.84	1.79	1.74	1.68	1.62
34	4.13	3.28	2.88	2.65	2.49	2.38	2.29	2.23	2.17	2.12	2.05	1.97	1.89	1.84	1.80	1.75	1.69	1.63	1.57
40	4.08	3.23	2.84	2.61	2.45	2.34	2.25	2.18	2.12	2.08	2.00	1.92	1.84	1.79	1.74	1.69	1.64	1.58	1.51
48	4.04	3.19	2.80	2.57	2.41	2.29	2.21	2.14	2.08	2.03	1.96	1.88	1.79	1.75	1.70	1.64	1.59	1.52	1.45
60	4.00	3.15	2.76	2.53	2.37	2.25	2.17	2.10	2.04	1.99	1.92	1.84	1.75	1.70	1.65	1.59	1.53	1.47	1.39
80	3.96	3.11	2.72	2.49	2.33	2.21	2.13	2.06	2.00	1.95	1.88	1.79	1.70	1.65	1.60	1.54	1.48	1.41	1.32
120	3.92	3.07	2.68	2.45	2.29	2.18	2.09	2.02	1.96	1.91	1.83	1.75	1.66	1.61	1.55	1.50	1.43	1.35	1.25
∞	3.84	3.00	2.60	2.37	2.21	2.10	2.01	1.94	1.88	1.83	1.75	1.67	1.57	1.52	1.46	1.39	1.32	1.22	1.00

Taken from Carlson, R., Design and Optimization in Organic Synthesis, Elsevier, Amsterdam, 1992,